ANTIBIOFILM FUNCTION-SPACER-LIPID COATINGS ON MEDICAL SURFACES

Pavithra Raghuraman

Thesis submitted to the fulfilment of requirement for the degree of Doctor of Philosophy

MARCH, 2021
AUCKLAND UNIVERSITY OF TECHNOLOGY
New Zealand

Table of contents

Abstract

The establishment of bacteria on surgical implants as a biofilm is a major problem and will significantly affect the morbidity and potentially the mortality of the patient. There are two basic approaches to prevent this from occurring being: (i) to prevent it from happening and/or (ii) to treat it afterwards. The first approach is the most desirable.

Surgical implant infections number in the range up to 4% of surgeries and new methods to prevent this are needed. The main objective of this research was to examine the potential of Kode FSL constructs to prevent the establishment of a biofilm. To determine this, FSL-antimicrobials needed to be designed and constructed; the ability of the FSL constructs to modify surgical surfaces established and then their ability to prevent the establishment of biofilms evaluated. During the research it was discovered that the best results were obtained by using FSLs to secondarily capture antimicrobials and this new approach was extensively evaluated. It was found that a combined product of crystal violet with silver captured by a charged FSL was the best at exerting significant reduction in adhesion and proliferation of both gram-positive (*S. aureus* and *S. epidermidis*) and gram-negative bacteria (*P. aeruginosa* and *E. coli*). FSL captured Cv was effective against gram-positive bacteria and gram-negative *E.coli* and had no activity against *P. aeruginosa*. While FSL captured silver nanoparticles were effective against gram-negative *P. aeruginosa*. FSL captured crystal violet and silver nanoparticle were effective in killing a minimum of 6 log initial bacterial (gram-positive and gram-negative) loading applied to surfaces.

FSL constructs such as FSL-Selenium, FSL-Spermine and FSL-RIP designed for this research, where the antimicrobial agent was a covalent part of the construct were not as good as secondarily captured crystal violet and silver. Among the three FSL's constructed, only FSL-Se on BAND-AID® surfaces at 0.5 mM concentration could bring about an antimicrobial effect against 4.6 log of gram-positive bacterial loadings. While FSL-RIP was able to prevent *S. aureus* attachment on to surfaces. But no killing effect was observed. Among the three constructs FSL-SPM unexpectedly showed enhancement bacterial growth (section 4.1.2.b) rather than inhibition of growth.

Further extension of the work has the potential to result in a novel antimicrobial coating suitable to commodity products such as bandage and surgical implants.

Attestation of authorship

I hereby declare that this submission is my own work and that, to the best of my knowledge and belief, it contains no material previously published or written by another person (except where explicitly defined by acknowledgement), nor material which to a substantial extent has been submitted for the award of any degree or diploma of a university or other institution of higher learning.

Pavithra Raghuraman

Auckland

2021

Intellectual property rights

Acknowledgements

Firstly, I would like to thank my supervisor Dr Stephen Henry for his constant support and encouragement throughout this research. His guidance, support, immense knowledge, understanding and patience allowed me to balance family and research. I would also like to thank my co-supervisors Dr Eleanor Williams and Dr Brent Seale for their support and assistance throughout the process.

A special gratitude goes to my colleagues in the AUT Centre for Kode Technology, Innovation who made my journey wonderful. It was fantastic to work with the facilities provided by them.

I would like to thank Manchester Trust for more than a year of stipend and I am grateful to AUT, School of Engineering for a full fees scholarship. I would also like to thank Kode Biotech for funding the fourth-year fees and providing a stipend.

Furthermore, I would like to thank Jim Clark for guiding me during the initial stages of my research.

A special gratitude to my parents, my sister, sister-in-law and their families for their moral and emotional support along the way. I am also grateful to my friends who have also supported me throughout.

Finally, I would like to thank my husband Raghu and my children Sahana and Tharan for being supportive and patient throughout.

Abbreviations

[-]Agnp	Negatively charged silver nanoparticle
[+]Agnp	Positively charged silver nanoparticle
agr	Accessory gene regulator
AMP	Antimicrobial peptide
Bn	Biotin
CMG	Carboxy methyl glycine
CRP	C-reactive protein
Cv	Crystal violet
DAIR	Debridement, antibitotic implant retention
DOPE	1,2-Dioleoyl-sn-glycero-3-phosphoethanolamine
E. coli	*Escheriscia coli*
EPS	Exopolysaccharide matrix
FITC	Fluorescein isothiocyanate
FSL	Function-Spacer-Lipid (Kode^{TM} technology construct)
FSL-Bn	FSL-Biotin construct with a biotin functional head
FSL-Se	FSL-Selenium construct with a selenium functional head
FSL-SPM	FSL-Spermine construct with a spermine functional head
FSL-Z	FSL-Zero construct with an amine functional head
HAP	Hydroxyapatite
MDR	Multi-drug-resistance
MRI	Magnetic resonance imaging
MRSA	Methicillin-resistant *Staphylococcus aureus*
NC	Sterility control/ negative control
P. aeruginosa	*Pseudomonas aeruginosa*
PC	Growth control/positive control
RAP	RNA III activating protein
RIP	RNA III inhibiting protein
ROS	Reactive oxygen species
S. aureus	*Staphylococcus aureus*
S. epidermidis	*Staphylococcus epidermidis*
Se	Selenium
SEM	Scanning electron microscopy
Se-np	Selenium nano particle
SPM	Spermine
TRAP	Target of RAP

Abbreviations FSL-complexes

A terminology was developed to allow for unique description of FSL-constructs which secondarily acquired antimicrobial compounds. This was required as the order and/or type of mixture had an effect on biological activity. First the FSL construct is described, which is then followed by the "+" symbol to indicate the secondarily associated antimicrobial component. The order in which the secondarily associated component are added, are indicated by the "+" symbols. e.g. FSL-Bn+Cv+[-]Agnp indicates the FSL-Bn was first added to the surface, followed by Cv, which was followed by [-]Agnp.Finally if the entire mixture was prepared and that was added to the surface then the brackets were used to indicate this. e.g. FSL-[Bn+[Cv+$AgNO_3$]], which means a mixture of [Cv+$AgNO_3$] was added to FSL-Bn, and that mixture was contacted with the surface. When a + symbol is in square brackets it relates to charge, e.g. [+] a positive charge. If the mixture is first made and then applied, the component of the mixture are indicated within brackets.

Name	FSL construct	Non-covalent association
FSL-SPM+[-]Agnp	SPM	[-]Agnp
FSL-Bn+Cv	Bn	Cv
FSL-Z+Cv	Z	Cv
FSL-Se+Cv	Se	Cv
FSL-Bn+Cv+[-]Agnp	Bn	Cv+[-]Agnp
FSL-Z+Cv+[-]Agnp	Z	Cv+[-]Agnp
FSL-Se+Cv+[-]Agnp	Se	Cv+[-]Agnp
FSL-Bn+Cv+$AgNO_3$	Bn	Cv+[-]$AgNO_3$
FSL-Z+Cv+$AgNO_3$	Z	Cv+[-]AgnNO_3
FSL-Se+Cv+$AgNO_3$	Se	Cv+[-]$AgNO_3$
FSL-[Bn+[Cv+$AgNO_3$]]	Bn	Premixed [Cv+$AgNO_3$]
FSL-[Z+[Cv+$AgNO_3$]]	Z	Premixed [Cv+$AgNO_3$]

List of tables

List of figures

Overview

The use of medical surfaces such as implants and surgical dressings have become a major part of modern medicine. Despite the advances achieved in surgical procedures, bacterial infections caused by biofilms arises from bacterial attachment to medical surfaces continue to be a major complication in health care. To reduce the incidence of such bacterial related infections a novel functional coating for the prevention of bacterial attachment onto the surfaces is constantly in need.

This thesis focuses on developing a novel antibiofilm coating on medical surfaces that effectively prevent bacterial attachment to the surface by killing or by stopping bacteria fixing on to the surface of the implant. The potential of Kode constucts to modify biological and non biological surfaces were employed to produce an antibiofilm surfaces.

Although the two benign Kode constructs (FSL-Bn and FSL-Z) were previously shown to modify any surface, investigation on its ability to modify medical surfaces was the first step employed to understand the mechanism, strength and stability of modification. These constructs were able to modify both medical surfaces and microorganisms. This abilty of FSLs to modify surfaces were utilized to deliver an antimicrobial on to the surface. Hence Kode constucts with antibiofilms such as Se, SPM and RIP were developed.

Before these antimicrobial FSLs were used on the surface their antimicrobial efficacy in solution were estimated against *S. aureus*, *S. epidermidis*, *P. aeruginosa* and *E. coli*. In this research, the antimicrobial efficacy of FSL in solution were characterised by a colour change using resazurin as an indicator. The in-vitro results demonstrated that FSL-SPM in solution was the only constructs with the ability to kill both gram-positive and gram-negative bacteria. While, FSL-Se demonstrated ability to kill gram-positive bacteria and FSL-RIP was ineffective in killing bacteria.

An antimicrobial coating on medical surfaces were then achieved by a simple drop dry technique. To prove the presence of antimicrobial FSL construct on medical surfaces a charge based detection method was employed. The presence of negatively charged FSL-Se was determined by a positively charged Cv and positively charged FSL-SPM by a [-]Agnp. Additionally, ninhydrin was employed to detect FSL-SPM on surfaces. The methodology employed indicated the presence of antimicrobial on the medical surface.

The antibiofilm properties of these labelled surfaces were estimated by studying the bacterial adhesion and colonisation using resazurin as indicator. The results obtained the resazurin assay were confimed by scanning electron microscopy, viability of bacteria removed from the BAND-AID® surface and crystal violet biofilm asays on bacteria removed from stainless steel.

The three antimicrobial coatings (FSL-Se, FSL-SPM and FSL-RIP) differ in their antimicrobial efficacy as a surface coating.The in-vitro results demonstrated that FSL-Se inhibit gram-positive bacterial attachment onto the surface by killing bacteria while FSL-RIP stop *S. aureus* bacterial attachment by merely preventing and not by killing. While FSL-SPM have shown to increase bacterial attachment to the surface. Owing to the inability to kill wide range of organism by covalent FSL- antimicrobials, an improved antibiofilm coating was required.

In order to achieve a multibacterial coating, that prevent and kill both gram-positive and gram-negative bacteria, FSL constructs labelled surfaces were biofunctionalized with other antimicrobials such as silver and crystal violet. Initially these antimicrobials were individually captured on FSL labelled surfaces. Benign FSLs, FSL-Bn and FSL-Z were also used along with FSL-SPM and FSL-Se. Negatively charged FSLs FSL-Bn, FSL-Z and FSL-Se on the surface captured positively charged Cv. These captured surfaces demonstrated antimicrobial activity against gram-positive bacteria. While positively charged FSL-SPM labelled surface that captured [-]Agnp has shown antimicrobial activity against gram-negative bacteria.

FSL with captured Cv or [-]Agnp had shown antimicrobial activity with gram-positive or gram-negative bacteria. A surface with antimicrobial activity against both gram-positive and gram-negative bacteria was prepared with both Cv and Agnp on the surface. For this the surface was first coated with a negative FSL which in turn had affinity towards positive Cv . This surface with negatively charged FSL and positively charged Cv was able to capture [-] Agnp. The presence of both Cv and [-]Agnp resulted in killing both gram-positive and gram-negative bacteria. The potential that FSL+Cv could capture $AgNO_3$ was considered possible instead of [-]Agnp and proved to be a better replacement with a increased antimicrobial efficacy.

To minimise the steps involved in delivering both antimicrobials to the surface, the ability to mix Cv and $AgNO_3$ solutions prior to contacting FSL was evaluated. It not only prevents bacterial attachment to the surface and inhibit bacteria growth.

The results from this study clearly demonstrate that FSLs associated with Cv and silver possess high antimicrobial activity against both gram-positive and gram-negative bacteria. The results prove a potential product with the ability to kill both gram-positive and gram-negative bacteria when applied to medical surfaces. It also reveals a prototype product with the ability to capture antimicrobials to the surface for the prevention of surface related infection

Chapter 1 Introduction

1.1 The need for novel antimicrobials to prevent implant infection

There has always been a need for novel antimicrobial products due to the rise in bacteria becoming resistant to conventional antibiotics. An endemic resistant bacterial infection could potentially harm millions of people. In the USA, 1.7 million bacterial infections occur resulting in hospitalisation. Everyone alive hs a bacterial infection at least once a year and account for 100,000 deaths annually[1]. Many deaths are due to infections caused by the re-emergence of bacteria that were thought to be eliminated with an antibiotic. Even though an extensive amount of research is ongoing, only a few novel antimicrobials have become available. As per a 2017 report, out of 33 existing antibiotics, only five classes could be considered as a novel[2].

The underlying cause for the need of novel antimicrobials includes antibiotic resistance by bacteria, difficulty in treating biofilm producing bacteria and challenges in sampling and treating implant infections will be discussed further in this section.

1.1.1 Antibiotic resistance by bacteria

Antibiotics are molecules that interact with bacterial inhibit or kill the microorganism. In due course microorganisms develop resistance which negates the ability of these molecules to attach the microbial target. Antibiotic resistance is not confined to pathogenic bacteria and can also occur in environmental bacteria. The emergence of antibiotic-resistant pathogenic bacteria results in inefficiency of antibiotics to clear the microorganism as shown in Figure 1, leading towards an increase in bacterial growth and eventually to severe illness and death.

In the 1950s resistance to the first antibiotic penicillin, had become a clinical concern and even today, resistance is seen to nearly all the antibiotics produced, leading to compromise in the success of therapy. When penicillin was first introduced, all *Staphylococcus aureus* were susceptible but some later developed resistance by the production of a β-lactamase enzyme[3] . This led to the production of methicillin to which resistance was also later formed resulting in by methicillin-resistant *S. aureus* (MRSA)[4]. In 2017, the World health organisation listed 12 pathogenic bacteria including *Pseudomonas aeruginosa* showed resistance to carbapenem a drug administered as the last line of defence against bacterial infections.

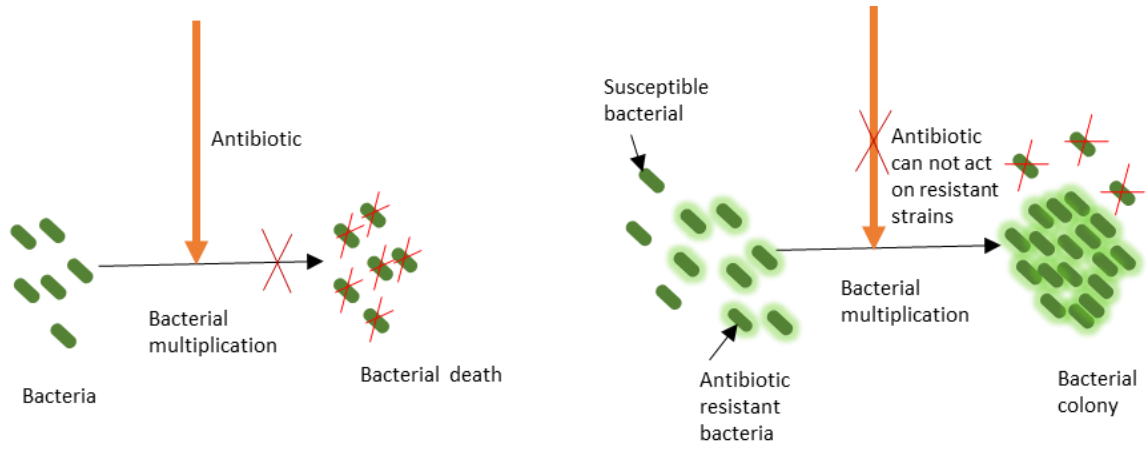

a) Effect of antibiotic on bacteria

b) Antibiotic kill bacteria that are susceptible to the drug resulting in multiplication of drug resistance bacteria caused due to effluxing of antibiotic or mutation of antibiotic target site or chemical modification of the antibiotic.

Figure 1. A diagrammatic representation showing a) the prevention of bacterial growth due to an antibiotic and b) bacterial colony formation resulted due to bacterial resistance to the antibiotic.

Resistance is a property of the bacterial community and achieved through various defence mechanisms such as effluxing of antibiotics, a mutation on antibiotic target sites and chemical modification. These mechanisms keep potentially toxic antibiotics normally fatal to microorganisms out or render them ineffective.

(i) Resistance occurs through the release of antibiotics by bacterial cell membrane-associated efflux proteins. Efflux protein pumps are associated with explusion of toxic substances including antibiotics, metals, toxins, dyes and detergents to the external environment from within the cell. This ability of explusion makes it possible for bacteria to force out antibiotic and gain resistance. In *E.coli* explusion of tetracycline is brought about by plasmid-encoded protein[5]. Over expression of efflux pumps by mutations or the presence of inducers may result in multidrug resistance for more than one class of bactericide[6]. In certain cases efflux pumps activated in the presence of antibiotics bring in resistance as in the case of *P. aeruginosa* biofilm resistance to azithromycin[7].

(ii) A natural mutation of the antibiotic target site leads to antibiotic resistance[8]. The peptidoglycan layer, transpeptidase and transglycosylase are some bacterial target sites for antibiotic attachment and it is possible for mutational changes to occur on these sites resulting in resistance to the inhibition of bacterial growth. For example, *Streptococcal* resistance to antibiotics is brought about by the alteration in the penicillin-binding protein with decreased affinity to the antibiotic[9]. These spontaneous mutational alterations of the target site by slow-growing bacteria also result in multi-drug-resistance (MDR)[10].

(iii) A major mechanism of resistance is brought about by chemical modification of the antibiotic with enzymes. Enzymes easily modify and inactivate an antibiotic derived from a natural product[11]. Covalent modification of the antibiotic by enzymes leads to lack of target sites for the antibiotic to act upon resulting in resistance[12,13]. Modifying enzymes could phosphorylate, adenylate or acetylate the antibiotic compounds rendering them ineffective[14].

Antibiotic-resistant mechanisms evolve with the introduction of new antibiotics[15]. A single bacterium could be resistant to a wide range of antibiotics and related to the extensive spread of human disease. If a super resistance gene is producing the effect, then bacterium with this effect are known as MDR[16]. MDR has extensively spread and accounts for nearly 25,000 deaths each year[17]. Apart from leading to death, these organisms can lead to inadequate or delayed outcomes of effective therapy. As MDR bacteria escalates the need for novel antibiotics or antimicrobial therapies escalates.

Antibiotic resistance can be ingated by the right prescription, proper dosing, controlled use supported by a novel multidrug synergy but never prevented. Potentially all bacteria are capable of becoming resistant to an antibiotic. It is juat a matter of time, hence the need for continuous development of a new antibiotic and antimicrobial stratergies.

1.1.2 Biofilm bacteria are difficult to treat

When bacteria attach to a surface, they form a biofilm. Biofilm bacteria are 10-1000 times more resistant and more difficult to treat in comparison to unattached planktonic bacteria[18]. Nearly 60% of infections are associated with biofilm formation[19], and infections on medical devices such as implants, catheters and ventilators are potentially life threatening. The efficiency of the antibiotic on biofilm depends on various factors such as the penetrative ability of the antibiotic, effective dose, the growth rate of the bacterial pathogen and the environment.

(i) Biofilms can limit the penetration ability of the antibiotic leading to failure of treatment. The specific drug penetration depends on the type of a biofilm, the thickness of the biofilm and the alteration in the membrane protein in response to antimicrobial agents[18]. Studies have demonstrated the inability of penicillin antibiotic to penetrate the β-lactamase positive bacterium by a diffusion barrier[20]. Similarly, a glycocalyx matrix contributes to cementing cells within the biofilm and leads to resistance by increasing the time for antimicrobial penetration[21]. This retarded diffusion of antibiotics decreases the concentration of antibiotic entering the biofilm, helping β lactamase enzymes to destroy the antibiotic[22].

(ii) Another mechanism that contributes to difficulty in treating microorganism depends on the phase of bacterial growth. For instance antibiotics such as β-lactam and tobramycin act on growth phase bacteria and may not affect the slow-growing bacteria in the deeper biofilm which are at the stationary phase[19].

(iii) Other factors include the environmental state brought about by the presence or absence of oxygen in which the bacteria grow[12]. Furthermore, the length of therapy also affects the antimicrobial efficacy. Ineffective abolition of bacteria by the first antibiotic therapy might lead to relapsing biofilms[22]. To avoid all these complications caused by a biofilm on medical implants, antimicrobials to prevent biofilm formation and kill bacteria are essential.

1.1.3 Challenges in sampling and treating implant infection

The implant is a valuable biomedical tool that is required to restore the normal or lost function of a body component. Some commonly used implants include dental, breast, hip and other orthopaedic implants. Many varieties are currently available and are made from different materials. Implant surfaces are prone to bacterial adhesion leading to biofilm formation and infection. An infectious complication related to an implant can result in a compromise in the quality of life and increased time of hospitalisation. In addition, it can lead to a revision of surgery and potential loss of life.

A higher rate of implant infections are reported than infections in implant free surgical interventions[23]. A minimally invasive surgical approach is an attractive treatment for both the patient and the clinician. An effective treatment accomplished by a high degree of clinical suspicion and an early confirmed microbial diagnosis achieves cure rates of greater than 80% and with retention of the implant[24]. Most colonised implants do not become infected so an ultimate proof requires an accurate diagnosis and would involve a sum up of all clinical signs symptoms, blood test, radiography, scans and microbiology findings.

Magnetic Resonance Imaging (MRI) and C-reactive protein (CRP) markers have been shown to be a useful tool for the diagnosis of postoperative spinal implant infection[25] and an implant retention treatment known as Debridement, Antibiotic Implant Retention (DAIR) is considered in most cases and involves a less extensive surgical procedure.

Non-operative cultures of blood for detecting infection vary in their sensitivity and possess a significant diagnostic challenge. The only clinical finding of implant-related infection is a pain at the implant site and no test is sensitive and specific for the infection caused. A definite diagnosis based solely on history and the physical finding may prove inaccurate while radiography may not

differentiate aseptic or septic loosening of the implant. CRP a critical parameter for the diagnosis of infection has shown low sensitivity and specificity of diagnosis of latent infection occurring by low virulent bacteria such as *Propionibacterium acnes*[26]. Many recent developments have helped in the detection of implant infection by MRI and other techniques, but in most cases, implant removal is required.

All implant infections require a microbiological detection to identify the microorganism involved in causing an infection. The microbiologic detection rate of implant infection is relatively low due to the culturing of swabs and small pieces of tissues and not the potentially infected surfaces. Microbiologic diagnosis of peri-implant tissue poses a challenge to detect biofilm bacteria adhered on the surfaces of the implant. Microbial culture and confocal laser scanning microscopy of the implant has enabled greater detection of infection than microbial cultures of tissues or swabs[27]. In such cases, specimens need to be obtained from explanted devices. Sonication of explanted devices has shown to be an accurate pathogen identification method when compared to peri-implant tissues[28]. Additionally, the diagnosis of all bacterial colonies is not possible. In the case of a facial implant, infection presentation could be late and could also show negative culture results. In these conditions incision and drainage, implant removal and antibiotic treatment for three months is the required treatment[29]. Finally, some detection methods can lead to misclassification of a polyclonal infection as monoclonal. Moreover, the lack of confirmation of the causative agent would lead to inappropriate treatment and finally lead to the rejection of the implant. Overall the traditional culture methods often turn out to be inefficient in reaching a proper diagnosis of the bacteria involved in the infection.

The success of treating an implant infection by DAIR treatment depends on the infecting microorganism, duration of symptoms, length of antibiotic treatment, the period between the onset of infection and initiation of treatment[30]. DAIR relies on the patient's immunity to clear the infection and has a low success rate[31]. In a case of early infection with local or systemic inflammatory reactions, they have a high probability of cure by DAIR treatment, whereas late infections require prosthesis revision due to difficulty in elimination of the biofilm on internal fixation devices[32]. Moreover, DAIR treatments have failed in conditions of fully developed biofilms and exclude the possibility of cure without removal of the implant. Even in the case of prolonged antibiotic treatment for more than six months, recovery is postponed and is not cured. In such cases revision of surgery would be considered and had proven to have a 100% success rate when compared to the retention of the implant[33,34]. Reports state that the cure of an MRSA infection fails in 72% of cases where revision is the only available option. In *S. aureus*-infected prosthetic valves, surgical replacement is the only cure[35]. Finally, there are cases where DAIR treatments have failed which has resulted in a revision surgery and even resulted in amputation[31].

Medical therapy includes identification of the infection causing microorganism, treatment with an antibiotic and in most cases involves re-implantation after the confirmed removal of the microbial infection. Due to the potential problems faced with successful implant surgery, there is a continuous need for an innovative antimicrobial coating to minimise and kill bacteria approaching the surface. Moreover, inhibition of biofilm formation inhibits infection which leads to the success of implant surgeries and reduces complications such as revision of surgeries. A novel antimicrobial approach to preventing biofilm formation rather than treating an infected implant is an increasing necessity.

1.2 The process involved in biofilm formation

Bacterial biofilms occur on surfaces where an initial bacterial attachment is achieved. The conventional transmission of bacteria to form an infection may be from normal skin flora or the environment. The human immune system maintains a balance with the presence of normal bacterial flora present in the environment, the skin and normal bodily function; when there is a loss of balance due to impairment of host defence mechanism or due to the increase in the bacterial load or bacteria being in a location that they should not be, biofilms may arise. The diagrammatic representation of the mechanism of bacterial biofilm formation is shown in Figure 2.

This involves initial adhesion through to a bacterial biofilm formation, which is a highly organised microbial community densely packed in an extracellular polymeric substance. The transition of free-floating bacteria (planktonic) to adhered biofilm infections occur through several stages such as adhesion, colonisation, biofilm formation and infection will be discussed further.

1.2.1 Adhesion

Bacteria may be present as planktonic, microcolony biofilms or dispersed bacteria[36]. Progression from planktonic bacteria to being surface-bound is due to the adaptation of the bacteria to the nutritional and environmental conditions[37]. Bacteria from the environment, the patient's body or the patient's health care provider find their way into the host and attach to surfaces resulting in the initiation of biofilm formation[38]. Surface sensing mechanisms result in a phenotypic change within the bacteria when interacting with the surface [39]. The microorganism attaches to the host tissue and may result in a stable irreversible attachment after the adaptation of the microorganism, because of strong attachment and detachment processes. Adhesion involves an initial reversible attachment to a surface which lead to an irreversible chemical and cellular adhesion phase[40].

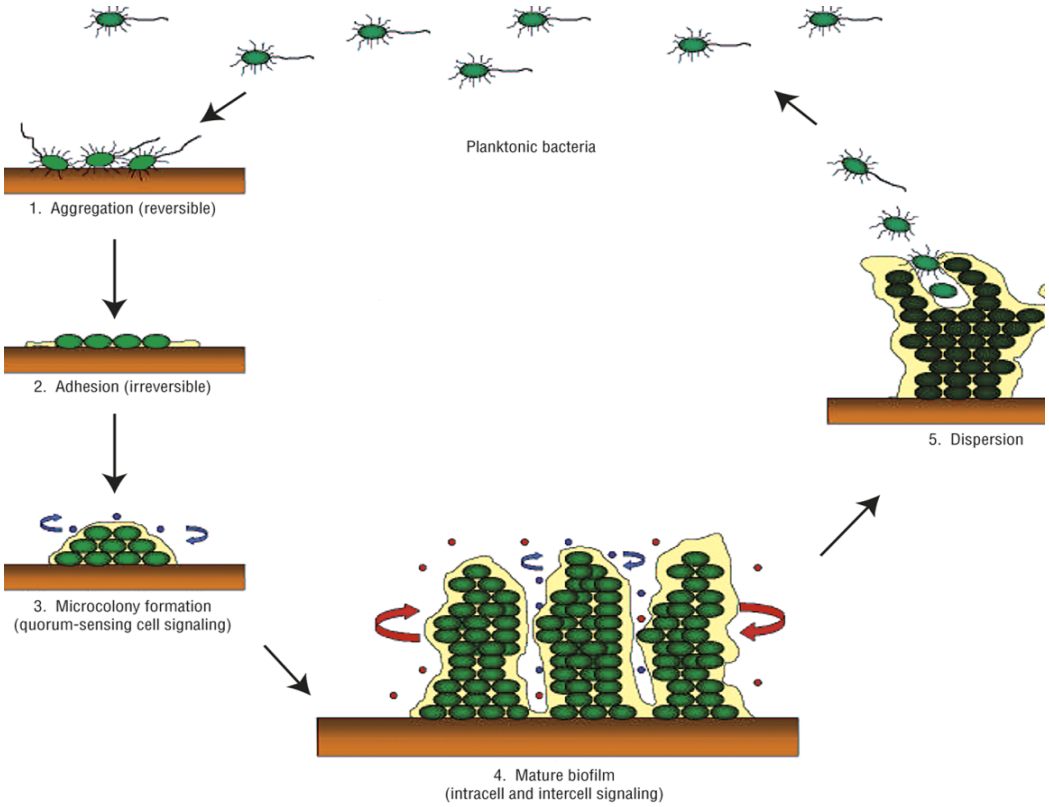

Figure 2. Representation of the stages involved in the formation of a biofilm[41]. Reversible adherence of bacteria, leading to irreversible attachment and formation of microcolonies and finally resulting in mature biofilms that release bacteria ready to infect a new region.

This attachment can be due to specific or nonspecific interactions. An example of specific interaction is *Staphylococcus* absorption onto implant material by a surface component recognising adhesive matrix, and the non-specific interaction example is type I pili of *Enterococcus coli* with mannose [42].

Many factors such as environmental, bacterial surface characteristics, material surfaces characteristics and the presence of proteins influence the mechanism of bacterial adhesion [40]. The mechanism of adhesion is quite complex and vary with species of bacteria. Two different organisms may show differences in adherence to the same surfaces and reports have shown that *P. aeruginosa* has shown to adhere better to silicone hydrogel contact lenses than *Staphylococcus* species[43]. Surface roughness plays an important role and is inversely proportional to bacterial adhesion[42,44]. Adhesin helps adhesion of bacteria with host proteins that help in spontaneous adherence to the material.

1.2.2 Colonisation

Colonisation occurs when firmly attached bacteria rapidly multiply forming small aggregates by the binary division of daughter cells resulting in microcolonies which eventually lead to larger colonies enclosed in a matrix. At this stage of rapid growth initial attachment ends and biological processes take over at the expense of the adjacent nutrients. Chemical signals result in the activation of genetic mechanisms where bacterial division takes place in an embedded exopolysaccharide matrix (EPS). The colonisation or biofilm stage of bacteria can escape the host immune response and induce a non-healing inflammatory phase [45].

1.2.3 Biofilm

Aggregates of bacteria that adhere to the wound bed or surface rapidly multiply resulting in a critical colonisation known as a biofilm. Biofilm can be beneficial in some situations such as the removal of contaminants such as metals, nitrogen and the purification of industrial waste[46]. However, the adverse effect of biofilms has become more significant. Biofouling is caused by bacterial biofilms in most industries. Biofilms on ocean-going vessels can cause mechanical blockage, material deterioration and a threat to health care[47]. Biofilms in the food industry are critical where numerous structures could serve as a source for biofilm formation and resulting in foodborne diseases[48]. Biofilm formation is involved in 65-80% of bacterial infection causing a severe concern to the health sector[49].

Chronicity of wound and wound infection is regulated by the quorum sensing mechanism of a biofilm. Quorum sensing is a phenomenon which occurs when a specific population density of bacteria is reached increasing the concentration of extracellular signalling molecules. Biofilm substances are composed of more than 75% EPS and up to 25% of bacteria[50]. The EPS mediates cell to cell interaction and cell surface interactions. Specific recognition patterns of bacteria bring in the ability to identify genetically distinct organisms and form clumps. Once a critical concentration of these molecules is reached, bacteria can undergo significant changes in phenotype such as metabolism and stress response. Moreover, it produces a cytotoxic effect on the host by the subsequent production of virulence factors[51]. EPS a key component of biofilms, play an important role in antimicrobial tolerance. The individual bacteria present in a biofilm are protected by the extracellular matrix, this can increase the resistance to antibiotic and has been reported to be involved in the pathogenesis of the skin, genitourinary tract, respiratory, epithelium, gut and dental caries[36,51]. Additionally, the ability of a microorganism in solution to adhere to previously attached organisms also contributes to biofilm interaction[50,52]. Biofilm formation on medical devices is thought to play a significant role in infection and only EPS slime

producing strains were infecting implants [53]. Central venous catheters, heart valves, ventricular assist devices, coronary stents, breast implants and dental implants are a few implant surfaces that could be compromised by bacterial biofilm. Figure 3 shows a scanning electron microscopy (SEM) image of a well-established biofilm formed on a fibre of cotton surgical dressing material. When a biofilm displays exceptional resistance to environmental stress, it forms an infection.

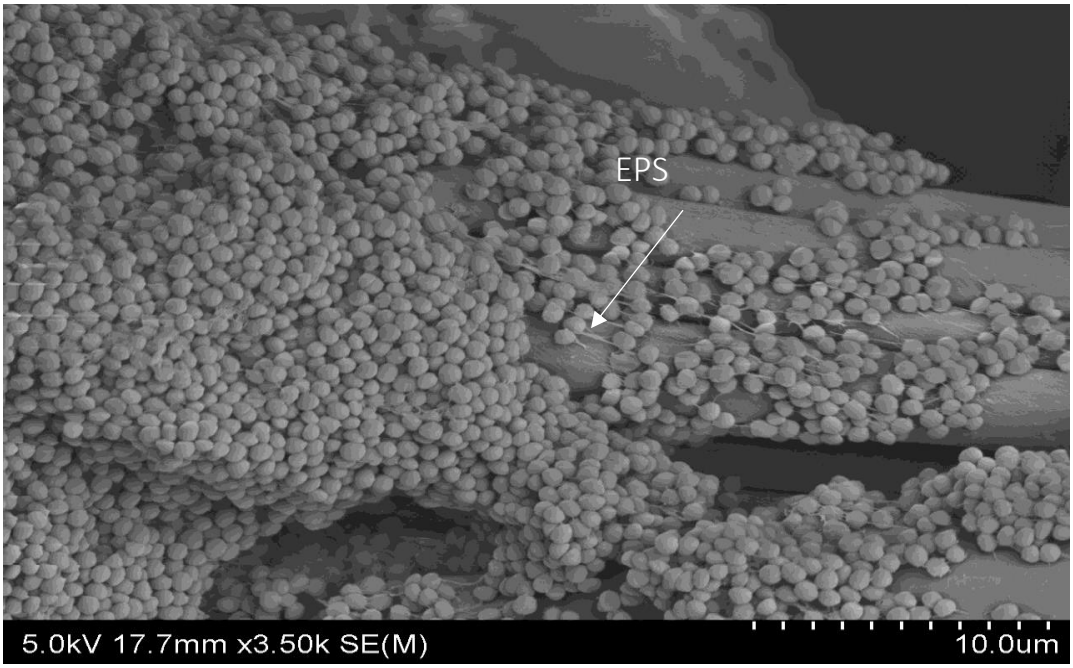

Figure 3. *Staphylococcus epidermidis* bacteria and probable exopolysaccharide matrix (EPS) threads visualised by scanning electron micrograph of a well-established biofilm on fibre of cotton surgical dressing.

1.2.4 Dispersion and Infection

Dispersion and mechanisms of infection are indicated in Figure 4 when harmless bacteria multiply, encapsulate by EPS formation and finally result in a harmful bacteria biofilm that produces virulent factors leading to infection. In addition, detachment of planktonic cells by a mature biofilm may lead to starting a new cycle of biofilm at a new region. The chronicity of persistent bacterial infection is due to bacterial biofilm formation[54]. Infection depends on the dose, the virulence of the bacteria, the resistance of the host[55] and is a life threatening complication. However, the point at which bacterial loading becomes an infection is still controversial. The number of organisms cannot always indicate bacterial invasiveness; for example, beta-haemolytic *streptococci* delay wound healing regardless of bacterial count[56]. Infections manifest on a wound caused by surgery, burns, minor cuts, diabetes, pressure and hospitalisation[37,57-59].

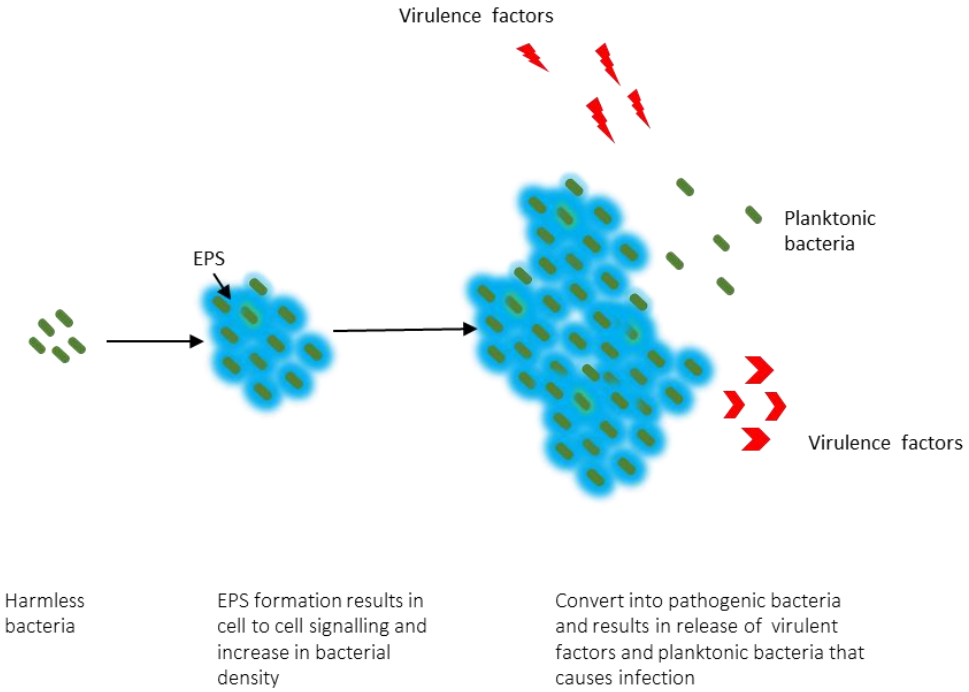

Figure 4. The principle of infection caused by the conversion of a harmless bacteria to a pathogenic bacterium that releases virulence factors leading to infection.

The clinical condition of the patient and the risk of hospital-acquired infection (HAI) co-occur with each other. For instance, ventilator-associated pneumonia occurs in patients on a ventilator for more than two days[60]. Such infections are responsible for high morbidity and mortality, prolonged hospital stay and finally result in increased health care cost[61]. The ability of a microorganism that has survived in an unfriendly environment including dry surfaces to then infect a patient has led to infections following surgery. For example, bacteria isolated from disinfected surfaces that were not from present patients indicate the survival of pathogens in the unfavourable environment and they are capable of forming an infection on patients hospitalised[62].

Also, HAI following major surgery is commonly occurring in patients between 5 -10 days of operation[63]. Infections associated with a variety of surgical implants have clinical and economic consequences and can also be life-threatening. Implants tend to potentiate bacteria on the surface so opportunistic microbes become virulent pathogens leading to infection. Bacteria causing an implant-associated infection that escape the first lines of intracellular defence lead to medical implant failure and often require the removal of the implant and aggressive and prolonged drug courses. Infection associated failure rates depend on the overall condition of the patient, material used, the surgical site, the sterility of the wound and surgical site, post-surgical care and the microorganism involved. Colonisation and infection are features that challenge

wound management. The possible source of infection on an implant is an adhered biofilm bacterium and can occur throughout the lifetime of the implant.

Some commonly infecting bacteria include *Streptococcus pyogenes, S. epidermidis, E. coli, P. aeruginosa* and *S. aureus*[56,57].

1.3 Microorganism in infection

A significant number of bacteria cause infection of implants. Infectious bacteria are in the atmosphere, surgical equipments, clothing, patients' skin or already in the body[64]. More than half of all the infectious disease is caused by normal flora that are commensals with the human body and the environment. The primary source of organisms is the skin of the host or a physician during implant insertion. About 90% of bacteria recovered from a clean wound could be a source of infection. These organisms are either introduced during implantation of the device or by temporary bacteria present in the bloodstream[65]. These microorganisms present in the environment attach to any surfaces and colonise to produce infection. About two third of surgical implant-associated infections are caused by *Staphylococcal* infection[35,66]. *P. aeruginosa* is the other significant gram-negative bacteria that causes implant-associated infection.

1.3.1 Gram-positive bacteria

Gram-positive pathogens present a global challenge in infection. Among the gram-positive bacteria, *S. aureus* infections present a significant health concern adding to the cost of health care. *S. aureus* is found among the normal flora of the skin and carried as a nasal commensal of 30% of the population[15]. *S. aureus* is considered the most virulent pathogen and the most prevalent biomaterial medicated infection causing agent. Adhesins of *S. aureus* bind to host protein, which helps in the initial attachment on implant surfaces and finally results in the production of extracellular toxins which are challenging to treat.

Polysaccharide intracellular adhesion, a significant component of EPS, contribute to infections in medical devices and influence the host response, and about fifty encoding genes may be responsible for the expression or secretion of virulent factors[65]. *S. aureus* and *S. epidermidis* are different species of the genus *Staphylococcus* and express various microbial surface components that recognise and adhere to surfaces. *S. aureus* adherence is more dependent on the presence of host tissue ligands, such as fibrinogen and collagen while that of *S. epidermidis* is by rapid attachment mediated by non- specific factors. *S. aureus* relies on protein for biofilm formation

while *S. epidermidis* relies only on EPS[66]. *S. aureus* is the main micro-organism that causes infections on orthopaedic, spinal, and breast implant.

S. epidermidis is a common skin and mucosal inhabitant in humans and is of clinical significance due to its biofilm being a major virulence factor, which leads to increased prevalence and resistance to various antibiotics[66]. These commonly produce infection in surgical and prosthetic implant devices and are also found in higher rates in a polymicrobial biofilm[67] and have shown the highest adhesion on implant surfaces[68] While considering pathogenicity, *S. epidermidis* is less pathogenic than *S. aureus.* However, under stress maintain a more stable growth rate than *S. aureus*. Antibiotic therapy on slow-growing *S. epidermidis* is difficult to treat by antibiotics which act on growing bacteria[68]. Various other gram-positive bacteria also contribute to implant infection, and Table 1 is a representation of the organism and the implant associated infections caused by them.

Table 1. Gram-positive bacteria that cause various implant-related infections

Microorganism	Implant	Reference
Listeria monocytogenes	Orthopedic Vascular	69-71
Staphylococcus aureus	Breast Ophthalmic Dental Orthopaedic Hearing	35,72,73
Staphylococcus epidermidis	Ophthalmic Breast Dental Orthopaedic	35,73
Streptococcus pneumoniae	Hearing	73,74
Streptococcus pyrogens	Orthopaedic	75-77
Streptococcus viridians	Ophthalmic	74
Enterococcus faecalis	Cardiovascular Orthopaedic	73,76,77

1.3.2 Gram-negative bacteria

Gram-negative bacterial infections are increasing in recent years. Gram-negative bacteria cause only 5% of infections on orthopaedic implants[78]. Table 2 represent gram-negative bacteria that cause implant-related infections.

Table 2. Representation of gram-negative microorganisms involved in medical devices and biofilm-related diseases

Microorganism	Implant	References
Pseudomonas aeruginosa	Ophthalmic Breast Hearing Orthopaedic cardiovascular	73
Enterococcus coli	Ophthalmic Hearing Orthopaedic Cardiovascular	73
Serratia spp	Ophthalmic	73
Haemophilus influenzae	Hearing	73
Proteus mirabilis	Orthopaedic	79
Klebsiella Pneumoniae	Orthopaedic Central nervous system shunt	80-82
Acinetobacter spp	Central nervous system shunt	80,82
Enterobacter cloaca	Orthopaedic	77, 83
Proteus mirabilis	Orthopaedic	77

E. coli a harmless gram-negative commensal in the intestinal flora evolve and adapt pathogenicity by producing virulent factors such as type I pili that are essential for adhesion and progress of infection to produce bone and uropathogenic biofilms[84].

P. aeruginosa is the second greatest cause of implant infections after *S. aureus*[85] and can grow in an anaerobic or aerobic environment possessing a vast genetic diversity contributing to challenges in eradicating the infection caused. *P. aeruginosa* is the most frequent infection that occurs among patients hospitalised for an extended period and infection can also occur in an existing infection caused by another microorganism such as *S. aureus. P. aeruginosa* transcribes specific genes for attachment of bacteria and hence initiate synthesis of the extracellular matrix that is resistant to drugs[86]. Bacteria use flagella, twitching and gliding motility to grow as a biofilm. *Pseudomonas* dispersed biofilm bacteria cause unique phenotype with their unproven role in

biofilm spread[87]. Mutation in the specific gene of this organism may lead to mutant biofilm which is more susceptible[49].

Klebsiella pneumoniae, *Acinetobacter spp*, *Enterobacter cloaca*, *Proteus mirabilis* are examples of a few other gram-negative bacteria that cause implant infections[77,80].

1.4 Factors affecting bacterial attachment onto the surface

Bacterial adhesion and biofilm formation on surfaces are influenced by many factors. One factor is the surface texture of implants. Texturing is mainly done to increase biocompatibility and also to enhance adhesion, growth proliferation and differentiation of the cells. However such textured surfaces could serve as a binding site for bacteria and initialise biofilm formation[88]. The roughness of the surface is a more critical parameter for bacterial adhesion. Additionally, binding may also depend on the surface free energy and material composition. Research shows that bacterial biofilm formation increases with surface roughness and for instance, a titanium nitride coated surface significantly reduced the bacterial adhesion of *Streptococcus pyogenes* and *Streptococcus sanguis* by reducing surface roughness[89]. When surface roughness increases to a threshold, surface free energy increases, therefore, facilitates biofilm formation[90]. Similarly, reduction in surface free energy reduces bacterial attachment, for example, polishing of zirconia blasted titanium surfaces reduces the surface free energy resulting in the decrease in *Streptococcus mitis* and *Provetella nigrescens* adhesion[89].

Similarly, the level of the composition of a component also plays a role in bacterial adhesion which may reflect on the surface free energy, surface roughness and surface protein binding ability. For instance, bacteria colonise stainless steel more readily than titanium.

Another factor that influences bacterial adhesion is blood proteins that rapidly absorb on the surface following implantation of a medical device. Serum proteins prevent bacterial adhesion due to nonspecific interaction of albumin with the implant surface while adhesive proteins such as fibrinogen form a specific ligand-receptor bond with the bacterial surface and enhance bacterial adhesion[88]. Also, shear forces caused by the blood flow influence bacterial adhesion. Although the parameters above state the influence of surface composition affects biofilm formation much research is primarily focused on the prevention of bacterial attachment to the surface.

1.5 Current surface coating strategies to combat bacterial biofilm formation

A broad spectrum of consideration has been proposed and tested for antibacterial features. At the biomaterial stage, a biocompatible implant alone is not sufficient for a successful surgery; a coating for prevention of infection is also desirable. To stop bacterial colonisation, researchers have studied a wide variety of surface modification techniques. Several mechanisms either interfere with bacterial growth processes or kill bacteria or prevent bacterial attachment to the surfaces and all these strategies are primarily aimed to discourage biofilm formation.

Figure 5 represents approaches that have been used in the battle against bacterial infection. Chemical modifications involve incorporation of antimicrobial agents into polymers (antibiotics, antiseptics, metals), and physical modifications are the development of materials with surface properties which repel microorganisms, or the fabrication of ultra-smooth surfaces with the ability to resist microorganisms attachment.

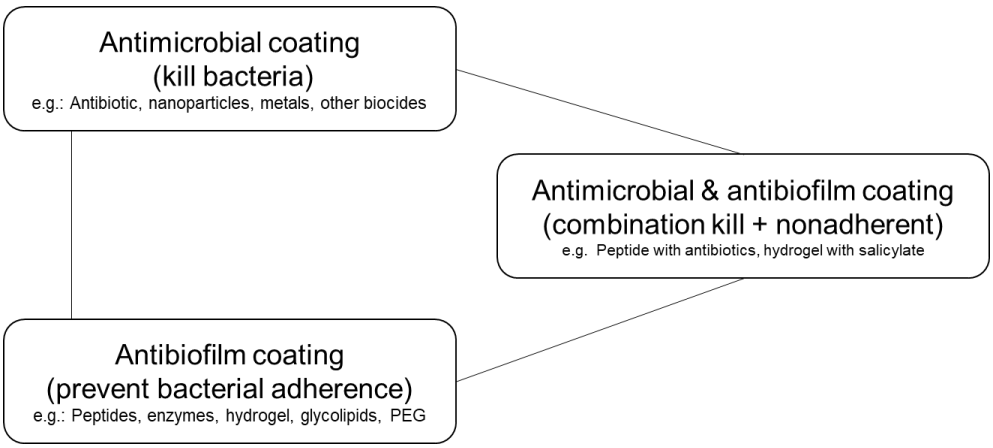

Figure 5. Schematic representation of the current trends in coating surfaces to combat bacterial infection.

1.5.1 Antibiofilm and antimicrobial coating

This section primarily involves the strategies followed by researchers to produce an active surface that prevents bacterial attachment (antibiofilm) or kill bacteria (antimicrobial). Many approaches have been stated in articles for preparing an antibiofilm coating on surfaces. Such coatings are an essential and significant approach to prevent infection by reducing bacterial attachment and colonisation. These molecules are targeted to prevent the first step of bacterial biofilm formation by inhibiting the tendency of bacteria to adhere.

One general approach is by impairing the production and assembly of bacterial adhesins. For example, cell-wall adhesins mediate *Staphylococcus* species adhesion to the host protein on implant surfaces. Such intracellular adhesins of gram-positive bacteria are a potential target to curb *Staphylococcus* derived infections[91]. For instance, synthetic short fibronectin peptide-coated surfaces have shown to inhibit *Staphylococcus* adhesion[92] .

Another approach by researchers for prevention of biofilms is brought about by preventing uncontrolled protein absorption on to biomedical surfaces is by perturbing the physio-chemical adhesive forces needed for bacterial attachment. For example, hyaluronic acid containing surfactant has proven to have reduced protein binding ability leading to a reflection on bacterial growth[93]. Bottlebrush coating with antimicrobial polypeptide and copolymer has seen to effectively reduce protein and platelet adhesions along with antimicrobial properties [94].

Researchers have also examined hydrogel coating on surfaces for an antimicrobial effect. Chitosan could prevent bacterial adhesion and biofilm formation and chitosan hydrogel has efficiently impaired biofilm formation of *C. parapsilosis*[95,96]. The underlying mechanism of this antimicrobial effect is the attraction of anionic microbial membrane by the cationic porous hydrogels leading to disruption of the cell membrane and finally leading to the prevention of bacterial attachment of the microorganism[97]. Similarly, an implant surface coated with polyethylene glycol has reduced bacterial adhesion to the surface[98]. Furthermore, a hydro fibre made of carboxymethylcellulose has been reported to have a strong bacterial removal capacity[99]. Additionally salicylic acid has shown to inhibit biofilm formation bacteria including *S. aureus*, *S. epidermidis* and *B. subtilis* [100].

Antimicrobial peptides (AMP) are receiving considerable attention as an alternative for antibiotic therapy and are a known mechanism of biochemical defence against potential pathogens. AMPs are small cationic peptides that ideally recognise and neutralise anionic microbes. AMPs result in bacterial peptide-mediated cell membrane rupture leading to bacterial death[101]. Due to the fast action of antimicrobial peptides, they decrease the ability of bacteria to produce resistance. Cathelicidins, proline-rich peptides, RNA III inhibiting protein (RIP) are among the reported AMPs to have an antibiofilm effect.

a) RNA III inhibiting protein (RIP)

RIP heptapeptide is involved in the interference of biofilm formation in *S. aureus.* This peptide inhibits the quorum sensing mechanism of bacteria that results in biofilm architecture of cell to cell communication through chemical signals and toxin production essential for disease progression. There have been two regulatory mechanisms proposed for activation of the quorum

sensing mechanism. Firstly, it has been reported that RNA III activating protein (RAP) phosphorylates target molecule (TRAP- target of RAP) and hence activate the *agr* (accessory gene regulator) quorum sensing mechanism by increasing toxin production and decreasing bacterial adhesion[102,103]. RIP (YSPWTNF-NH2) a heptapeptide was reported to inhibit the phosphorylation of TRAP, disrupting the regulation of *agr* resulting in strong activity against biofilm formation[25,104]. TRAP phosphorylation inhibition leads to inhibition of bacterial toxin production and bacterial adhesion[105]. RIP and RAP could bind to the same receptor and one act as an antagonist and the other as an agonist.

In contrast, there have been reports that RAP depends on cell lysis rather than cell density which would be essential for quorum sensing. The *agr* quorum sensing system up regulates aggressive virulence factors by maturation and export of pheromone proteins resulting in activation of the quorum sensing mechanism. These proteins help high-density bacteria to adapt to the environment with a low supply of nutrients[106] . Self *agr* pheromones, induce quorum sensing while others inhibit the response. RIP a coagulase-negative S*taphylococcus agr* inhibits *agr* of *S. aureus*, and this explains its inhibiting activity[104] .

In summary, RIP results in a target-oriented highly effective peptide for the prevention of staphylococci infections. This protein diminishes the ability to produce toxins and interferes with cell-cell communication and prevents formation of virulent phenotypes[107]. These do not kill or stop growth but prevent bacterial toxin production which influences establishment of a biofilm. In theory RIP surface coating could be used on an implant and other biofilm forming surfaces to inhibit bacterial infection. This approach has been handled by researchers and has also has been reported that RIP administration prevented biofilm formation and abolished infection of *S. aureus* and *S. epidermis* including MRSA[108]. RIP incorporated in Polymethylmethacrylate (PMMA) beads has shown the *in-vivo* capability of preventing MRSA infection[109]. Urinary stents biofilm prevention demonstrated by infected mice models *in vivo* that received RIP coated stents had shown to have decreased bacterial count on stent and urine samples[102] .

b) Enzyme coatings

Another strategy to combat infection is the use of enzymes that actively interfere with bacterial adhesion and minimises chances of resistance. Enzymes have been considered as aiding directly to attach microorganisms, interfere in biofilm formation and disperse biofilm bacteria[110]. For example, DNase I, dispersin B, lysozymes, proteolytic enzymes are a few enzymes that have shown to inhibit bacterial attachment and hence biofilm formation[111,112]. DNase I, non-specifically breaks phosphodiester bonds of the phosphate backbone of extracellular DNA that is

an essential component of all matrices of all biofilms formed, and finally results in the prevention of biofilm formation[113]. DNase I could dissolve initial stages of biofilm but is not effective in the removal of a mature biofilm due to the proteolytic enzymes that inactivate the enzyme[113]. DNases can inhibit both gram-positive and gram-negative biofilms[114]. Similarly, disperin B a β-N-acetylglucosamine mediates the attachment and detachment of biofilms of some microbial species including *S. epidermidis, E. coli, Pseudomonas fluorescens* and *Actinobacillus* ac*tinomycetemcomitans*[115].

c) Biosurfactants

Biosurfactants have emerged to be effective in controlling biofilms by reducing surface tension thus reducing bacterial adhesion. Biosurfactants are amphipathic molecule consisting of both hydrophilic and hydrophobic groups. These molecules can self-assemble into complex arrangement mediated by non-covalent bonds, vesicles or micelles. Through self-assembly they alter the surface hydrophobicity resulting in interfering with the process of bacterial adhesion[116]. Some microbial biosurfactants are useful as antimicrobial due to their low toxicity and biodegradability, and a broad range have been described including glycolipids.

Glycolipids are present in large amounts in living organisms and contain one or more saccharides covalently bound to a lipid tail. These mediate many biological and pathological processes such as cell growth, fertility, immunity, microbial and viral invasion[117]. Glycolipids can prevent the adhesion of bacteria onto the surfaces and also can disrupt preformed biofilms[118]. However glycolipids can also potentially act as microbial receptors and some glycolipids also possess antimicrobial activity[119].

Among the antimicrobial glycolipids, rhamnolipid has shown to have greater importance. Rhamnolipid has been studied widely for the involvement of biosurfactants in adhesion and development of pathogens. Rhamnolipid produced by *P. aeruginosa* contains β-hydroxy fatty acid connected to rhamnose sugar via a glycosidic linkage and the rhamnose sugar is composed of one or two moieties[120]. *P. aeruginosa* the primary producer and many other *Pseudomonas, Burkholderia, Acinetobacter* species have been reported to produce rhamnolipid. Rhamnolipid has the potential to alter the cell-cell interaction and cell to surface interaction and overproduction inhibits biofilm formation. Reports suggest inhibition of bacterial adhesion by rhamnolipid against *S. aureus*, *S. epidermidis* species and has inhibited the growth of *B. subtilis* and *P. aeruginosa.* Rhamnolipids are also shown to inhibit marine biofilm caused by *B. pumilus*[121].

Rhamnolipid also were to have antimicrobial activity along with anti-biofilm activity against both gram-positive and gram-negative bacteria including *P. aeruginosa*. It was reported to affect the

bacterial cell surface[122]. The antimicrobial action of Rhamnolipid is brought about by the interaction of rhamnolipid with the bacterial cell membrane. Rhamnolipid at low concentration interacts with cell surfaces increasing the hydrophobicity of the bacterial cells resulting from lipopolysaccharide alteration. Such hydrophobic alteration enhances the degradation rates of bacteria[123] . The antimicrobial effect is concentration dependent and results in binding to the membrane and altering membrane permeability[124]. An increase in protein leakage was noted on *P. aeruginosa* and *B. subtilis* probably due to the rhamnolipid forming molecular aggregates due to the formation of channels for proteins, alternatively it could also directly solubilise the protein resulting in higher leakage[125] .

Rhamnolipid could affect the interaction of bacteria with the surface and with each other. This inhibition in colonisation activity is caused by the property of surfactants. Hence Rhamnolipid can modulate cell-cell and cell to surface interactions disrupting the bacterial attachment. Researchers have used Rhamnolipid on surfaces, and the anti-biofilm activity of Rhamnolipid on polystyrene surfaces has been reported to inhibit biofilm formation of *L. monocytogenes* [126,127].

d) Antibiotics

An antimicrobial coating protects a surface against a wide range of microorganisms. Various approaches could bring in a protective effect. The protective effect could be brought about by the release of an antimicrobial molecule from a surface that kills planktonic bacteria and/or an antimicrobial effect when the bacteria meets the surface with the bound antimicrobial coating.

Several studies have shown use of antibiotics in treatment against bacterial infection. For example gentamicin, an antibiotic against S*. aureus* was effective against planktonic bacteria while biofilm bacteria showed increased tolerance[128]. Such reduced antibiotic susceptibility contributes to persistent biofilm infections. Because of the limitation of antibiotics to treat biofilm bacteria the development of antibiotic incorporated surfaces for the prevention of bacteria to form a biofilm was an approach used by many researchers.

Incorporation of antibiotic onto/ into surfaces

Reports on various antibiotic incorporation within implant surfaces are available. Ciprofloxacin and streptomycin incorporated into waterborne polyurethane polymers have been shown effective for inhibition of *S. aureus* and *E. coli* biofilms and substantially reduced the biofilm formation of *P.mirabilis.* Similarly, antibiotics such as minocycline and rifampin on implants were proven to be more effective at inhibiting bacterial adhesion when compared to silver

sulfadiazine–chlorhexidine-coatings[129]. Likewise, ciprofloxacin containing polymer additives in dental resins have shown antibacterial activity against *Streptococcus mutans*[130]. Researchers have also reported a long- term antimicrobial wound dressing, achieved with the incorporation of gentamicin sulfate and ciprofloxacin[131].

The slow release of antibiotics from surfaces was another approach that has been used for a localised, long lasting and controlled release of antibiotics. Hydrogel has been used as a drug delivery system. However, such systems were more rapid and release limited by minimal loading. Cyclodextrin-based hydrogel systems were found to be efficient in antimicrobial drug delivery[132]. Del Real et al. used Hydroxyapatite (HAp) bone cement composed of gentamycin sulfate for the controlled release of antibiotics from the surface to prevent infection[133]. Similarly, insoluble titanium dioxide nanotubes with antibiotic loaded bone cement has proven to show enhanced slow drug elution, without compromising the mechanical property of the bone cement[134] . Some researchers have used soluble polymers and water-soluble substances such as dextran for antibiotic diffusion from surfaces. However, the rate of release of the drug from a surface with the antibiotic depends on solubility, binding capacity and a net charge of the drug[135].

Though the antibiotic releasing system is a powerful tool for effective eradication of contamination, it seems to have several shortcomings. Firstly, a bacterial biofilm is possible on the surrounding tissues where antibiotic is not released. Secondly, when antibiotic level reaches lower than the therapeutic levels, chances for surviving bacteria to re-establish a biofilm also becomes high. The effectiveness also depends on the spectrum of activity of the drug.

e) Metal elements with an antimicrobial coating

The choice of metal implant is crucial in biofilm formation; for example, increased S. *epidermidis* adhesion has been seen on cobalt-chromium when compared to titanium alloy and stainless steel. Metal antimicrobial agents are attractive alternatives to antibiotics with a lower risk of drug resistance, excellent stability and biocompatibility.

Titanium has been revealed to have high antimicrobial activity and based on this ability implant surfaces made of titanium have been widely used. Surfaces modified with titanium were often a choice for implants. Similarly, other metal modified surfaces have been seen to inhibit bacterial growth, for example copper impregnated surfaces have been reported to clear 99% of pathogenic bacteria such as *S. aureus, E. coli* and *P. aeruginosa* within 2 hr of contact. Metal impregnated surfaces enhance antimicrobial activity, for instance, hydro fibre dressings delay the growth of bacteria when impregnated with silver[136,137]. Similarly, magnesium oxide containing

hydroxyapatite granules were considered in the prevention of dental and orthopaedic infection for eradicating S. *aureus* infection[138]. Hence surface modification with metals has been proved to enhance the antibacterial effect of implant surfaces

The antimicrobial activiy of metals is to cause release of sodium, calcium, phosphorus from the bacterial cell membrane causing weakening[139] and additionally, involved in denaturing the protein and enzyme imbalance in the bacterial cell. For example, metals such as copper and zinc have affinity to the binding site of bacterial proteins, and result in toxicity[140].

(i) Metal elements as nanoparticles

Metals as nanoparticles are considered key to new trends in antimicrobial surface coatings. Metal nanoparticles are nano-sized metals that contain a higher surface to volume ratio compared to the particle molecule that constitutes it. These molecules are more reactive in carrying an antibacterial property with lower toxicity to the patient, and Silver and gold nanoparticles are currently used as antimicrobials to fight the bacterial infection and its direct effect on bacteria has been well investigated[141].

There are several proposed mechanisms for antimicrobial activity of metal nanoparticles. Firstly, the size of these nanoparticles allows them to interact with the bacterial membrane and enter the cell. Secondly, these molecules dissolve faster with a release of a higher amount of metal ions, resulting in the induction of pits and gaps in the membrane, leading to disruption of metabolic processes. Furthermore, these molecules can generate oxidative stress by the generation of Reactive Oxygen Species (ROS) such as superoxide, leading to induction of programmed cell death. In addition, these metal nanoparticles are also proposed to interfere with the electron transport mechanism. The mechanism of antimicrobial activity of the metal nanoparticles is illustrated in Figure 6.

The common nanoparticles used as antimicrobial agents include zinc, magnesium, copper, titanium, gold, platinum, silica and nickel. For example, magnesium oxide nanoparticles were shown to have anti-biofilm ability against both gram-positive and gram-negative bacteria when tested *in vivo* but had a dose-dependent cytotoxic effect on MCF-7 cells[142]. Copper and silver nanoparticles demonstrated efficiency to a wide range of microorganisms[143]. However, a higher concentration of copper nanoparticles was needed when compared to the silver nanoparticle required to bring in a lethal effect against a wide range of microorganisms[144]. Based on the antimicrobial effect of metals, metal nanoparticle incorporation into/onto surfaces has been a recent route for prevention of bacterial infection. At present it appears that metallic nanoparticles are the most promising antimicrobial.

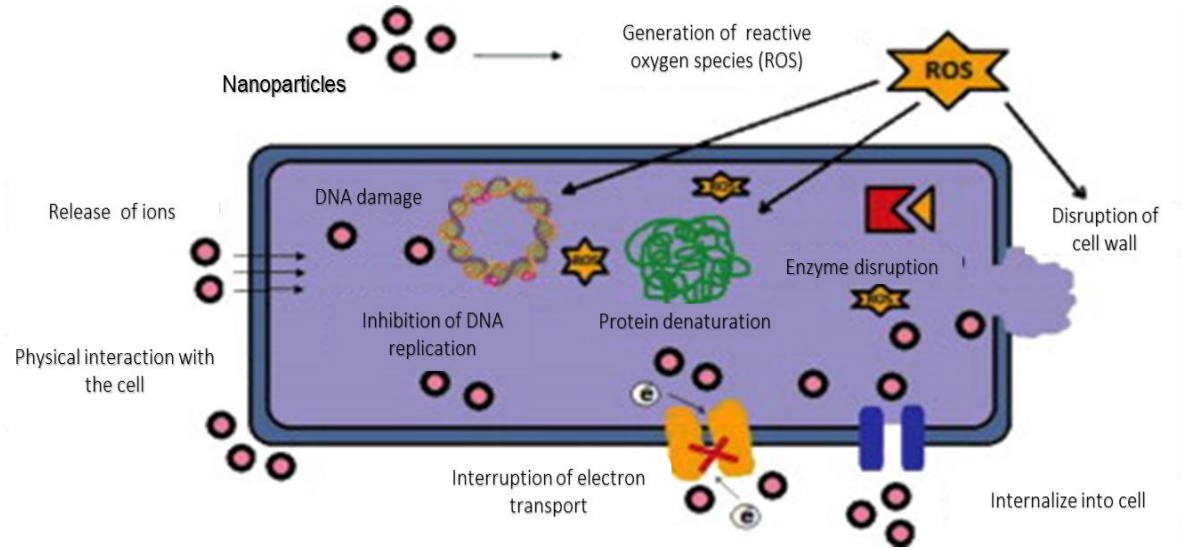

Figure 6. Proposed mechanism of antimicrobial activity of metal nanoparticles brought about by production of superoxides that disrupt the cell wall, enzymes, denature proteins and also result in DNA damage (Dizaj SM et al., doi: 10.1016/j.msec.2014.08.031)[145].

(ii) Silver

Silver is extensively known as a broad-spectrum antibacterial agent. Silver as an elemental metal itself has no antibacterial effect but when oxidised releases silver ions that are responsible for the antibacterial efficacy. Silver ions and silver-based compounds have a strong growth inhibitory effect on microorganisms and have been used as an alternative to overcome drug resistant bacteria. Silver coating is one of the most publicised coatings to prevent biofilm formation and is currently in use to reduce microbial activity on burn wounds, diabetic and leg ulcers and also widely used as dental implants[146,147]. Silver incorporation onto metallic surfaces and dressing

material and textiles, seems like a promising strategy for obtaining an antibacterial surface and reducing bacterial resistance. Silver impregnated surfaces decrease not only adherent bacteria but also bacteria adjacent to the implant surface.

The silver antimicrobial effect occurs by microbial membrane damage. Two mechanisms have been proposed, firstly by an electrostatic attraction with the microbial membrane resulting in binding of silver onto the surface. This binding results in the prevention of bacterial respiration by formation of superoxide ions[148]. Silver ions can also penetrate the cell as silver ions and inhibit bacterial DNA replication[149].

Another mechanism suggested by Kim *et al*. is that metal depletion causes irregular pits on the outer membrane and changes the membrane permeability resulting in a progressive release of membrane proteins and lipopolysaccharides causing denaturation of membrane leading to death[150]. Denaturation can also occur by silver ions binding to electron donor groups of proteins based on the chemical affinity of the silver ions for sulphur or thiol groups, which results in denaturation and loss of enzymatic functions which can kill bacteria by inactivation of vital functions[151].

To overcome the interfering effect caused by silver salts and silver ions, cost-effective silver nanoparticles were developed[150]. The silver nanoparticle interaction with microorganisms also appears to be shape dependent. Truncated triangular nanoparticles have higher antimicrobial activity in contrast to rod-shaped and spherical nanoparticles[152]. The antimicrobial efficacy also depends on the type of bacteria and greater efficiency was noted against gram-negative *E. coli* in comparison to *S. aureus*[150]. Similar results of higher *E. coli* reduction were seen on catheters coated with silver[153,154]. In contrast, Ruparelia et al. reported that two strains of *E. coli* were resistant in comparison to *S. aureus* and silver incorporated into transparent sol-gel coatings which has been shown to have antibacterial activity against *S. aureus, E.coli* and *P. aeruginosa*[155,156].

Silver nanoparticles have been reported to possess high antibacterial activity against multidrug-resistant strains of both gram-positive *S. epidermidis* and *S. aureus*[129]. Silver is considered broad-spectrum antimicrobial as its mechanism of action is not only against bacteria but effective against fungi and viruses too.

Most of the approaches for achieving an antibacterial surface with silver include dip coating, spray coating, sputtering, drop and deposition[153,157]. Deposition of silver includes electrophoretic deposition, ion-beam-assisted deposition, anodic spark deposition[158]. However, in some cases, silver ion coatings on surfaces have been achieved by merely immersion of the matrix into silver nitrate solution that finally gets reduced to silver nanoparticle.

Silver ions that potentially leach out in minute concentrations are not of concern but at high concentrations are cytotoxic and reported to affect the basic mammalian cellular function leading to cell death. Silver nanoparticle coated surfaces have been generally shown to be biocompatible at 0.5% of the weight of silver, on a catheter did not affect fibroblast cell survival but did result in reduced proliferation and contraction of the cytoskeleton, which indicated the start of the apoptotic cascade[153]. Silver ions can change the cell permeability of sodium or potassium ions, which is a well-known cytotoxic effect brought about by heavy metals[159]. Silver nanoparticle might enter the alveoli of the lungs and produce oxidative stress on cells and also accumulate in the liver[160]. Furthermore, silver ions have been proven to negativelly affect the male reproductive system by affecting the sperm cells[161].

All these possibilities of silver toxicity have not threatened the use of silver in the medical field and it is widely approved. Silver, apart from antimicrobial activity seems to have other benefits in human health such as anti-inflammatory properties by promoting apoptosis of damaged cells[162]. Silver also promotes the healing process and reduces scarring[163].

Incidents of bacteria developing resistance to silver have been reported. This resistance is developed by the over expression of enveloped proteins protecting the microbial DNA and preventing silver ions being able to exhibit antimicrobial activity. Several bacterial genes have been identified to promote resistance to silver[164,165]. Additionally, the concentration of silver ions used, also play a role in bacterial activity. At low concentrations of silver ions, bacterial cells can establish and survive while higher concentrations lead to death. Hence determination of effective concentration is crucial, as the silver ions not only interact with the bacterial cell but at high concentrations could interact with the mammalian cell and be cytotoxic.

f) Non-metal elements as an antimicrobial coating

Non-metallic compounds are reported to possess antimicrobial activity hydrogen, chlorine, iodine, nitrogen, selenium and oxygen are a few examples of non-metals that are used in biomedicine for their anti-infective properties. For instance, nitric acid a compound of nitrogen has been reported to possess antiplatelet and antimicrobial properties to prevent thrombus fixation and reduce bacterial adhesion. However, selenium a non-metal is widely used on implant surfaces to prevent bacterial infection.

Selenium

Selenium belongs to metalloids and exists as selenide, selenite and selenate. Selenium is a naturally occurring essential trace element that is necessary for the normal functioning of the human body. It has a critical role in different physiological functions including the regulation of the immune response and maintaining bone strength. Selenium in humans is found in selenoproteins, and around 25 selenoproteins are known and are involved in maintaining biological functions[166]. This element is also found to reduce toxicity caused by other metals by forming metal selenide compounds. Selenium deficiency may result in retarded growth and bone diseases, while at higher concentrations than the beneficial requirements can be toxic.

Selenium exhibits antibacterial, antinflammatory and anticancerous properties making it interesting for research[167]. Selenium and its compounds antimicrobial properties to inhibit bacterial growth and biofilm formation has been well studied. A component of selenium, when used in dressing materials, for wound infection, proved to be an active element to inhibit growth of bacteria[168]. The antimicrobial effect of selenium occurs by its ability to attach to many surfaces and catalyse the production of superoxide radical that are cytotoxic to bacteria[168-170]. This bacterial cell toxicity takes place when the superoxide radical gets converted into a neutral hydroperoxyl radical in the presence of the negatively charged bacterial cell membrane. This hydroperoxyl radical is capable of passing through the cell membrane and forming a free radical chain with unsaturated fatty acids of the bacterial cell, resulting in bacterial cell death[171]. Such antimicrobial activity of selenium is shown on both cocci and bacilli[172].

Previous studies reveal that selenium in the form of selenium compounds (Table 3) or selenium nanoparticles can inhibit bacterial growth[173,174]. The form of selenium used depends on the device on which a coating needs to be established. Organoselenium compounds were attached to contact lens, cellulose and bandages by covalent bonding. This prevented bacterial attachment and colonisation. Additionally, organoselenium was active on bacteria at 4˚C, implying that the activity of selenium does not require metabolically active bacteria and possibly will serve as an alternative to antibiotics that act only on active growing microorganism[175]. The superoxides formed by the organoselenium coating on lenses did not affect corneal epithelial cells of the rabbit leading to the conclusion that selenium toxicity is dose-dependent and can reach a concentration at which selenium has no toxic effect on mammalian cells growing near the medical device but only affect bacterial growth.

Selenium in the form of selenium nanoparticles (Se-np) (Table 4) have been extensively used by researchers due to their high penetration power and for being biocompatible and biodegradable. Se-np have shown antibacterial activity by the strong interaction with polyelectrolytes within the

charged cell membrane of the bacteria. Moreover, Se-nps also led to oxidative stress and DNA damage[176]. Additionally nanoparticulate elemental selenium has a protective effect on fibroblast cells[177]. However, reports do suggest that Se-np are toxic when compared to inorganics or organic seleno compound but less when compared to elemental selenium[176]. Se-np had greater antibacterial activity compared to oxyanion selenite[178].

Table 3. Selenium compounds and technology used for rending an antimicrobial surface against various bacterial species.

Surface	Coating technology	Microorganism inhibited	References
Orthopaedic implants	Sodium selenite coatings on titanium discs. Coated by drying on the surface under laminar flow	*S. aureus* *S. epidermidis*	179
Reverse osmosis (RO) membrane	Organo-selenium by joining amine group of selenocysteine and selenocyanatoacetic acid on a RO membrane	*S. aureus* *E. coli*	180
Cellulose	Organoselenium-methacrylate polymer coated on to cellulose by placing at 60 ˚C	*P. aeruginosa* *S. aureus*	173
-	Organoselenium compound in solution without a surface	*S. aureus* weakly active against *E. coli, P. aeruginosa*	181
Cellulose/ Bandage/ contact lens	Organoselenium covalently attached to surfaces	*S. aureus* *P. aeruginosa* *S. marcescens*	166
Titanium discs	Sodium selenite dried on to surfaces	*S. aureus* *S. epidermidis*	182

Table 4. Selenium nanoparticle antimicrobial activity against microorganisms with and without coating on surfaces

Surface	Coating technology	Microorganism inhibited	References
-	Se-np in solution	*S. epidermidis* No effect against *E. coli*	183
Glass, Catheters	Se-np 24 hrs at four ˚C	*S. aureus*	184
Silicon Surfaces	Se-np printed onto silica surfaces	*S. aureus* *P. aeruginosa*	185
PCL Poly (Ɛ-caprolactone)	Se-np on PCL- prolonged and slow release	*S. aureus* *S. epidermidis*	176
-	Se-np in solution	*E. coli* *P. aeruginosa* *K. pneumonia* *S. typhimurium* *S. aureus*	186

g) Other biocidal coatings

Other biocidal coatings such as chitosan, alginate, polyamines, and crystal violet have also been employed for the prevention of surface-related bacterial attachment[187-189]. The underlying mechanism of antibacterial effect is caused by the anionic microbial membrane attracting the cationic biocidal molecules, resulting in disruption of the cell membrane leading to the death of the microorganisms[97].

(i) Polyamines

The biogenic polyamine is an essential cationic compound found in all living organisms and is important in the regulation of cell growth and proliferation in plants and animals. Polyamines include putrescine, spermidine and spermine. The function of binding depends on the positive charge of the molecule and they electrostatically bind to negatively charged molecules such as DNA, RNA and protein[190]. Spermine, the most active compound when in higher concentration and protects cells from reactive oxygen produced by hydrogen peroxide, leading to regeneration of tissues . It has also been shown to possess growth-inhibiting properties against various bacteria [191,192,193].

Nearly all living organism produce polyamines. In humans, spermine is produced by the prostate at a concentration 50-350 mg/mL in seminal fluid.

Spermine and spermidine antimicrobial activity is seen at concentrations higher than 100 μg/mL[194]. The mechanism of antimicrobial activity is by the agglutination of bacterial cells forming complexes with nucleic acid and phospholipids and inhibiting protein synthesis[195]. Additionally, spermine can generate disruption of the barrier produced by calcium uptake of lipopolysaccharides of gram-negative bacteria. Spermine is protective against lethal sepsis by inhibiting damage-associated molecular patterns which contribute to uncontrolled systemic inflammation and pathogenesis of sepsis[196]. Spermine has been effective in the reduction of planktonic bacteria growth and prevents biofilm formation[197,198.] However, spermine is unable to disperse biofilm bacteria. Casein, lecithin and basic organic and inorganic salts can alter the antimicrobial action of spermine[199].

The antimicrobial efficacy of spermine against *S. aureus* was caused by its inability to produce these polyamines so when externally administered they inhibit bacterial growth. The lack of *de novo* synthesis of polyamines was seen in many gram-positive bacteria and few gram-negative bacteria due to the lack of a gene encoding the synthesis[200]. Antimicrobial activity widely depends on concentration and spermine has been able to outperform gold standard antibiotic coatings. For example, spermine inspired CZ-01127 a bis-alkylnorspermidine-terphenyl antibiotic coating on silicone outperformed gold standard antibiotic coatings against bacterial growth[201].

Spermine has been used on surfaces for other properties too. Spermine based solid phase coatings were used in gene therapy for its ability to bind and release DNA[202]. Spermine incorporation into polyurethane urea matrices was done based on its ability to regenerate bone tissues and not for its antimicrobial ability [203].

(ii) Crystal violet coatings

Crystal violet also known as gentian violet, is an active ingredient of gram staining. This triphenylmethane dye has been utilised for its antifungal, antiparasitic, antibacterial and anti-tumour properties[204,205]. Crystal violet was first used as an antiseptic and early in the 19th century crystal violet was used to treat superficial skin infections[206]. Crystal violet has been used as an external skin disinfectant on skin lesions for the treatment against MRSA bacteria[207]. Based on crystal violet's antimicrobial properties this molecule was recommended by the World Health Organisation for inclusion in the inter-agency emergency kit.

Crystal violet in combination with other compounds has been reported to provide an antimicrobial coating on surfaces. It has been proposed that crystal violet in combination with zinc nanoparticles on medical grade silicone possess increased antimicrobial activity[208]. Similarly, crystal violet in combination with chlorhexidine (known as gendine) impregnated onto catheters by simple dipping proved high antibacterial activity against broad spectrum microorganisms and additionally was potentially safe, when assessed by *in-vitro* cytotoxicity tests[209]. Similar experiments using gendine on central venous catheters carried out by Hanna et al. showed broad-spectrum antimicrobial activity against both gram-positive and gram-negative bacteria, and in yeast[210].

Crystal violet dissociates into a positive ion that can penetrate the bacterial cell and bind to DNA. Crystal violet is involved in the hindrance of ATP synthesis in the mitochondria thus preventing mitochondrial respiration[211]. Additionally, it was postulated that crystal violet on light activation generates superoxides causing oxidative damage of cells leading to death[212]. Crystal violet readily penetrates gram-positive bacterium and covalently bind proteins, but the inability to penetrate the gram-negative bacterium cell wall renders less effective[205]. Crystal violet is reported to be slightly active against *P. aeruginosa* by Bakker et al.[206]. There have been reports that crystal violet disrupted *P. aeruginosa* biofilms, but continuous exposure and a high concentration of crystal violet was required to bring about this effect[204]. *E. coli* reacts poorly with dye due to the high isoelectric points leading to increased resistance to the cationic dye[213].

A cytotoxic effect of crystal violet has been observed in mammalian cells caused by inhibition of oxidase complex of NADPH resulting in superoxide formation[205].

1.5.2 Antibiofilm and antibacterial combined coating

Although many modifications are available, none of these have been individually successful. The exception being, silver which has been extensively used for the development of putative infection-resistant catheters. Thus an alternative approach is the combination of two or more compounds. Such types of coatings containing a combination of both antibiofilm and antimicrobial properties will prevent bacterial attachment and kill bacteria which come in contact. Figure 7 represents the effect of coating implant surfaces with an effective antimicrobial or antibiofilm coating that could prevent bacterial adhesion and kill bacteria that meet these surfaces.

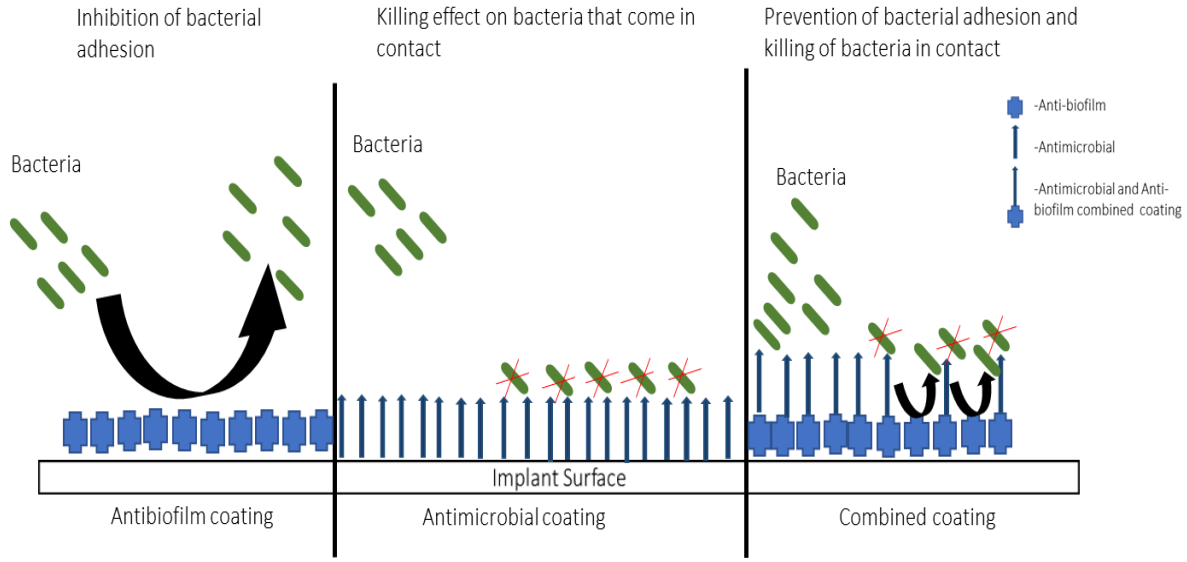

Figure 7. Diagram representing the effect of coating implant surfaces to prevent bacterial infection.

A salicylate combined with the hydrogel has been shown to initially serve as an antimicrobial followed by an antibiofilm by repelling protein absorption[214]. Immobilisation of nitric oxide (NO) in polydopamine (pDA) nanoparticles was found to be both antibiofilm due to the antifouling capacity of pDA, and kill bacteria due to the presence of NO[215]. Similarly, triclosan and enzyme dispersin B in synergy had an antibiotic activity and antibiofilm efficacy against *S. aureus, S. epidermis* and *E.coli*[216]. Likewise, RIP in synergy with an antibiotic has shown to have antibiofilm and anti-microbial effect. DNase I and antibiotic in combination resulted in a decrease in the establishment of biofilm in comparison with the antibiotic or DNase I used alone[217]. Anti-adhesive glycolipid coating on metal nanoparticles have proven to have both anti-biofilm ability and bactericidal effect. Rhamnose lipid at high concentration was sufficient to bring about an anti-biofilm activity, but the combined effect of treatment with a silver and iron metal nanoparticle has shown an increased anti-biofilm effect at a lower concentration[218].

1.6 Coating technologies used for rendering an antimicrobial medical surface

Implant surface interactions with the environment play a key role, and modification techniques can render the surface to have specific properties and characteristics. Many processes have been used to modify surfaces with bioactives having antimicrobial or anti-biofilm properties. Technologies vary from simple dipping to more complex coating methods such as ion

implantation, physical vapour deposition, chemical vapour deposition and plasma electrolytic oxidation have been implemented for coating a surface with an antimicrobial molecule.

Simple dip coating or drop coating was enough to modify a surface with an antimicrobial surface. For example, polymer-based on poly (D, L-lactic acid) PDLLA was coated with gentamicin sulphate by simple two dip-coating and dried in laminar air flow[219]. Similarly, sodium selenite coatings were achieved on titanium discs with desired concentration and dried under laminar flow. Fei Fang et al. used a dipping technique to layer by layer assemble positively and negatively charged polyhexamethyleneguanidine phosphate- ammonium polyphosphate (PGHMGP-AMP) nanoparticles on cotton fabric to render the surface both anti-flammable and with antimicrobial properties[220]. Deposition of ions on titanium discs was carried out by placing in 60˚C and shaking for 24 hr[221].

More complex coating technologies using complex instruments have been used by many researchers. For example, ion implantation was carried out using ion implantation machines and metal vapour for silver ion implantation on titanium[222]. Another coating technology using plasma electrolytic oxidation involves an electrochemical modification technique resulting in activation of a polymer film with organic precursors with electric impulses. Plasma technology can be used for deposition of molecules on a broad-spectrum of surfaces including metals, polymers, and ceramic. The plasma oxidation technique renders the surface with a homogenous oxide layer. Using this technology hydroxyapatite coatings have been achieved on titanium surfaces[223-225]. However it should be noted most of these techniques are incompatible with biological coatings.

1.7 FSL technology an opportunity to deliver an antimicrobial surface

Kode Technology is a novel surface modification technology with an ability to functionalize any surface with a small molecules by a simple mechanism of attachment of the Functional Spacer Lipid (FSL) molecule. This technology has been used both *in vitro* and *in vivo*. The FSL molecule consists of a Functional head (F), a Spacer(s) and a Lipid tail (L) with a large number of variants of the spacers and also a range of different lipids. Figure 8 is a schematic representation of the Kode construct as building block toy figure, representing the functional head with a toy head, a spacer with a red body and lipid tail with grey legs.

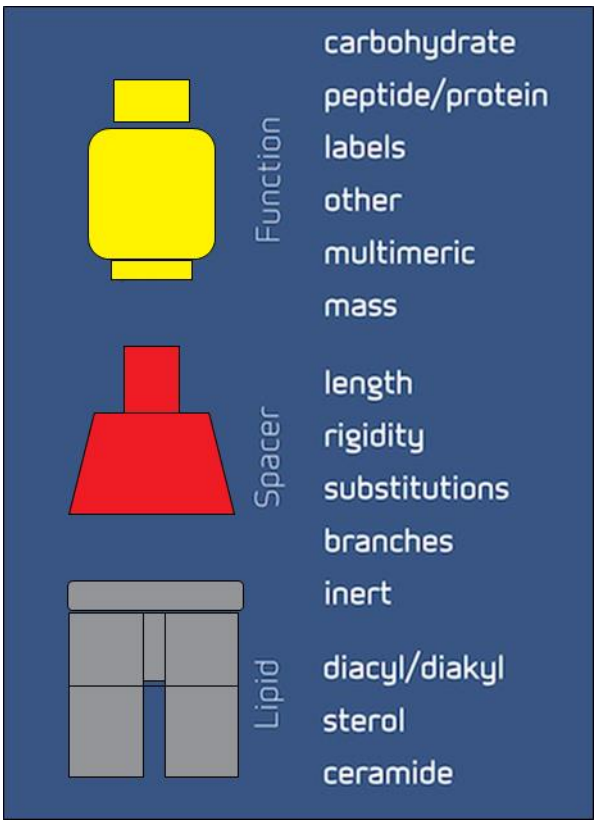

Figure 8. Representation of FSL with a functional head, a spacer and a lipid tail. Variation in the primary head group is possible to bring about the desired activity.

The functional head usually carries the desired molecule for functionalising of the surface to produce application prospects. The choice of a functional head group is limited only by solubility and chemical conjugation issues[226]. Functional moieties to date include biotin, fluorophores, hyaluronic acid, polysaccharides, peptides and glycans. The spacer arranges the functional molecule away from the surface. The length of the spacer reflects the needs for a specific application. The spacer also has been shown to impart water solubility of the FSL construct making the molecule ready to use in biocompatible media. The most common spacers are based on carboxymethyl glycine (CMG) and adipate. These spacers are either short, long, branched, clustered or even functionalized to modify the surface and result in an optimised bioactivity as shown in Figure 9[227]. More recently the spacers have also been used to secondarily associate with bioactive compounds (this research). The lipid tail not only helps to anchor the construct onto the surface, it also imparts an amphiphilic nature to the FSL and along with hydrophilic head render the molecule able to self-assemble on to any surface [228]. The most common lipid tail is 1,2-Dioleoyl-sn-glycero-3-phosphoethanolamine (DOPE) while other lipids such as ceramide, cholesterol have also been used for the construction of FSL to impart specific membrane association.

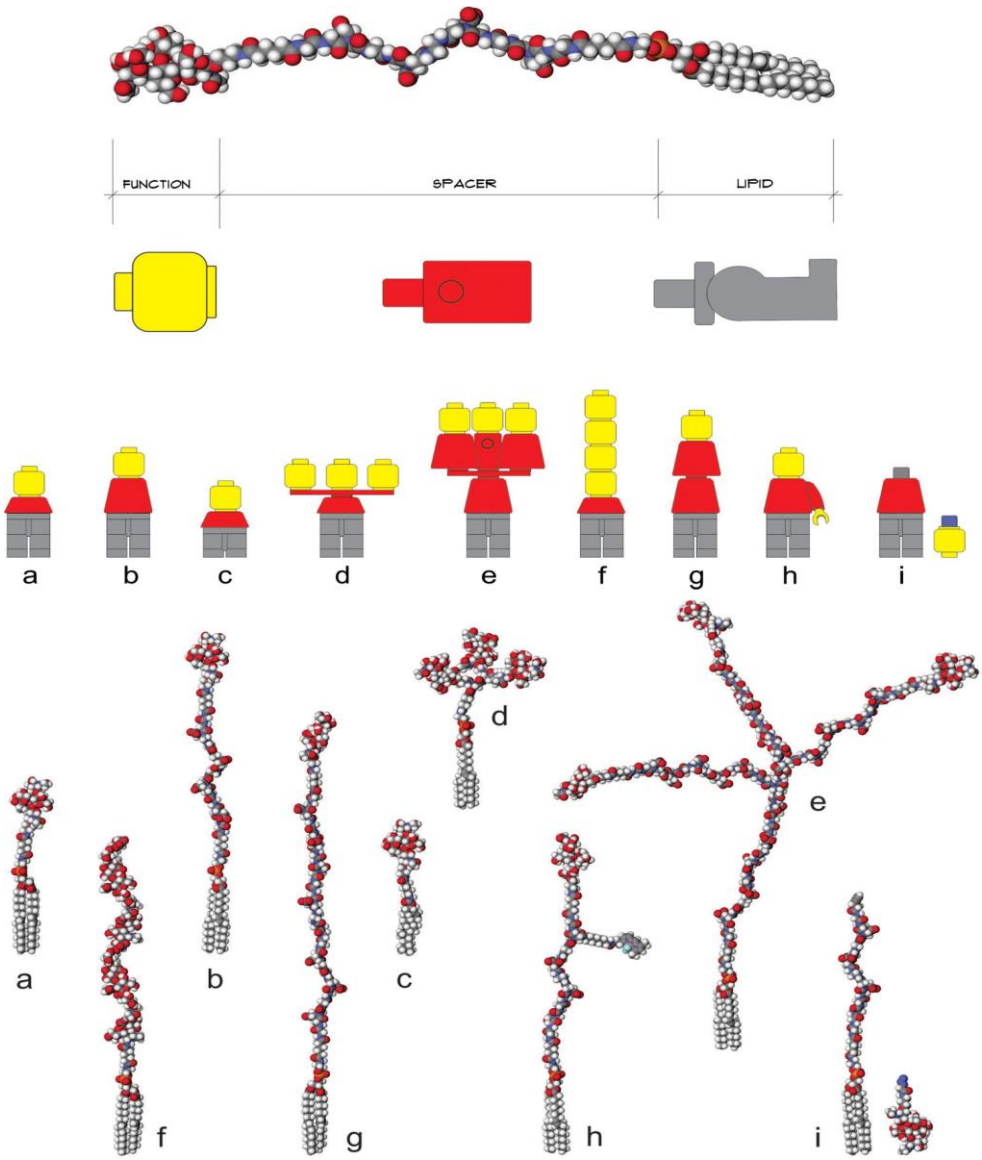

Figure 9. Schematic representation of different Kode function-spacer-lipid (FSL) construct presentations of functional heads. Upper image shows a generic Kode construct based on a carboxymethylglycine spacer linked to a DOPE lipid tail. The 'building block toy figure' representations beneath show a yellow head representative of a single type of functional head, the red body represents a spacer, and the grey legs represent a lipid tail. The 9 structures shown at the bottom of the figure are space-filling molecular models of the building block toy figures with each having the same tetrasaccharide blood group A functional head except model f which has an (8-mer) hyaluronic acid functional head. Variation representations shown are (a) short 1 nm adipate spacer, (b) CMG 7 nm spacer, (c) sterol lipid instead of DOPE, (d) clustered head, (e) trimeric CMG spacer, (f) linear repeating functional heads, (g) double CMG spacer and (h) functionalized CMG spacer where the spacer can undertake a secondary function, in this example, the fluorophore BODIPY is attached, (i) secondarily attached functional head, which is this case uses click coupling chemistry. Reproduced with permission of Kode Biotech [227].

The change of functionality of a surface using a FSL construct has been well established. These molecules were initially designed to attach blood group glycans to red blood cells and have been expanded to modify many cells, viruses, zebrafish, embryos and liposomes[227,229].

Surface modification with FSL technique uses simple, easy to use procedures to label the desired component onto any surface. For example, biotinylation of any surface can be done within minutes using this technology to bring about the desired effect[230]. Similarly, surface coating of FSL molecules had led to various other applications including diagnostic and quality control systems. For example, surface coating of RBC with FSL was used as a model to mimic blood groups, and to neutralise circulating antibodies in incompatible transfusion in animals models[231]. FSL incorporation ability has also led to the spontaneous insertion of monospecific antigen on the erythrocytes that can be used for routine serological methods to map monoclonal and polyclonal blood grouping reagents[232].

FSL surface modification of microorganisms is proven with biotin, and fluorescein isothiocyanate (FITC), functional group attachment to viruses and bacterial surface. Influenza virus labelling with two different FSL has shown the integration of the construct into the cell membrane, without significantly affecting the virions ability to bind to the target[233]. Similarly, bacterial labelling with FSL-Biotin (FSL-Bn) has shown that both gram-positive and gram-negative bacteria can be biotinylated. Such modifications on microorganisms also indicate the possibilities of an antimicrobial FSL to attack the bacteria by attaching directly to the microbial surface. This technology has been applied in the attachment of synthetic molecules to almost any non-biological surfaces such as silica, nitrocellulose, plastics and stainless-steel surfaces which implies the possibility of coating an antimicrobial molecule on to medical surface[234,235].

FSL surface coating is a passive, generally harmless modification brought about by the hydrophobic lipid tail and/or hydrophilic spacer for adding a functional component onto the surface and can be further modified after attachment with other compounds. This amphiphilic molecule self assembles on to any surface, mediated by both the hydrophobic lipid tail and hydrophilic spacer[235]. Based on this ability, FSL constructs have the potential immobilise an antimicrobial functional head on to dressing material or stainless-steel surfaces to prevent bacterial infection. Figure 10 shows the possibility of labelling a surface with an FSL molecule that may not be possible in the absence of the molecule. Metals surfaces which could serve as an implant material have already been proven to be modified using this technology[234].

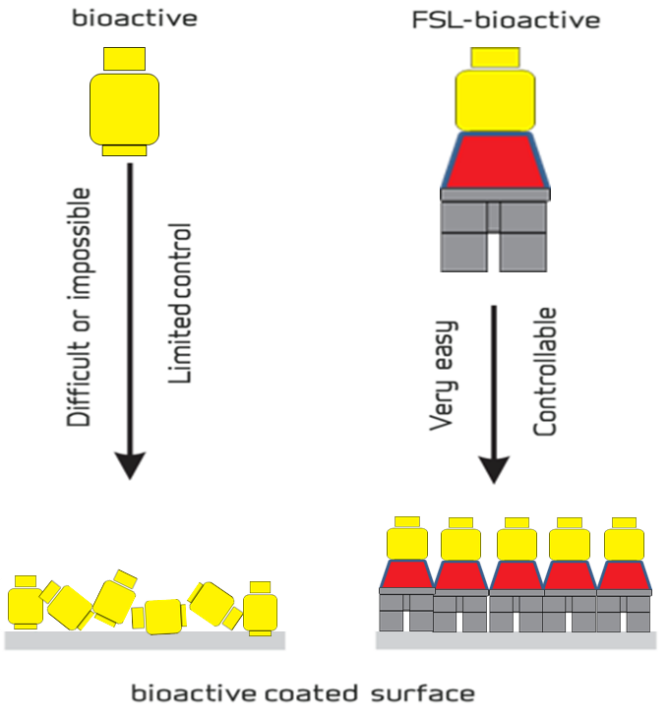

Figure 10. Representation of possibility of bio-functionalising a surface with an FSL construct.

1.8 Potential advantages of using an FSL molecule to render a surface with antimicrobial features

Preventing the early establishment of infection acquired during surgery is the most critical target in preventing failure of implant surgery. That is, if the surface gets contaminated during surgery, and can self sterilise itself that would prevent infections being able to stop the race before its begins. There are many possible approaches which may provide a template for a new group of antimicrobials. In this research RIP, crystal violet, silver, selenium and spermine with Kode technology enhancement were considered for their ability to prevent biofilm establishment on surfaces.

- FSL constructs can modify almost any surface including those surfaces known to be used in surgical procedures. Surfaces such as titanium, silicone,plastics, stainless steel are common implant materials that have previously been modified with FSL construct.
- FSL can potentially be made into a range of FSL-antimicrobial constructs.
- FSL constructs are capable of bearing one or more functional moieties and can secondarily associate with other bioactive compounds.

1.9 Aims

The primary goal of this PhD was to develop Kode Technology based antibacterial coating for the prevention of bacterial adhesion and biofilm formation on medical device surfaces. The strategies followed in this project, were:

- Establish the ability of FSL constructs to coat medical device surfaces (e.g. dressing synthetic fibres, stainless steel (SS) and silicone)
- Develop a range of different FSLs with antimicrobial/ antibiofilm activity
- Evaluate the efficacy of these FSLs against representative microorganisms (*S. aureus*, *S. epidermidis*, *E. coli* and *P. aeruginosa*)
- Determine antimicrobial activity (solution phase/ solid phase)
- Determine and optimise antibiofilm activity (solid phase)
- Develop a prototype product with antimicrobial/antibiofilm features

Chapter 2 FSL baseline experiments

The main objective of this research was to establish if antimicrobial FSLs can prevent bacterial growth and biofilm formation. Before this could be determined, a series of baseline experiments were undertaken to assess the ability of the FSL construct to adhere to biological and non-biological surfaces. Later the research focuses on the performance of antimicrobial FSLs on bacterial growth and biofilm formation on dressing material and stainless-steel as a model for topical and implant surfaces respectively.

2.1 FSL constructs used

2.1.1 Benign FSL

The ability of FSL constructs to modify both living and non-living cells has already been established[234]. However, standardisation of modification on each surface used is essential. A series of baseline experiments were carried out to demonstrate the ability of FSLs to modify surfaces using benign easily measurable FSLs such as FSL-Bn and FSL-FLRO4. These constructs have been widely used for functionalisation of RBC, virions and other non-biological surfaces. The modifications brought about by these molecules can be readily visualised either by using an enzyme conjugate or by direct fluorescence.

FSL-Bn consists of a biotin functional head, a carboxymethyl glycine (CMG) spacer and a DOPE lipid tail as illustrated in Figure 11. FSL with biotin as the functional head but variation in the lipid tail, such as ceramide was also used for specific experiments (FSc-biotin).

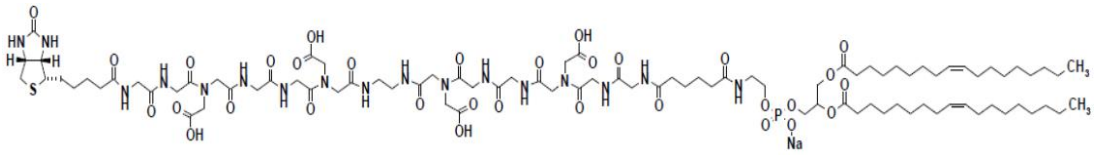

Figure 11. Schematic diagram of an FSL construct presenting a biotin functional head linked to the spacer CMG and a DOPE tail.

FSL -FLRO4 consists of a fluorescein isothiocyanate function head (FITC), short adipate spacer and a DOPE tail as shown in Figure 12.

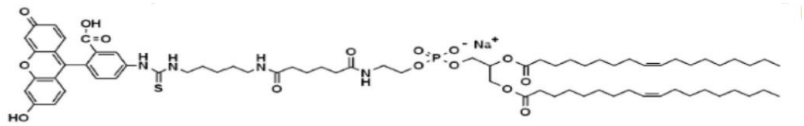

Figure 12. Schematic diagram of FSL-FLRO4 with functional FITC head, an adipate spacer and DOPE tail.

2.1.2 FSL -Zero (FSL-Z)

FSL-Zero (FSL-Z) is an FSL construct with a minimal (NH_2) functional head on a CMG spacer and DOPE lipid tail were also utilized in this research to render the surface with a negative charge (Figure 13).

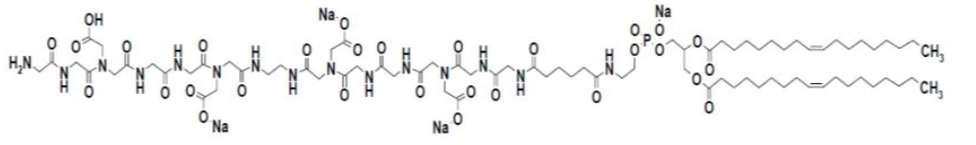

Figure 13. Schematic representation of FSL-Z with a minimal NH_2 functional group a CMG spacer and DOPE tail.

2.1.3 Bioactive antimicrobial FSLs

Antimicrobial coatings are required to have an antimicrobial activity. FSLs with potential antimicrobial/antibiofilm functional heads selenium, spermine and RIP were specifically built for this research by Shemyakin and Ovchinnikov, Institute for Bio-organic chemistry, Moscow, Russia.

a) FSL-Selenium (FSL-Se)

Selenium has shown to be a source of the antimicrobial and antibiofilm agent, for controlling the growth of pathogenic bacteria[169,175,182,236]. FSL-Selenium (FSL-Se) based on a negatively charged carboxymethyl glycine (CMG) spacer and DOPE lipid tail was constructed as illustrated in Figure 14.

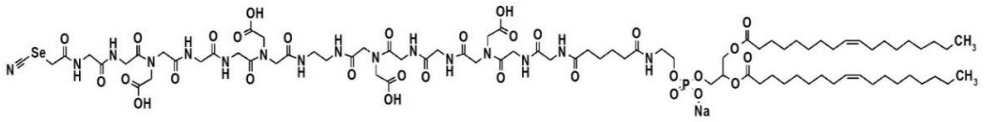

Figure 14. Representation of FSL-Se with a selenium functional head, CMG spacer and a DOPE lipid tail.

b) FSL-Spermine (FSL-SPM)

Spermine was also considered for construction of an antimicrobial FSL due to its ability to reduce and inhibit the growth of microorganisms on surfaces[197,198].

Spermine was incorporated as the functional head of an FSL along with a DOPE lipid tail and an adipate spacer Figure 15.

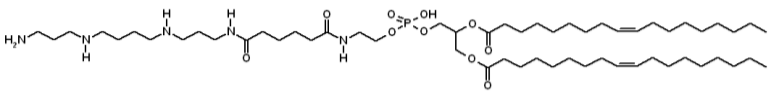

Figure 15. Representation of FSL-SPM with DOPE tail, adipate spacer and spermine functional head.

c) FSL-RNA III inhibiting protein (FSL-RIP)

The heptapeptide RIP (YSPWTNF-NH2) has been established to have antimicrobial and antibiofilm activity[104] . An FSL construct with RIP peptide head, a CMG spacer and DOPE tail was constructed as shown in Figure 16 .

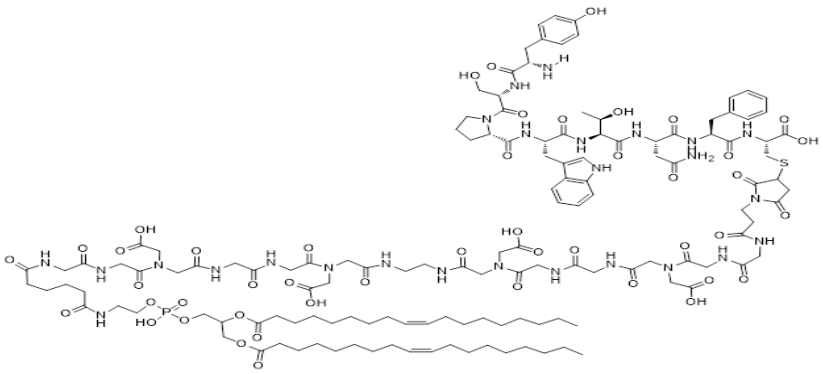

Figure 16. Schematic diagram of FSL-RIP constructs with a function RIP peptide, CMG spacer and DOPE tail.

2.2 Zeta potential of FSL constructs

The charge of the antimicrobial surface coating could influence the bacterial mobility. Hence estimating the charge of the construct was important.

FSL-Se, FSL-Bn and FSL-Z were considered to be negatively charged due the presence of the negatively charged CMG spacer. FSL-SPM was considered positively charged due to the presence positively charge amine. To establish this zeta potential analysis was carried out on the FSL constructs used. Zeta potential is the measure of electro kinetic potential and is caused by the net electrical charge of the dispersed particle. In this study the primary purpose was to verify the electrical charge of the FSL construct in water, in which FSL constructs were to be dissolved.

Methodology

FSL constructs were prepared at 0.5 mg/mL in water and analysed for Zeta potential using a Malvern Zeta sizer Nano ZSP at 25 ˚C. For the analysis the sample was prepared in the desired concentration and slowly filled into the cell covering the electrode. The zeta potential measurement was taken immediately.

Results and interpretation

The zeta potential for the FSL constructs prepared in water is shown in Table 5. The Zeta potential results reveal as expected FSL-Se, FSL-Bn and FSL-Z are negatively charged (due to the presence of CMG spacer), and FSL-SPM positively charged (due to presence of positively charged functional head). This experiment confirms the charge on the construct although dilutions were not analysed in order to obtain an accurate interpretation as suggest by Tantra et. al.[237].

Table 5. Zeta potential of FSL constructs

FSL construct	mV
FSL-Se	-26.7
FSL-SPM	19.5
FSL-Bn	-25.5
FSL-Z	-30.1

2.2.1 Microorganism interaction with FSL

a) Bacterial cultures used

The strains of bacteria used in this study were originally clinical isolates stored at - 80 ˚C. *S. aureus, S. epidermidis, E. coli* and *P. aeruginosa* were confirmed by culturing on Columbia sheep blood agar followed by gram staining, oxidase and catalase reaction. The results of quality control testing are shown in Table 6.

Table 6. Conformation of identity of clinical isolates.

	Haemolytic activity	Gram staining	Catalase activity	Oxidase Test
S. aureus	Positive	Positive cocci	Positive	Negative
S. epidermidis	Negative	Positive cocci	Negative	Negative
P. aeruginosa	Positive	Negative bacilli	Positive	Positive
E. coli	Negative	Negative bacilli	Positive	Negative

b) Bacterial cultivation

One colony of each bacteria were inoculated onto 100 mL of Mueller Hinton (MH) broth for 24 hr. These 24 hr culture were stored at - 80 ˚C with equal volumes of glycerol prepared from stock glycerol (Sigma-Aldrich, USA) to give a 15% final concentration of glycerol. These cultures were stored until required. Bacterial inoculum of the desired strain were prepared by streaking a loop of bacterial culture, retrieved from - 80 ˚C, on to Columbia sheep blood agar (Fort Richard Laboratories, NZ). Plates were then incubated (Sanyo CO_2 incubator) at 37 ˚C overnight.

Fluorescent staining of bacteria and yeast with FSL-Biotin (FSL-Bn)

A preliminary experiment of FSL insertion onto bacterial surfaces was carried out. This was done to study the interaction between FSLs and the microorganisms. Previously reports shown preliminary data of microorganism and FSL interaction by K. Barr[234]. Similar protocol was followed and all the four -microorganisms used were tested for FSL-Bn insertion.

Methodology for FSL modification of bacteria

One colony of bacteria grown on Columbia sheep blood agar was placed in 50 µL of 0.13 mM FSL-Bn and mixed well by vortexing for 30 sec. The cultures were incubated at 37 ˚C for 2 hr and washed three times in PBS by centrifugation at 10,000 RPM for 1 minute. To the pellet 20 µL of streptavidin -AlexaFluor ® 0.1mg/mL in PBS, (Life Technologies, USA) was added, then vortexed for 30 seconds and incubated at 37 ˚C for 30 minutes. The pellet was washed three times in PBS and finally reconstituted with 50 µL of PBS. Then 2 µL of cell suspension was placed on a clean slide and visualised under the fluorescence microscope at 488 nm excitation wavelength (Olympus Fluorescence microscope BX 51) and unlabelled controls were included.

Results and interpretation

Immunofluorescent staining using streptavidin AlexaFluor ® confirmed the attachment of FSL-Bn on the bacterial surface when visualised using fluorescent microscopy. No fluorescence with the controls was noted. Figure 17 results show clear evidence of FSL attachment to both gram-positive cocci and gram-negative bacilli irrespective of the large difference between the lipid composition of their cytoplasmic membranes.

These results demonstrate the ability of FSLs to attach to both gram-positive and gram-negative bacteria. Similarly, it is expected that when antimicrobial FSLs are used, they will also attach to the bacterial membrane. In this scenario FSL labelled bacteria may actually kill bacteria adjacent to themselves as well as themselves.

2.3 FSL constructs interaction with biological surfaces

Biological surfaces such as bacteria and yeast causes implant infection and FSL with covalent antimicrobials need to come in direct or very close contact with these microorganisms to have an antimicrobial effect. To understand if there is a consequence of such interactions, independent of the bioactive head, benign FSLs were used to examine the interaction of FSL with bacteria and yeast without intrinsic antimicrobial activity.

Gram-positive

S. aureus

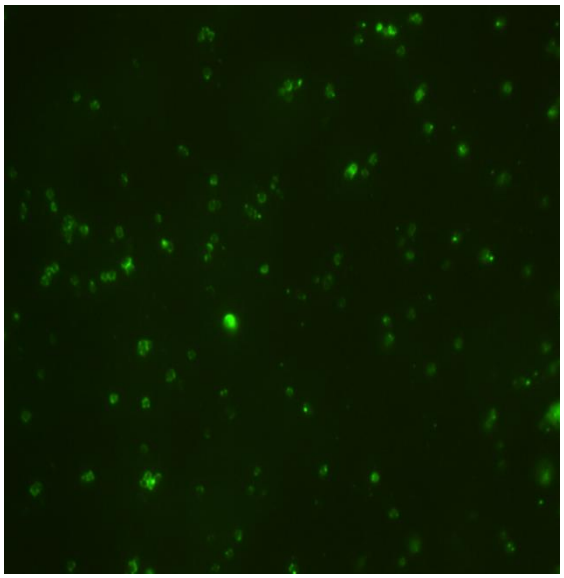

Gram-negative

P. aeruginosa

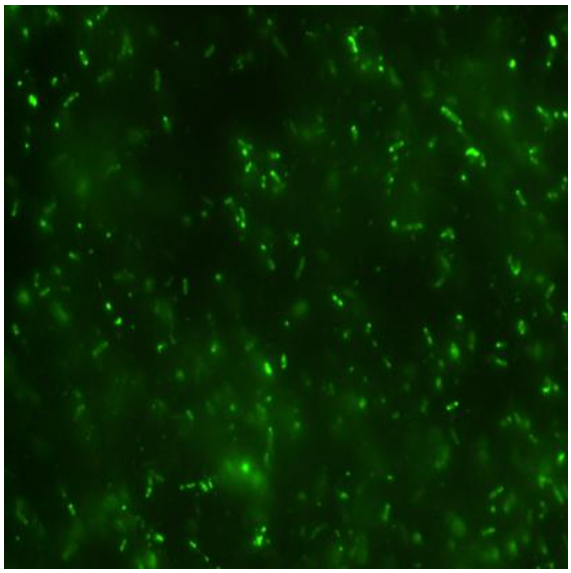

Figure 17. Attachment of FSL-Bn on the surface of both gram-positive *S. aureus* and gram-negative bacilli *P. aeruginosa* detected by immunofluorescence. All cells were first labelled with FSL-Bn for 2 hr at 37 ˚C washed and wet mounted for fluorescence microscopy after being reacted with fluorophore labelled streptavidin. Magnification x1000

2.3.1 Single-celled fungi

Yeast, like bacteria causes implant infections[238]. It was important to consider yeast cells interaction with benign FSLs to obtain the possibility of antimicrobial FSL coating on yeast cells. *Saccharomyces cerevisiae* were chosen as a model eukaryotic surface for FSL interactions followed by *Candida albicans* and *Rhodotorula sp.*.

Methodology

Saccharomyces cerevisiae, Candida albicans, Rhodotorula were treated with FSL-Bn to estimate the ability to modify eukatryotic surfaces. Yeast cells were cultured at 25˚C in Sabouraud Dextrose (SAB, Fort Richard Laboratories, NZ) agar for 48 hr (kept alive with periodic sub culturing). One yeast colony was washed in PBS, and a 6% yeast cell suspension was prepared in PBS. 50 µL of 6% yeast suspension was then treated with 0.48 mM FSL-Bn incubated at 25 ˚C for 2 hr. Treated cells were washed in PBS and then treated with 40 µL of avidin AlexaFluor ® 0.1 mg/mL in PBS, (A-21370, Invitrogen) for 30 minutes before visualization under fluorescence microscopy. Unlabelled control surfaces were included.

Results and interpretation

Unlike bacterial labelling with FSL-Bn, yeast cells were not readily labelled with the FSL-Bn construct. Figure 18 (A) shows clear evidence of the failure of FSLs to label the entire surface of yeast cells. However, results demonstrate that FSL-Bn was deposited in specific regions of the yeast cells. Of note, fluorescence was detected only at high exposure of nearly 3 seconds indicating poor labelling. It is already established that the lipid tail of the FSL constructs facilitates attachment onto the cell surface and other non biological surfaces[239,240]. Therefore, it was investigated if a variation in the lipid tail of FSL constructs could produce a better labelling effect. FSL constructs with different lipid tails such as ceramide, at a similar concentrations to that of the DOPE tail was used. The results suggest that the ceramide lipid tail can be more favourable than DOPE Figure 18 (B), but again it did not result in labelling of all the yeast cells present. No fluorescence was detected on control surfaces.

FSL-Bn treatment of other fungi such as *Candida albicans* and *Rhodotorula sp.* was assessed and demonstrated similar results as seen on *Saccharomyces cerevisiae.* Our results showed the inability of FSL to label all fungi tested, since fluorescence was seen in only specific regions, as shown in Figure 19 .

FSL-Bn (DOPE)

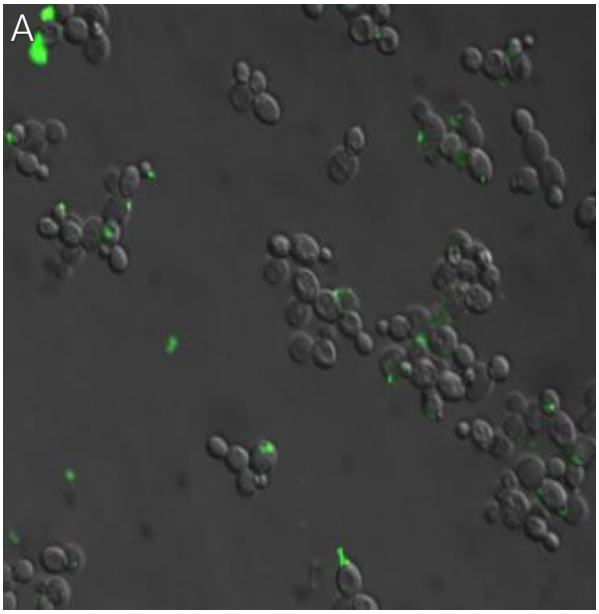

FSc-biotin

(ceramide)

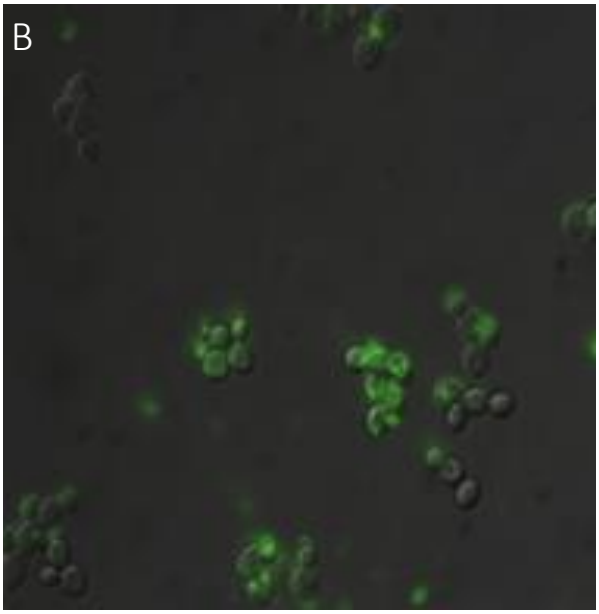

Figure 18. Superimposed fluorescent images onto DIC images to show FSL labelled regions of *Saccharomyces cerevisiae.* (A) Fluorescence displayed on a specific region of the cell when labelled with FSL-Bn (DOPE). (B) Better attachment was noted with a variation of the lipid tail from DOPE to ceramide. However, it did not result in labelling all the cells.

Candida albicans

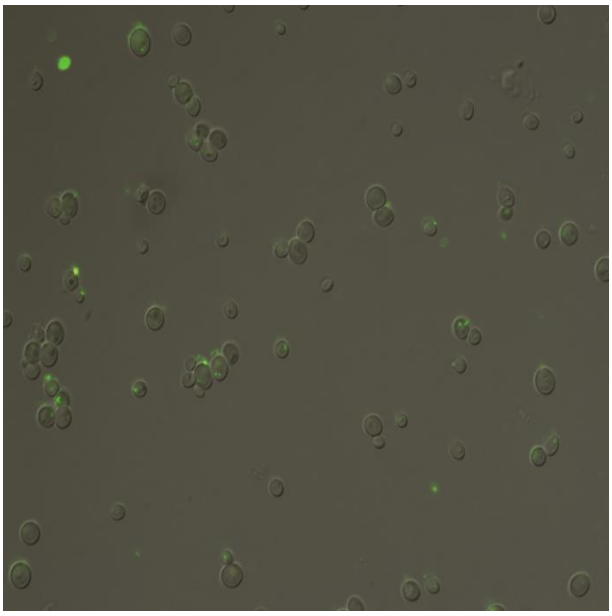

Rhodotorula sp.

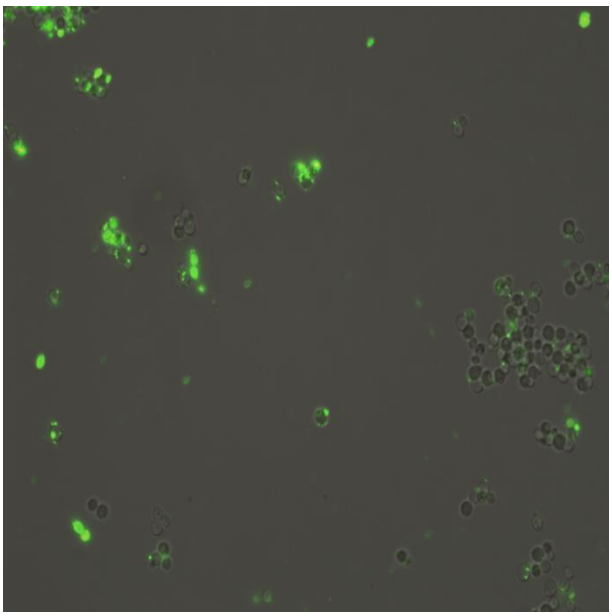

Figure 19. DIC and fluorescent images superimposed to identify the labelling of FSL-Bn on *Candida albican*s and *Rhodotorula sp*. The results show fluorescence at specific regions of the fungi.

Extensive further experiments of treating the surface of the yeast were undertaken such as treatment with acetic acid, ethanol, citric acid etc. However quality labelling of yeast cells could not be established and the reason for poor labelling was unknown. However, the labelling appeared to be associated with the bud scars. Although the fungi memebrane did not label the ability of the FSL to impart an antimicrobial effect when present on a surface is still valid.

2.4 Non-biological surfaces labelling with benign FSL

Non-biological surfaces such as BAND-AID®, implants and contact lens can serve as surfaces for bacterial dwelling and biofilm formation. Investigating the ability of FSL to interact with these surfaces was crucial before proceeding with examining the efficacy of antimicrobial FSL on microorganisms, biofilms and its ability to inhibit biofilm formation.

2.4.1 BAND-AID®

a) Binding characteristics

The binding of FSL on to surfaces depends on various factors such as surface hydrophobicity or hydrophilicity and is also influenced by many forces including hydrogen bonding, Van der Waals and electrostatic forces[241]. While strength of coating depends on various factors such as dose, contact time, the method of layering, thickness of layer (single or multiple) and stability against solvent system used and environmental factors like plasma[230]. Hence considering these factors that influence attachment and strength it was essential to optimise the labelling of FSLs with each surface used.

Methodology for streptavidin conjugated staining for biotin molecules (Enzyme assay EA)

A sensitive staining method for FSL-Bn on the surface, streptavidin conjugated to alkaline phosphatase was used. The high affinity of streptavidin to biotin makes this extremely sensitive reaction for the detection of FSL-Bn on the surface[234].

After FSL-Bn labelling, surfaces were blocked with 2% bovine serum albumin (BSA) (Gibco, 30063572, USA) in phosphate buffered saline (PBS) for 1 hr. Streptavidin conjugated to alkaline phosphatase (S2890-250UG, Sigma, USA), diluted in 2 % BSA to 1 µg/ mL, was incubated for 30 minutes at room temperature. Surfaces washed six times in PBS. NBT/NCIP substrate (nitro-blue tetrazolium chloride and 5 -bromo-4 chloro-3'-indolyphospate p-toluidine salt, 11681451001, Roche, Germany), diluted in Tris substrate buffer (100 mM Tris, 100 mM NaCl, 50 mM $MgCL_2$) and flooded onto the surface for colour development (precipitate). The reaction was stopped by washing in tap water for ablour 2-5 minutes.

(i) Molar concentration

In this section, experiments were carried out to determine the minimum amount of FSL detectable on BAND-AID® (Johnson & Johnson BAND-AID®, Plastic, Quilt-AID technology) surfaces.

Methodology overview

A series of dilutions of FSL-Bn from 0.2 µM to 48 µM was prepared in PBS, 3 µL of each concentration were contacted with BAND-AID® for 10 minutes and visualised using the enzyme assay as described above.

Results and interpretation

As can be seen in Figure 20, the FSL spot was readily detectable at 0.4 µM/mL and higher concentrations of FSL-Bn (not shown). However at 0.2 µM, the result was negative/ weak suggesting a minimum of 0.4 µM concentration of FSL constructs is required to be detectable on BAND-AID® surfaces. The effect of darkening increased by increasing the concentration of FSL-Bn.

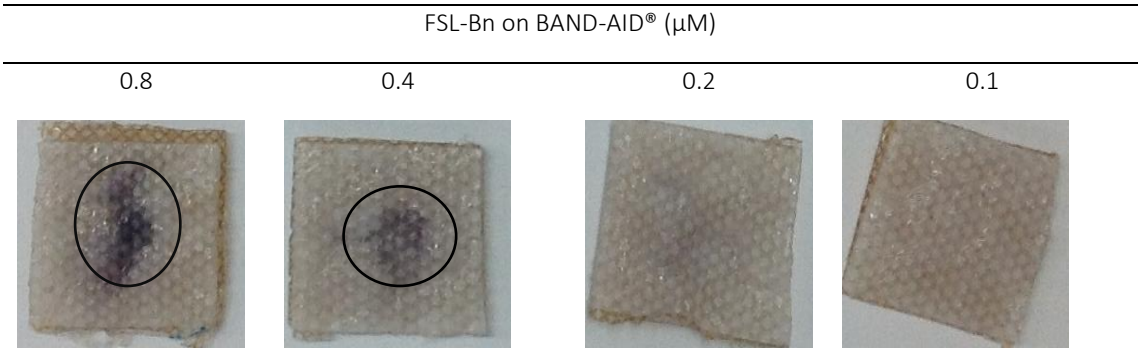

Figure 20. The minimum detectable concentration of FSL-Bn when applied as a 3 µL spots on BAND-AID® surfaces. Clear purple staining on the surface is detected at 0.4 µM of FSL-Bn. The detectable colour change on the surface is denoted by a circle.

(ii) Stability on PBS washing of labelled surfaces

Estimation of stability of the FSL construct with the surface is essential. To evaluate the strength and mechanism of binding, FSL-Bn labelled surfaces were exposed to diluent systems such as PBS. Influence of increased number of washing FSL labelled surfaces with PBS was also determined.

Methodology overview

To establish the stability of the interaction of the molecule with the surface, BAND-AID® surfaces were labelled with 3 µL of 0.4 µM, left in contact for 10 minutes and then washed in PBS from one to five times before interaction with phosphatase labelled streptavidin.

Results and interpretation

The results in Figure 21 show the coating of FSL-Bn was present even after five washes. The analysis confirmed the distribution of the FSL construct across the surface, as well as the durability of the attachment. However, increase in the number of times the labelled surface was washed with PBS resulted in smudging of the construct onto the surface, which is potentially due to dislodging layers, which then interacts with unlabelled areas [239].Results almost suggests better results with one wash with PBS. The greater number of washes would distribute the FSL as shown in the figure below.

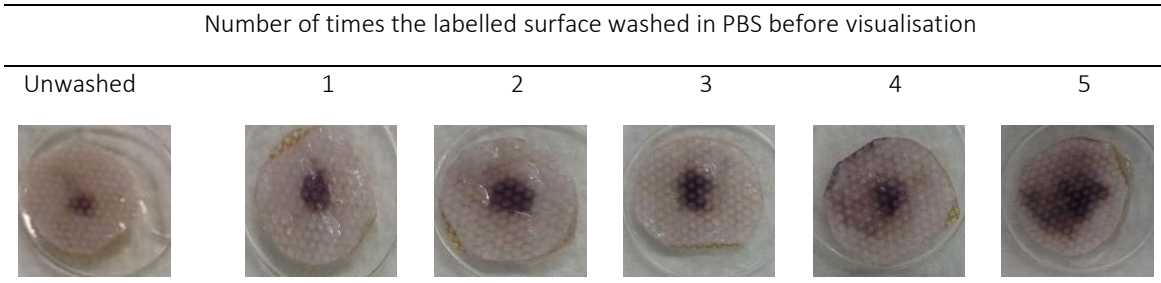

Figure 21. Effect of the number of PBS washes of FSL construct labelled surfaces.

(iii) FSL stability on solvent washed labelled surfaces

Methodology Overview

The stability of FSL-Bn construct on the surface was evaluated by exposing labelled BAND-AID® to varying solvent systems in comparison with PBS. Surfaces were labelled with 3 µL of 0.4 µM FSL-Bn, left in contact for 10 minutes and soaked in either 1 mL of water or PBSor 70% acetone, 70 % methanol or 70% ethanol. After five minutes of exposure, the surface was washed with water and treated by enzyme phosphatase labelled streptavidin.

Results and interpretation

Results show exposure with solvents minimally disrupts the binding of FSL onto the surface. Figure 22 demonstrates that 70% of ethanol partially elutes FSLs from the surface in comparison to water and PBS.

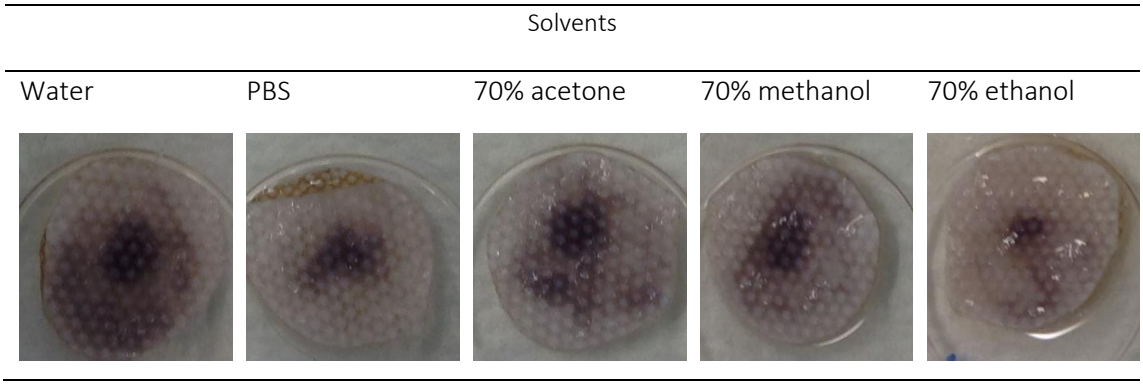

Figure 22. Elution of FSL construct on BAND-AID® material exposed to water, PBS and 70% acetone, 70% methanol and 70% ethanol. Swatches are stained to visualise the presence of remaining construct.

Further investigation on the effect of exposure of FSL-Bn labelled surfaces to 70% ethanol from 5 minutes to 20 minutes were investigated. Only minimal changes in staining is visible even in comparison with 70% ethanol in contact with labelled swatches for increased contact time with the surface Figure 23.

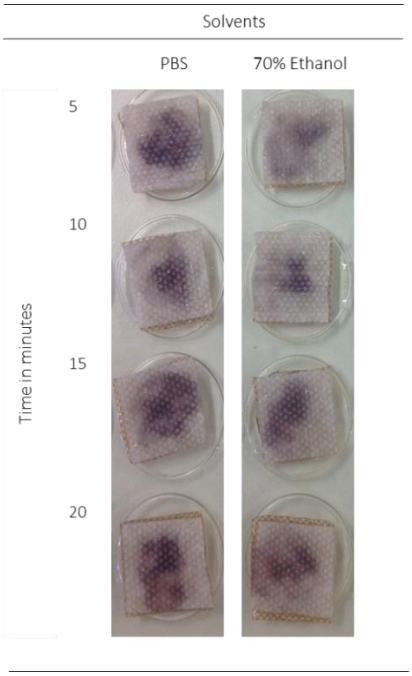

Figure 23. Binding stability of FSL constructs on BAND-AID ® in the presence of ethanol.

2.4.2 Contact lens surfaces

Contact lenses are often associated with a high risk of microbial keratitis[242]. Development of an antimicrobial coating on contact lenses could prevent eye infection. Preliminary studies were performed to investigate the ability of FSL-Bn and FSL-FLRO4 coating on contact lenses, as a baseline for antimicrobial coating and as a surrogate for other medical silicone surfaces.

Methodology overview

An artist's brush cleaned with 70% ethanol was used to paint one half of a 1•DAY ACUVUE® TruEye® Brand silicone contact lenses of FSL-Bn. Left at room temperature for 10 min. The surface both painted and unpainted regions were visulaised with the enzyme assay using streptavidin phosphatase conjugate. Additionally, 48µM FSL-FLRO4 was used for direct fluorescence microscopy.

Results and interpretation

Purple precipitate indicated the ability of FSL-Bn to bind to the coated region of the contact lens caused by the enzyme immune assay. It should be noted that poor adherence of the precipitate to the lenses can also affect the results observed. The presence of the FSL on the surface was also visualised using FSL-FITC and fluorescence microscopy. Figure 24 demonstrate the ability of FSL constructs with two different functional heads to coat contact lens surfaces.

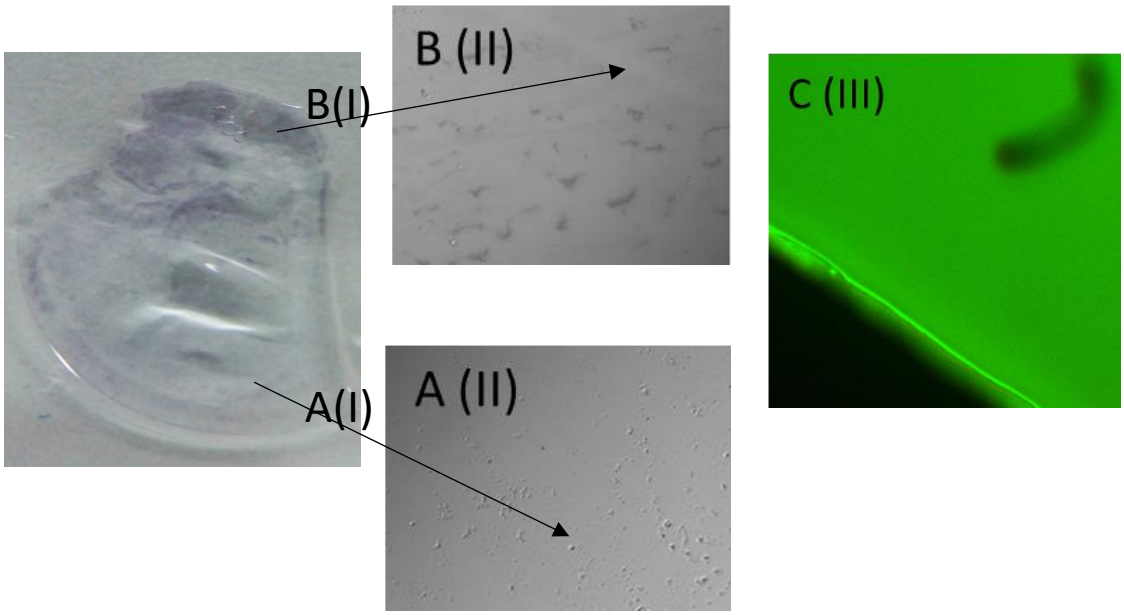

Figure 24. FSL-Bn and FSL-FITC labelled contact lens. (I) Immuno stained FSL-Bn image (II) microscopic image. (III) fluorescent image of FSL-FLRO4 labelled contact lens. (A) FSL uncoated region of contact lens (B) FSL coated region of contact lens showing positive enzyme assay precipitates. (A II) shows no precipitate formation (B II) precipitate is seen.

2.5 Non-biological surface labelling with antimicrobial FSL

In the above section 2.4 benign FSL-Bn were detected on surfaces. The next step was to establish if antimicrobial FSLs could be detected on surfaces. Two antimicrobial FSL's FSL-Se and FSL-SPM were applied on to non-biological surfaces such as BAND-AID®.

2.5.1 Antimicrobial FSL-Se constructs on BAND-AID ® Surfaces

a) Detection on surface

FSL coating on BAND-AID® material was achieved by using drop and dry technique and label of surfaces was detected with crystal violet which binds to the spacer.

Methodology

BAND-AID® surfaces were cut into 0.25 cm^2 squares. To the surfaces 50µL of FSL-Se at 0.13 mM was pipetted and dried at 80˚C (until the surfaces were completely dry) . To detect the negatively charged FSL-Se labelled surface (via its spacer) was treated with 0.04% crystal violet diluted in water for 10 minutes and washed 6* with water. No- FSL, FSL-Bn (which has the same spacer as FSL-Se) and positively charged FSL-SPM were included as controls.

Results and interpretation

The presence of FSL-Se was indicated by capture of the purple dye (Cv). To determine that cationic dye binds to negatively charged FSLs, the surface labelled with other negatively charged FSLs such as FSL-Bn and a positively charged FSL-SPM were used (see table 5).

Figure 25 demonstrates crystal violet binding to FSL surface as a purple colour coating on negatively charged FSL coated surfaces and not on positively charged FSL- SPM. It is of note that the FSL-SPM surface stained less than the uncoated surface (No- FSL) indicating that charge is responsible for the result, and the unmodified surface is able to bind some dye.

FSL-Bn (CMG)	FSL-Se (CMG)	FSL-SPM	No -FSL
			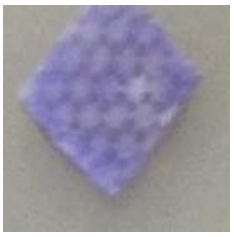
A	B	C	D

Figure 25. Crystal violet binding to negatively charged FSL labelled surfaces. Photograph of the crystal violet capture labelled BAND-AID® (A) negative charge FSL-Se, (B) negative charge FSL-Bn (C) positive charge FSL-SPM (D) unlabelled surface.

b) Stability

Since the surface coating was achieved the next step was to determine the stability of the the coating.

Methodology overview

It is essential to determine the stability and strength of the antimicrobial coating on the surfaces. Therefore, 50 µL of FSL-Se at a concentration ranging from 2 µM- 0.5 mM were placed on BAND-AID® surface and dried at 80 ˚C. One lot of FSL-Se labelled surfaces (2 of each concentration) were washed 6 times in water and compared to surfaces not washed before treating with 0.04% crystal violet solution.

Results and interpretation

Differences in binding were observed with washed and unwashed surfaces (Figure 26). Unwashed surfaces have higher optical densities in comparison to washed surfaces and higher concentrations result in loss from the unwashed surface as seen by reduced optical densities. The amount of crystal violet bound to washed surfaces was reduced, affirming that washing results in removing ablative FSLs from the surface, leaving behind a probable monolayer. The observed reduction of optical density values of unwashed 0.25 mM and above could be attributed to FSLs being washed away when adding crystal violet solution.

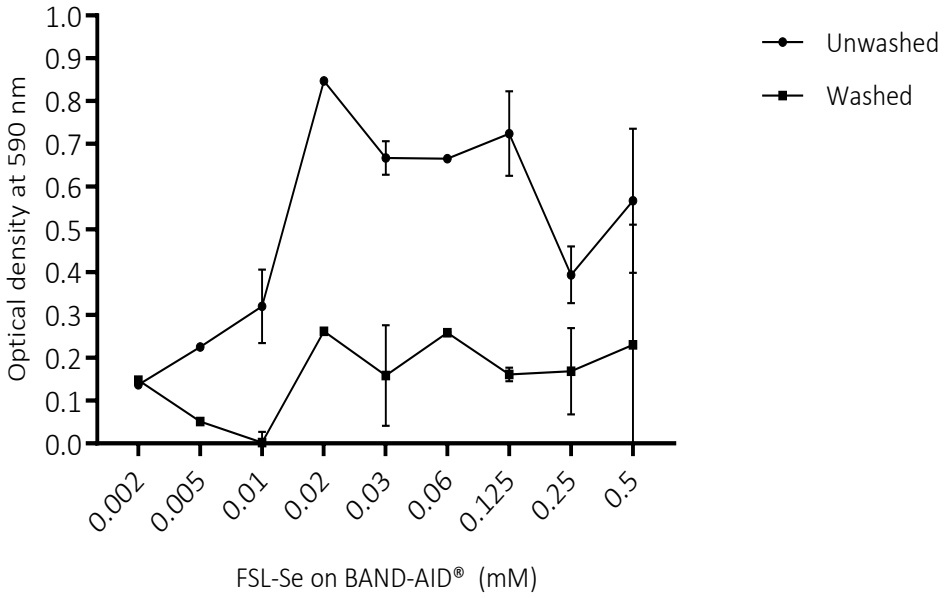

Figure 26. Performance comparison between washed and unwashed FSL-Se labelled surfaces. Unwashed surfaces have higher optical densities in comparison to washed surfaces and higher concentrations result in loss from the unwashed surface as seen by reduced optical densities.

Statistical software graphpad prism software was used to analyse the washed and unwashed FSL-Se labelled surfaces. The statistical significance was determined by the application of Sidak's

multiple comparisons test. Two way Anova yielded a very low p value at 0.02,0.03, 0.06 and 0.125 mM concentration of FSL-Se on unwashed surfaces in comparison to washed surfaces (Table 7). This Indicate that a significant amount of FSL-Se is present on unwashed surface compared to washed surfaces.

Table 7. ANOVA analysis of washed and unwashed FSL-Se labelled surfaces.

Unwashed – washed (mM FSL-Se)	Significance	Adjusted p value
0.002	ns	>0.999
0.005	ns	0.964
0.01	ns	0.146
0.02	*	0.034
0.03	**	0.008
0.06	*	0.035
0.125	**	0.004
0.25	ns	0.504
0.5	ns	0.112

The greater number of * indicate a geater significant difference between the washed and unwashed surfaces. ns=not significant.

c) Wettability of labelled surface

Cell surface characteristics such as surface roughness, surface charge and the composition of material play a critical role in influencing bacterial adhesion[243,244]. Studies have shown that hydrophobicity favours bacterial adhesion and modification of a surface alters hydrophilicity and hydrophobicity of surfaces[245,246]. Surface characteristics such as hydrophilicity or hydrophobicity of FSL modified surfaces can be verified by the capacity of water absorption and contact angle analysis.

(i) Water absorption of labelled surfaces

Methodology

BAND-AID® surfaces were cut into 0.25 cm^2 square. BAND-AID® surfaces were then labelled with 50 µL of 1 mM FSL-Se and dried at 80 ˚C. 5µL of water was then placed on the labelled area and observed by eye for the rate of absorption.

Result and interpretation

A droplet of water remians for about 10 seconds indicating a decrease in hydrophilicity results in decreased absorption in comparison to surfaces that readily absorb water in <1 second. The water droplet as seen as remaining on the surface (Figure 27) shows the change in hydrophilicity

of the FSL-modified surface in comparison with unlabelled surfaces, which readily absorb water. This suggests that FSL-Se modification reduces hydrophilicity.

Table 8. The time water droplet remains on a BAND-AID® surface

FSL-Se	Time (in seconds) droplet remain on surface
Modified surfaces	10
Unmodified surface	<1

FSL-Se labelled surface (1 mM)

Figure 27. Presence of water droplet on FSL-Se labelled BAND-AID® surface. A droplet of water remains for about 10 seconds indicating a decrease in hydrophilicity results in decreased adsorption in comparison to surfaces readility absorb water in <1 second.

(ii) Water contact angle measurement

Methodology

The contact angle measurement of fibrous surfaces like BAND-AID® is difficult, however, measurement of the drop angle overtime was calculated using Attension® complete Theta optical tensiometer by (Bioline Scientific). Water contact angle measurements were used to estimate the wettability of 50 µL of 1 mM FSL-Se labelled surfaces by the sessile drop method. 1 µL of a water droplet on the surface was captured and analysed.

Results and interpretation

Using an optic tensiometer the contact angle for uncoated surfaces could not be determined due the high hydrophilic nature of the unmodified BAND-AID® surface. When using FSL-Se lablelled

surfaces the contact angle increased to 77.9 ˚ and lasted for 0.09 seconds, signifying that the FSL-Se altered the surface properties resulting in a noticeable decrease in hydrophilicity.

2.5.2 FSL-SPM detection on BAND-AID®

FSL-SPM modified surfaces readily absorbed to the surface and hence the contact angle could not be measured. This signifies that these labelled surfaces were highly hydrophilic. FSL-Se detection on surfaces was carried out using crystal violet while FSL-SPM detection was determined using ninhydrin and negatively charged silver nanoparticles ([-]Agnp). Ninhydrin detection was based on the presence of primary amino group of the spermine functional head of FSL-SPM, while the [-]Agnp method was a charge-based capture detection method.

a) Ninhydrin detection method

Ninhydrin is widely used for the colorimetric estimation of the primary amino group present in compounds and produces a purple colour (Ruhemann's purple) which can be used for estimation[247].

Methodology

BAND-AID® cut into 1 cm^2 circles and labelled with 50 µL FSL-SPM. Surfaces were then dried. To determine the molar range in which FSL-SPM spermine would produce detectable purple colour, a series of FSL-SPM dilutions over a range of concentration 0.05-1.6 mM/ mL were prepared in water. FSL-SPM dried onto the surface and then 0.2% ninhydrin (Applichem, Darmstadt) in ethanol (LabServ, Thermofischer)was sprayed on the surfacce and baked at 100˚C for 1 minute for colour development.

Results and interpretation

Colour development indicates spermine based FSL constructs can interact with ninhydrin and produce colour on the surfaces when applied as a 50µL spot. Presence of ninhydrin on FSL-SPM labelled surfaces indicate as concentration decreases colour development decreases. At 1.6 mM concentration, clear colour development was visualised but at lower concentrations such as 0.1 mM colour development could not be observed (Figure 28).

FSL-SPM (mM)		FSL-SPM (mM)	
0		0.4	
1.6		0.2	
0.8		0.1	

Figure 28. Representation of colour development on labelled FSL-SPM BAND-AID® surfaces by ninhydrin. Presence of ninhydrin on FSL-SPM labeeled surfaces indicate as concentration decreases colour development decreases.

(i) Stability of the FSL-SPM on the surface when washed with water

Methodology overview

The stability of FSL-SPM coating on washed surfaces was evaluated. 1.6 mM FSL -SPM modified surfaces were washed one to three times in DI water. Labelled washed surfaces were then stained with 0.2% ninhydrin solution and dried at 100˚C for colour development.

Result and interpretation

Figure 29 demonstrates the efficiency of FSL-SPM binding of the surface unaffected by the number of times a surface is being washed after labelling.

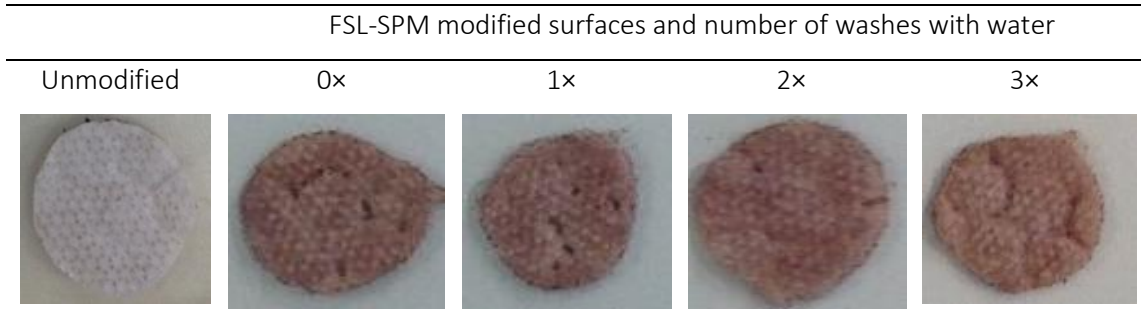

Figure 29. The photographic image showing FSL-SPM on BAND-AID® after different washing regimes and stained with 0.2% ninhydrin solution. The colour produced on the surface remains unaffected with an increased number of washes indicating high adhesion of the molecule to the surface.

(ii) Stability of FSL-SPM on surfaces when in contact with PBS, alcohol and acetone.

Methodology overview

The effect retention of FSL-SPM and free SPM (spermine) to surfaces when in contact for 5 minutes with various such as water, PBS, 70% methanol, 70% ethanol or 70% acetone was evaluated. FSL-SPM labelled surfaces after immersion in solution were rinsed in water before dipping to remove excess solution/solvent before being stained with ninhydrin solution. Unlabelled and free SPM labelled surfaces were included as controls.

Results and interpretation

Water did not affect the binding ability of FSL-SPM, as colour was observable on surface, but efficiently removed free SPM control from the surfaces. SPM control on the surface was completely removed by solvent washing as shown in Table 9. However, 70% of methanol, 70% ethanol and 70% acetone affected the retention of FSLs on the surface, unlike PBS that retained FSL even after 5 minutes of exposure.

Table 9. Elution profile of FSL-SPM when exposed to water, PBS and 70% methanol, 70% ethanol, 70% acetone for 5 minutes. The reduction in colour after exposure to solvents revealed its ability to remove FSL from the surface when compared to water and PBS. Presence of colour on the surface is denoted by +, and – denotes no appearance of the colour on the surface. +/- denotes a faint colour on the surface.

	Solvent system used					
	Unwashed	Water	70 % methanol	70 % ethanol	70 % acetone	PBS
Unlabelled	-	-	-	-	-	-
SPM 0.5 mM	+	-	-	-	-	+
SPM 0.4 mM	+	-	-	-	-	+
FSL-SPM 1.6mM	+	+	+/-	-	+/-	+
FSL-SPM 0.8 mM	+	+	-	-	+/-	+
FSL-SPM 0.4 mM	+	+	-	-	+/-	+
FSL-SPM 0.2 mM	+	+	-	-	+/-	+

b) Silver nanoparticles detection method

The second charged based detection method was by using [-]Agnp to detect positively charged FSL-SPM surfaces. [-]Agnp dispersed in water were used for visual detection of positively charged FSL-SPM coated surface. In house nanoparticles were syntheised for the following experiments as per the methodology mentioned by Poudyal.

[-]Agnps were synthesised using the following protocol

2 g of glucose and 1 g of PVP was dissolved in 40 mL of MilliQ water and heated to 90°C. 0.5 g of silver nitrate ($AgNO_3$, >99.9% pure) was dissolved in 1 mL MilliQ water and was quickly added to the heated mixture. The appearance of brown colour indicated the formation of [-]Agnp. The dispersion was kept at 90°C for 1 hr and then kept to cool at room temperature. The particles were collected by centrifugation at 7200 rpm for 90 minutes for three times. The centrifuged particles were suspended in MilliQ water to remove excess glucose NO_3^- oxidation products, excess PVP and Ag^+. (Ultracentrifugation at 30,000 rpm for 30 minutes is preferred but this alternative was chosen in the absence of ultracentrifuge).

[+]Agnps were synthesised using the following protocol

1 g of polyethyleneimine (PEI) was dissolved in 40 mL of water and heated to 90°C. 0.5 g $AgNO_3$ was quickly added to the mixture and the dispersion was kept at 90°C for 1 hr. Since the particles did not settle down as quickly as [-]Agnp, the suspension was diluted almost 5 times before centrifuging using MilliQ water and centrifuged at 7200 rpm for 120 minutes three times. Final suspensions were kept at 4°C, covered with aluminium foil to protect from light.

Methodology

FSL-SPM on surfaces rendered a negative charge to the surface due to the cationically charged spermine. The capture of positively charged silver nanoparticles by FSL- SPM labelled surfaces could be visualised on the surface and efficiency estimated colorimetrically. Surfaces labelled with FSL-SPM (as described in after washing three times in DI water were placed in one mL of seven per cent [-]Agnp prepared from the suspension stored in the fridge. These 0.25 cm^2 BAND-AID® swatches were incubated at room temperature shaking for one hr. For colorimetric estimation the remaining liquid in the 24 well plates was read at 424 nm optical density FSL-SPM capture of negatively charged silver nanoparticles was estimated at 424 nm and 0.25cm^2 FSL-SPM labelled surfaces were washed three times before placing in 7% silver nanoparticle solutions, shaking for 1 hr. BAND-AID® surface removed from the solution and optical density (OD) of the remaining solution was estimated.

Results and interpretation

Visual detection

BAND-AID® removed after 1-hr incubation were visualised for a colour change on the surface. Silver nanoparticle adsorption was seen in 0.03-0.13 mM of FSL-SPM labelled surfaces with an increasing concentration of above 0.25 mM, there is no absorption of silver nanoparticles indicated by no colour change (Figure 30). FSL -SPM above 0.25 mM concentration could not be detected on the surface and probably washed when placed in silver nanoparticle solution.

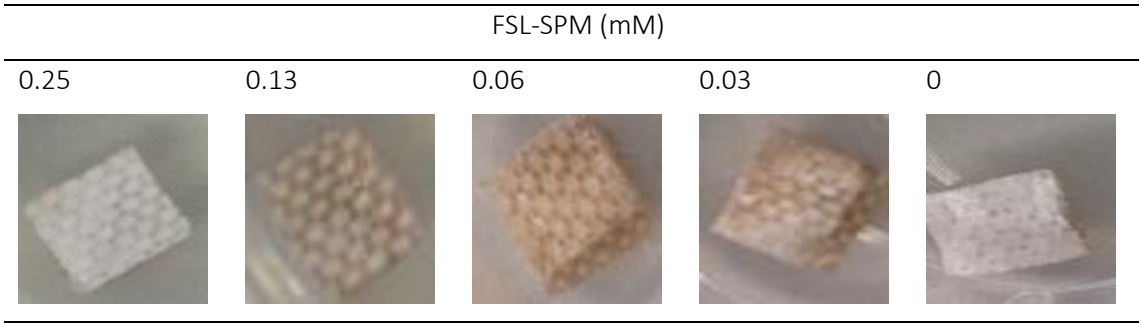

Figure 30. Silver nanoparticles capture by FSL-SPM labelled surfaces. Visualised by silver nanoparticle capture detected by a brown colour change on the surface after 1h contact with 7% negatively charged silver nanoparticles.

(i) Colorimetric detection

The efficiency of FSL-SPM capture (Figure 31) Illustrates at lower concentration FSL-SPM labelled on the surface was able to capture silver nanoparticles while as concentration increased the ability to capture reduced when the remaining liquid in the 24 well plates was read at 424 nm optical density

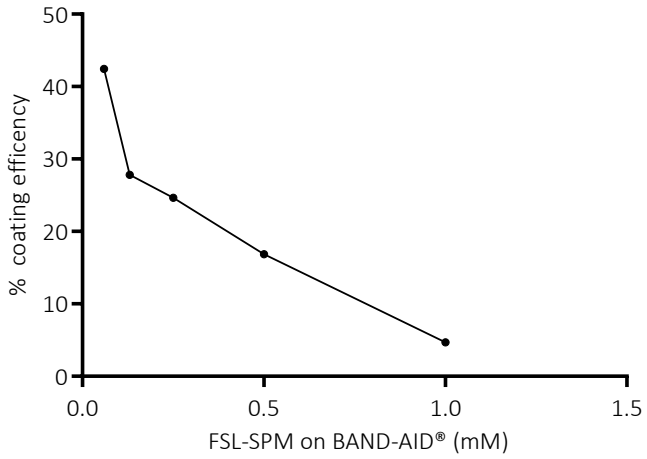

Figure 31. Graphic representation of efficacy of FSL-SPM labelling the surfaces detected with silver nanoparticle capture.

The ninhydrin and [-]Agnp methods were not compared but both the methods were only used as a confirmation for the presence of FSL-SPM on the surface. FSL-SPM labelled surfaces capturing [-]Agnp have other purpose that will be discussed later in this research.

c) FSL-SPM particle size

Methodology

The effect shown above is probably due to the presence of FSL-SPM as nanoparticles. To confirm the presence as nanoparticles, FSL-SPM construct were measured for particle size using a Zeta sizer. Zeta sizer is used to measure the size of particles. In this experiment 0.5 mg/mL of FSL-SPM was measured in water.

Results and interpretation

The sample when prepared as 0.5 mg/mL solution in water were approximately 100nm in diameter size when measured with a Zeta sizer (Figure 32). Hence at higher concentration FSL-SPM could be washed away when placed in silver nanoparticle solutions. Additional investigation of FSL-SPM in solution using Zeta potential will explain the characterisation of the construct. Since it was not within the scope of this research, further analysis was not carried out.

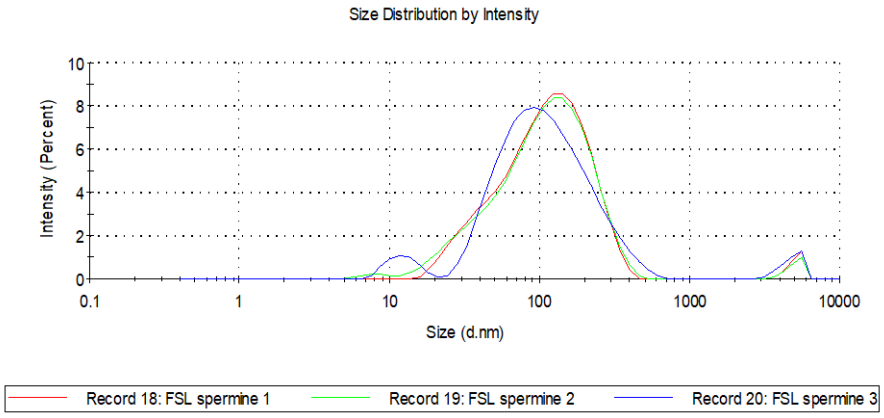

Figure 32. FSL-SPM size distribution when analysed at 25˚C in a Zeta sizer. The particle size of FSL-SPM when prepared as 0.5 mg/mL were ~ 100 nm in diameter.

2.6 Summary

In this chapter FSL attachment on the surface were established by a simple drop method that has been previously reported[248]. However, this coating is likely to leach over time and its susceptibility over time was not analysed in this research.

Characterisation of antimicrobial FSL-Se shows that FSL-Se reduces the hydrophilicity of the surface while FSL-SPM did not change the surface property. The effect of changes in surface properties on bacterial adhesion will not be discussed in this research due to all FSL construct labelled surfaces were hydrophilic.

Both FSL-Se and FSL-SPM detection methods illustrate that FSLs on surfaces could be detected by a charge- based method. The antimicrobial efficacy of the FSL construct in solution and on surface will be discussed in the following chapters.

Chapter 3 Antimicrobial activity in solution phase

FSL antimicrobials before attaching them onto surfaces were analysed for antimicrobial activity as a solution. This is because when a large quantity of FSL is applied to a surface, some will ablate into the solution phase and have an antimicrobial effect. In such a case the antimicrobial activity of FSLs in solution will give knowledge on the antimicrobial activity of the ablative layer. However it is to be expected that a final prduct will utilise both the solution and surface bound effects.

Antimicrobial activity is measured by estimating the Minimum Inhibitory Concentration (MIC). MIC values signify the susceptibility of the organism to a particular molecule. MIC is the lowest concentration at which visible bacterial growth is inhibited and is commonly used as an indicator for antibiotic dose response for a bacterial infection. The MIC can be determined using resazurin as a growth indicator to allow the identification of viable bacteria causing a dye colour change from blue to fluorescent pink. The resazurin based assay is a simple and reliable assay which has been employed in many antimicrobial screening assays[249,250].

3.1 Bacterial cultivation and inoculum preparation

S. aureus, *S. epidermidis*, *P. aeruginosa* and *E. coli* were the microorganisms used in this research. Fresh culture was prepared from frozen stock when required. Two colonies were inoculated into 10 mL MH broth (prepared as per manufacturer's instructions Becton Dickinson, USA) and propagated to log phase in a shaking incubator for 4 hrs at 37 ˚C and 200 rpm mixing with an orbital shaker (Grant Bio POS- 300). All the four organisms used reached log phase in four hours of incubation. The optical density (OD) of the bacterial culture was measured in MH broth and diluted to 0.08 OD which is equal to approximately 0.5×10^{8} CFU/mL. A validation check was carried out each time the OD approximated suspension was prepared to determine the actual concentration of bacterial loading used for each experiment.

Inoculum validation

The inoculum check was prepared by making 10^{-1} to 10^{-7} dilutions of the 0.08 OD culture in 0.1% peptone water (Becton Dickinson, USA) and plating out 100 µL onto Columbia sheep blood agar plates. These plates were incubated at 37 ˚C overnight. The colony forming units (CFU) were counted, and the concentration of bacterial inoculum was calculated.

3.2 Bacterial concentration and resazurin colour development

Resazurin a non-fluorescent blue redox indicator is reduced by a cellular activity to highly fluorescent pink. This dye helps in visible growth identification by a colour change[251]. To establish the accuracy of this method the performance of resazurin was evaluated determining the relationship between the bacterial concentration present and colour produced.

Methodology

10 µL of approximately 2 log bacteria were added to the 96 well plates wells that contain 50 µL of FSL constructs at different concentrations. Then 10 µL of (0.02%) resazurin dye was added followed by 30 µL of MH broth, and then incubated at 37 ˚C for 24 hr. The colour produced for each bacterial concentration of the suspension was measured. A growth control (PC) and a sterility control (NC) were included in all the experiments. Viability count was checked by removal of bacteria from the solution preparing serial dilutions in 0.1% peptone and plating onto Columbia sheep blood agar. Plates were incubated at 37 ˚C for 24 hr. After 24 hr, the number of colonies counted and CFU (colony forming units) were calculated.

Results and interpretation

The colour results in Figure 33 show that blue correlates with no bacterial growth while pink indicates bacterial activity. The slight change in colour from blue to purple indicates reduced bacterial growth. Hence this assay is able to detect presence of lower number of viable cells as previously shown in literature [251].

Examples of colour produced by resazurin solution		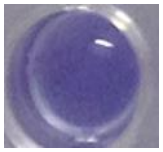		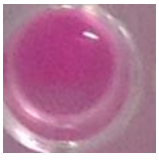
Log CFU of viable bacteria present / well	*S.aureus*	0	3.6	5.8
	S.epidermidis	0	3.2	4.8

Figure 33. Representation of detection limits of resazurin dye. Blue indicates the absence of bacterial growth, while a slight change in colour indicates bacterial growth. Each well were infected with 2 log bacterial loading.

3.3 Minimum inhibitory concentration with resazurin as an indicator

Methodology

A stock solution of 2 mM of FSL construct in water was prepared and pipetted into the first row of the 96 well plate. To all other wells, 50 µL of sterile water was added. Serial dilutions were then made using a multichannel pipette so that each well had 50 µL of the test material in serially descending concentrations. To each well was added 10 µL of resazurin indicator solution was added(0.02% prepared from R7017, Sigma Aldrich, USA) and 30 µL MH broth to give a final volume in all the wells of 90 µL. Finally, 10 µL of desired *S. epidermidis* bacterial suspension was added to each well. The bacterial concentration was added in decreasing concentrations from the first column to the last starting from 1×10^3 to 1×0^5. Plates were incubated at 37 ˚C for 18-24 hr, and observed colour changes were photographed and MIC determined.

Results and interpretation

3.3.1 Antimicrobial activity of FSL-Se in solution

Figure 34 shows the colour change brought about by viable bacteria and MIC for FSL-Se determined by visual reading. Pink observed indicates presence of viable bacteria while blue indicates bacterial growth inhibition.

MIC determination in the presence of FSL-Se in solution indicates that a 0.5 mM and 0.25 mM concentration of FSL-Se was bactericidal to about 4 logs bacterial loading of *S. epidermidis.* FSL-Se concentration of 0.13 mM and 0.06 mM could inhibit 3 bacterial logs of initial loading.

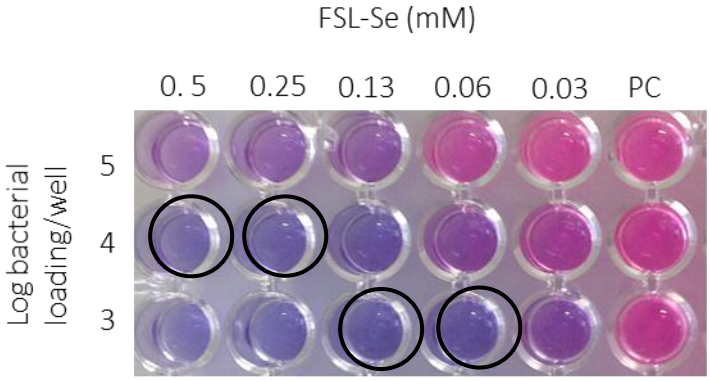

Figure 34. MIC for FSL-Se at each concentration of using resazurin dye. The black circle denotes the minimum concentration of FSL required for each concentration of *S. epidermidis* bacterial loading.

a) The MIC of all microorganisms

Four concentrations of FSL-Se (0.5, 0.25, 0.13 and 0.06 mm) were tested against four concentrations of microbes (S. aureus, *S. epidermidis*, *P. aeruginosa* and *E. coli*) at two initial loading concentration (10^3 and 10^4) using the same method in 3.3.1. and incubated for 24 hr at 37˚C with the resazurin dye indicator. MIC data presented in Table 10 revealed FSL-Se exhibited strong antimicrobial effect against gram-positive bacteria but no activity against gram-negative bacteria. Similar MIC were exhibited with both the gram-positive bacteria used, in the range of 3-4 log reduction for gram-positive bacteria. Of the four-concentrations tested FSL-Se was not effective against the two gram-negative bacteria tested.

Table 10. MIC data from resazurin assay demonstrating FSL-Se antimicrobial activity against two gram-positive and two gram-negative organisms.

		FSL-Se (mM) log inhibition			
		0.06	0.13	0.25	0.5
Gram-positive	*S. aureus*	3*	3	4	4
	S. epidermidis	3	3	4	4
Gram-negative	*P. aeruginosa*	No inhibition			
	E. coli	No inhibition			

* Numbers indicate log bacterial loading per well that could be inhibited by each concentration of FSL-Se.

b) Comparison with selenous acid

Equimolar concentrations of selenous acid and FSL-Se were compared to determine the efficacy of the construct. Each well contains a 50 µL dilution of either FSL-Se or selenous acid, 10 µL of 0.2% resazurin reagent, 30µL of MH broth and 10 µL of bacterial suspension (*S. aureus* concentration – 2.9 log bacterial loading per well). Plates were then incubated at 37˚C for 24 hr and observed for colour change.

The ranges of MIC values obtained for FSL-Se and selenous acid showed that 1mM of selenous acid and 0.06 mM of FSL-Se in solution are the lowest concentrations able to cause sterility (Figure 35). The antimicrobial efficacy obtained for FSL-Se was eight-fold higher than that obtained by selenous acid. These results were reproduced on three separate occasions and the plate layout for the experiment was adjusted to allow direct comparision for endpoint of the MIC. FSL-Se control with no bacteria had no activity with resazurin dye. However, note that the higher

concentrations of selenous acid (>4 mM) with resazurin gives brownish colour artefact with the resazurin dye. This comparison was only carried with *S. aureus* as a model bacterium.

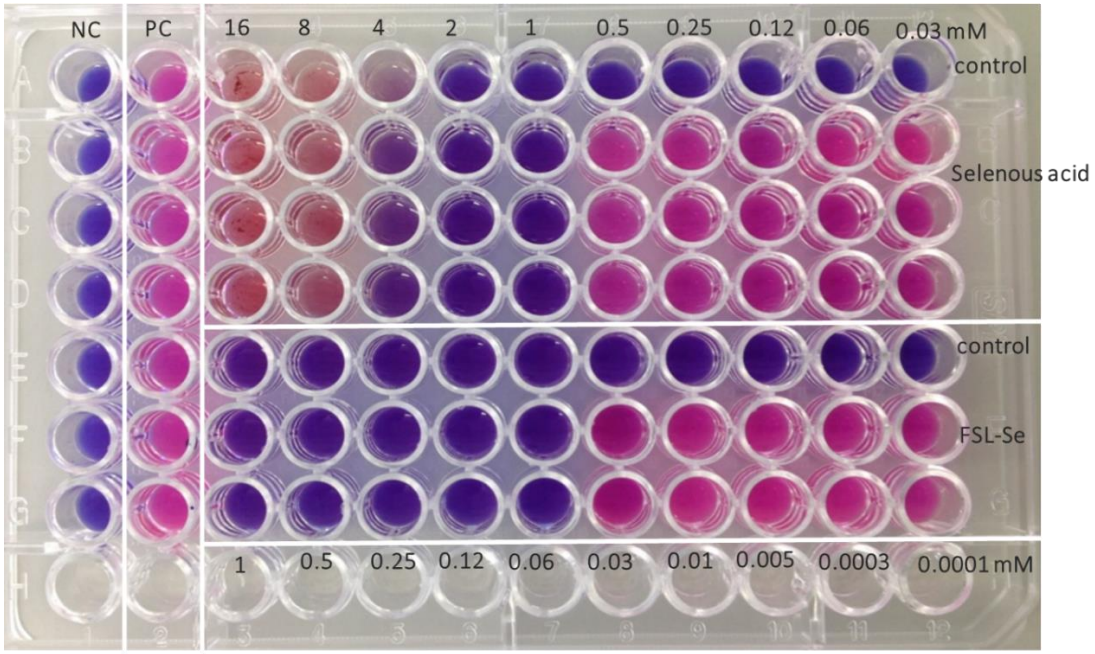

Figure 35. Resazurin-based MIC for FSL-Se against *S. aureus*. Control wells were with the test solution alone and no bacteria. Concentration of selenous acid >4 mM gave a brownish colour with resazurin dye. Concentrations 1 mM of selenious acid and 0.06 mM for FSL-Se showed were taken as MIC values for 2.9 initial log bacterial loading.

3.3.2 Antimicrobial activity of FSL-SPM in solution

The antimicrobial efficacy of FSL-SPM constructs in water as evaluated by determining the MIC for each bacterial loading in the presence of resazurin growth indicator. The microtitre plate method with a range of concentrations of bacteria from 10^2-10^5 were tested in the presence of MH broth and resazurin dye. The results indicated that FSL-SPM in solution has inhibitory action against the 4 micro-organism tested, and the MIC for each bacterial loading varies between microorganisms (Table 11).

Table 11. MIC of FSL-SPM against all four microorganisms tested with resazurin indicator.

		mM FSL-SPM concentration log inhibition			
		0.06	0.13	0.25	0.5
Gram-positive	*S. aureus*	3	3	4	4
	S. epidermidis	0.5	3	4	5
Gram-negative	*P. aeruginosa*	0	2	3	4
	E. coli	0	2	4	4

3.3.3 Antimicrobial effect of FSL-RIP

The antimicrobial efficacy of FSL-RIP as a solution was analysed.

Methodology overview

The MIC activity of FSL-RIP as a solution was measured using the resazurin indicator. Decreasing concentration of FSL-RIP were incubated with 10 µL of *S. aureus* suspension, MH broth containing resazurin at 0.02%. Each test was prepared in triplicate and incubated at 37˚C for a colour change in 24 hr. Each plate had growth control (PC) and sterility control (NC).

Results and interpretation

Figure 36 indicates pink in all the wells showing the inability of FSL-RIP in solution to inhibit bacterial growth when infected with 3.5 logs of *S. aureus* loading. It should be noterd that the RIP peptide is normally internalised to bring about it antimicrobial effect, so these result indicate that RIP is not internalised, as has no effect.

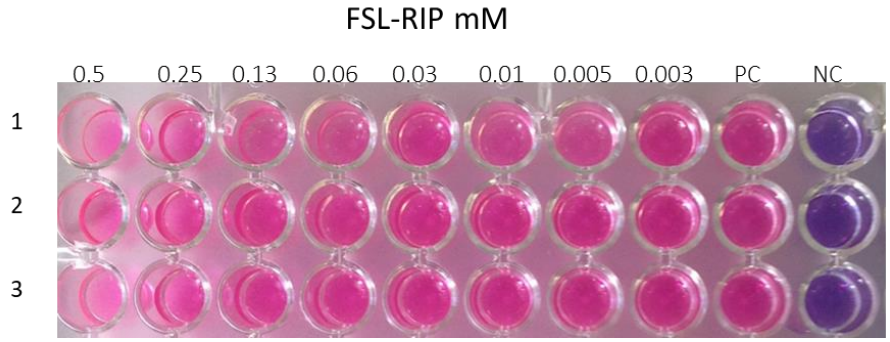

Figure 36. Antimicrobial activity of FSL-RIP in solution against *S. aureus* at 3.5 logs bacterial loading per well. A pink colour indicates the inability of FSL-RIP constructs to inhibit bacterial growth. Rows 1-3 are triplicates. Sterility controls are NC-negative and PC- positive growth control.

3.4 Summary

The results demonstrate that the antimicrobial FSL-SPM in solution was the only construct to show antimicrobial activity against both gram-positive and gram-negative bacteria. FSL-Se in solution had antimicrobial activity only against gram-positive and not gram-negative bacteria. FSL-RIP in solution had no antimicrobial activity. These results suggest that ablative layer of antimicrobial FSL when come into solution can exert an strong antimicrobial effect, and if the surface effect is to be measured then the ablative layers must be first washed away before adding bacteria.

Chapter 4 Antimicrobial activity of surface bound FSL

4.1 Ablative layer plus adhered layer

FSL molecules, when contacted with a surface, self-assemble as a surface adhered layer and as a multilayer (when at high concentrations). These additional layers are called the ablative layers and can be removed with PBS or when in contact with a growth medium and become solution phase FSLs . Previously it was shown the solution phase FSLs also extent antimicrobial activity Both the surface monolayer and the ablative layer will exert separate and additive antimicrobial effect. Washing of the surface is generally considered sufficient to remove the ablative layer, allowing for measurement of the surface monolayer.

Methodology

First, 50 µL of FSL-Se was pipetted a 0.25 cm^2 square BAND-AID® swatch. FSL-Se labelled swatches were then dried at 80˚C for approximately 45 minutes. 10 µL of a 10^5 of bacteria suspension was then applied to the surface. The contaminated swatches were incubated for 10 minutes to allow the bacteria to settle and then they were placed in 96 well microtiter plates. To each well was added 50 µL of water and 150 µL of MH broth containing 0.02% resazurin indicator. A growth control PC and a sterility control NC were included in the each assay. Microplates were incubated for 24 hr at 37˚C. *S.aureus* was chosen as the model bacterium for determination of factors contributing to FSL-Se antimicrobial efficacy. After a standard protocol was established the other microorganisms were tested. Bacterial cultivation and desired inoculum concentration were prepared as per section 3.1. From 0.08 OD of prepared bacterial concentration, 1 in 10 dilution was done to get $0.5\times10^{7,}$ further serial dilutions were done. The 10^5, 10^4 and 10^3 were used as bacterial inoculates.

4.1.1 The antimicrobial ability of FSL-Se on BAND-AID®

a) FSL-Se concentration vs bacterial loading

The antimicrobial capacity of FSL-Se on BAND-AIDs® was evaluated using resazurin dye as an indicator of bacterial growth. Note these surfaces were not washed so the effect observed is due to both the surface bond and ablative (solution phase) FSL constructs.

Methodology overview

First 50 µL of FSL-Se was placed on to 0.25 cm^2 BAND-AID® swatches, dried at 80˚C (for 10 minutes until the surfaces are completely dried) and inoculated with the desired concentration of bacteria in a 96 well microtiter plate along with resazurin dye containing growth medium (MH broth). The plates were incubated at 37˚C for 24 hr to observe the colour change. The antibacterial activity was analysed by plotting bacteria loading versus FSL concentration. The last well with blue indicates the concentration at which bacterial inhibition is seen. *S.aureus* was chosen as the model bacterium for these initial measurements of FSL-Se antimicrobial efficacy.

Results and interpretation

(i) Colour change

Figure 37 shows that the 0.5 mM concentration of FSL-Se on a BAND-AID® can kill an initial log 4.3 bacteria loading. In contrast 0.25 mM of FSL-Se on a BAND-AID® could inhibit 3.7 log of bacterial loading while 0.13 mM had no effect on bacterial growth inhibition.

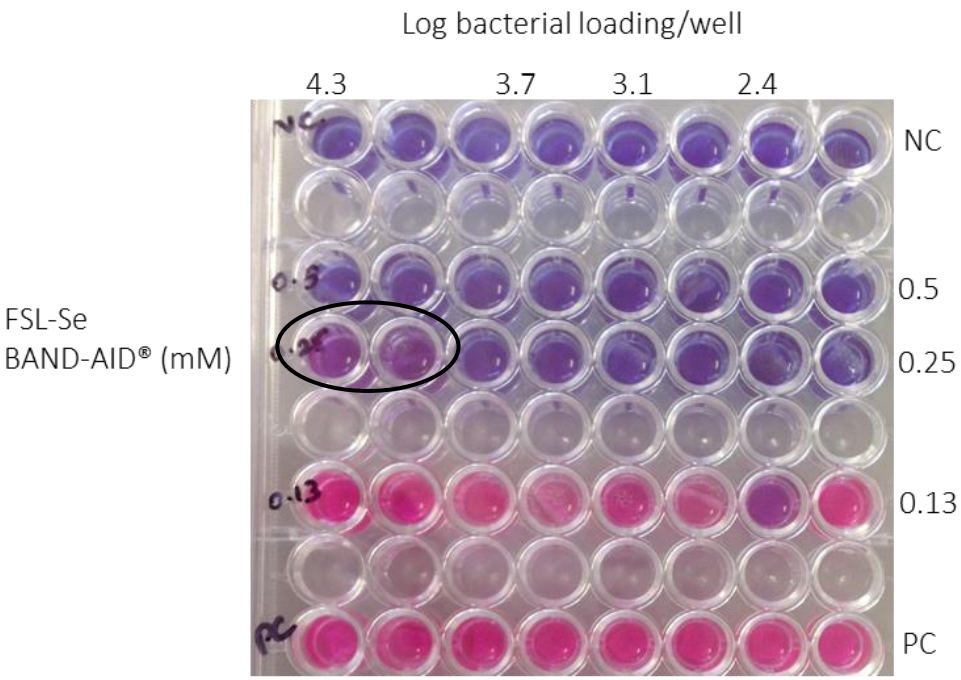

Figure 37. Bacterial inhibition of FSL-Se on BAND-AID®. Columns are of decreasing bacterial loading, while rows represent decreasing FSL concentration on BAND-AID® surfaces. The black outline denotes the last concentration below which bacterial growth occurs. Blue=no growth, pink=growth

Figure 38 shows the effect of bacterial loading vs FSL-Se concentration at three different concentrations of *S. aureus* and the MIC of bacteria of FSL-Se coated BAND-AID®. At 0.13 mM, FSL-Se did not inhibit the growth of 2 logs of bacterial loading. At 0.5 mM concentration FSL-Se could inhibit the growth of 4 logs of bacterial loading.

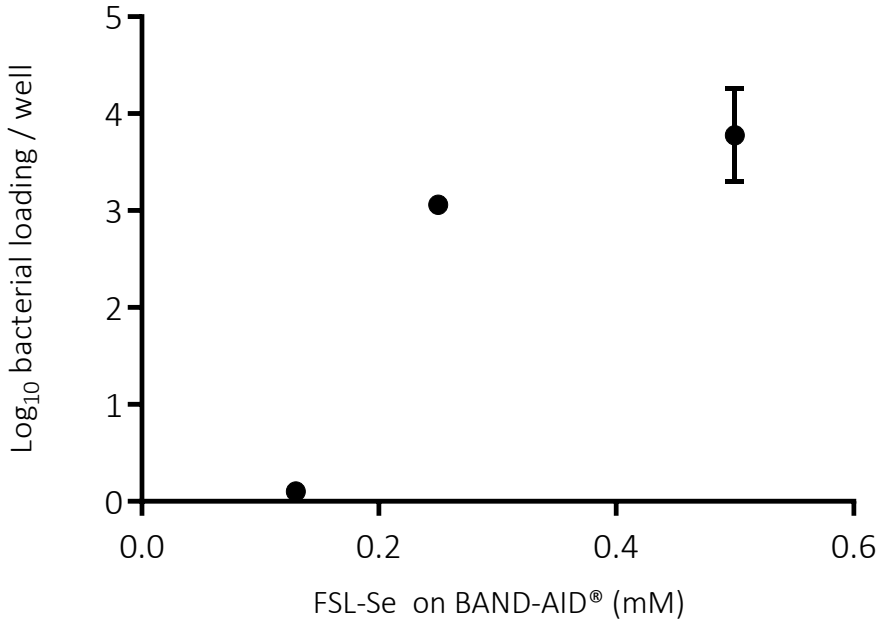

Figure 38. Initial bacterial loading vs concentration of FSL-Se on BAND-AID® that had an inhibitory effect against *S. aureus*. The graph represents values obtained from triplicate experiments.

(ii) SEM analysis

After 24 hr incubation with the resazurin indicator, swatches were washed 1× with water and then fixed with 2.5% glutaraldehyde (Sigma Aldrich, USA). Swatches were not ethanol dehydrated due to the potential of ethanol to remove FSL from surfaces. Swatches were dried at room temperature, platinum sputter coated and visualised by SEM (Hitachi SU-70).

Each sample was viewed at ten random regions to estimate the presence of bacteria. Results found that where colour is blue (i.e. at 0.5 mM FSL-Se labelled surfaces) there was no growth on while at lower concentrations where a slight change in colour from blue to pink was seen with resazurin has shown bacterial colonization (Figure 39).

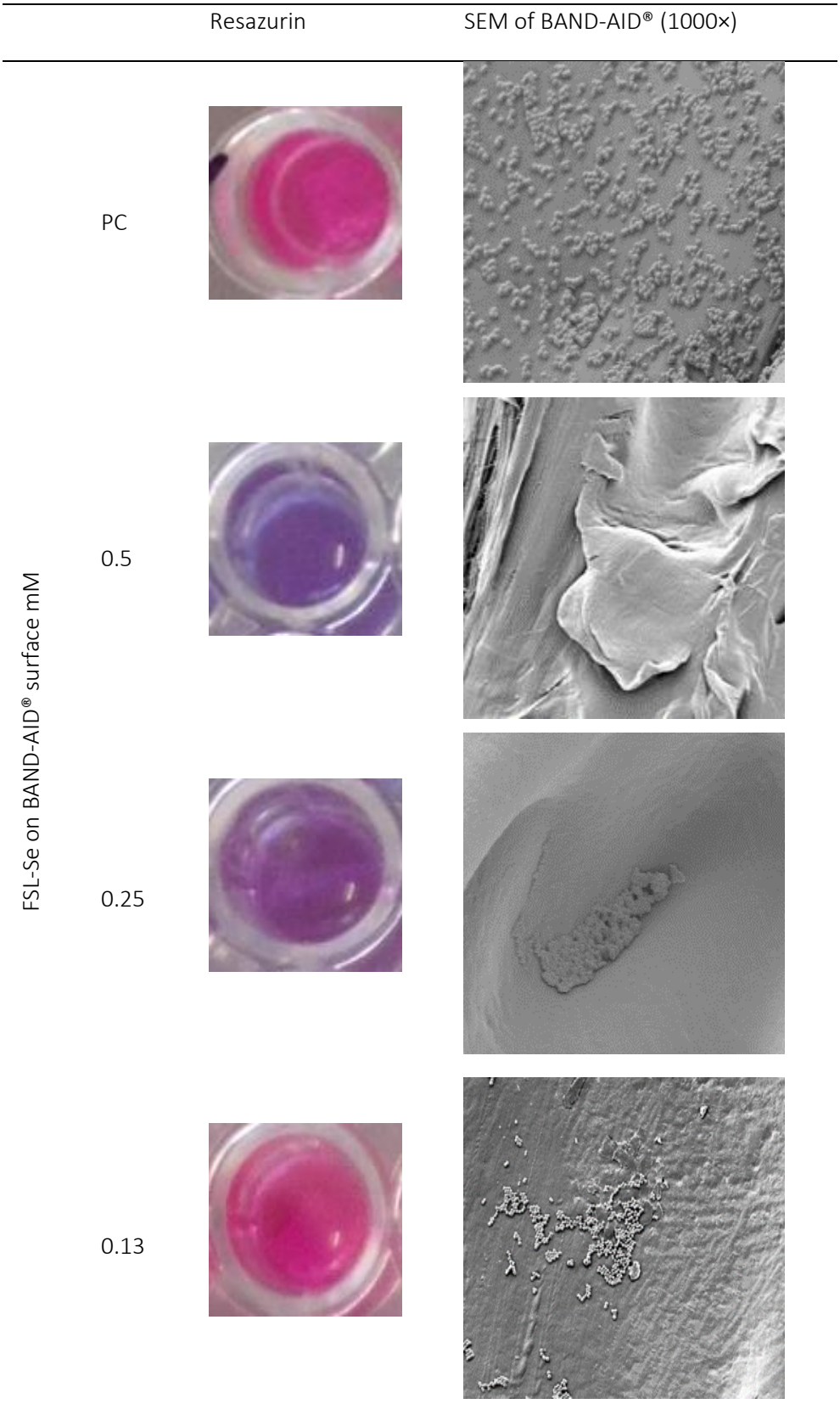

Figure 39. Images of both resazurin reactions with corresponding SEM image after 4.3 logs initial bacterial loading and 24 hours incubation at 37˚C loading.

b) Factors affecting the antimicrobial effect

This section focuses on establishing the factors involved in altering the antimicrobial efficacy of labelled surfaces. In the previous section 3.3.1 FSL-Se in solution was shown to have antimicrobial activity against *S. aureus and S. epidermidis.* Based on this knowledge, in this section a comparison between FSL-Se in solution and FSL-Se on surface were undertaken. Additionally, experiments were carried out to study contact time of bacteria with a labelled surface and its effect on antimicrobial efficacy.

(i) FSL in solution vs FSL on BAND-AID®

Methodology overview

This section is a comparison of FSL-Se on surfaces as described in section 4.1.1.a.and FSL-Se in the solution treated at the same bacterial concentration. FSL-Se in solution were added to the well instead of placing onto the BAND-AID® surface. FSL-Se at varying concentrations on BAND-AID® and surfaces treated with bacteria were incubated along with MH broth with 0.02% resazurin indicator.

Results and interpretation

Figure 40 shows slight pink colour formation at 0.13 mM concentration of FSL-Se in solution while at other concentrations no colour change was observed. FSL-Se on BAND-AID® were blue in colour at all the concentrations used. This clearly shows that 0.25 mM concentration of FSL-Se in solution and on a BAND-AID® surface cause sterility. At 0.13 mM the FSL-Se present in solution was slightly less effective than that present on dressing, but the difference was 0.13 mM. Overall the results suggest the total amount of FSL-Se in the well was eqivalent regardless at present on bandage or as free in solution.

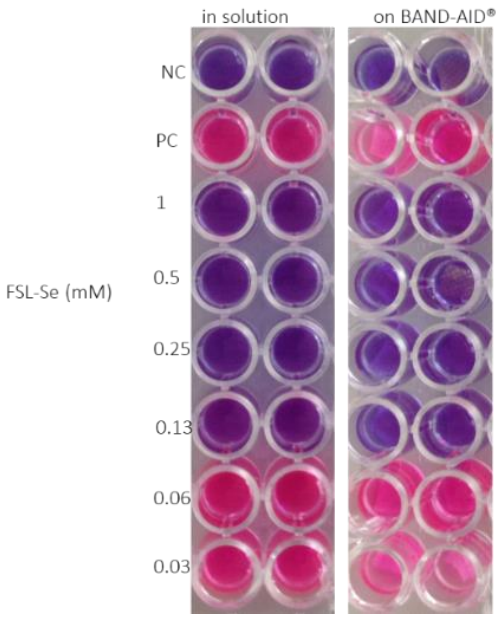

Figure 40. *S. aureus* growth inhibition of FSL-Se in solution and on BAND-AID® surfaces with a bacterial loading of 3 log bacterial loading.

(ii) FSL-Se swatch vs swatch placed in FSL-Se in solution

Overview

Antimicrobial activity of FSL-Se labelled swatches were compared with FSL-Se in solution along with unlabelled swatches placed in MH broth. Experiments were carried out with *S. aureus* loading, incubated at 37˚ C for 24 hr in the presence of resazurin indicator.

Results and interpretation

Figure 41 below shows that free FSL-Se in solution (when present with unlabelled swatch) had a slightly higher antimicrobial activity when compared to FSL-Se bound to swatches when in solution. FSL-Se in solution could inhibit 4.4 log bacterial loading while FSL-Se swatches could inhibit 4 log bacterial loading, and the difference was considered minor and insignificant.

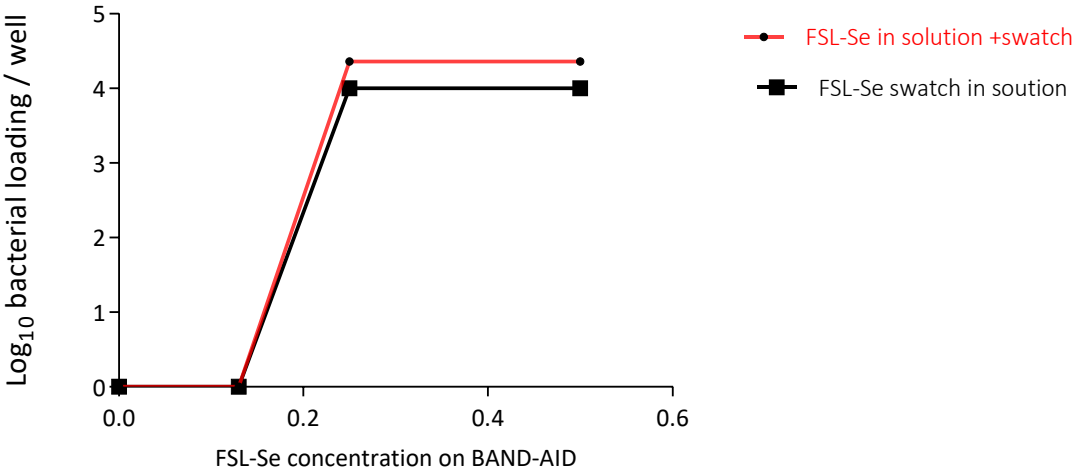

Figure 41. Representation of the antimicrobial activity of FSL-Se caused by comparing FSL-Se in solution + swatch and FSL-Se loaded swatches placed in solution. FSL-Se in solution had shown 0.4 log increased efficiency in removal of *S. aureus.*

(iii) FSL-Se swatch and bacterial contact time

Methodology overview

The effect of bacterial contact time with FSL-Se labelled BAND-AID® was determined. 50 µL of FSL-Se labelled and dried surfaces were contacted with 10ul of bacteria and left in contact for 2 hr at room temperature in a closed humid chamber. After 2 hr contact time they were placed in MH broth and resazurin solution and incubated at 37 ˚C for 24 hr with shaking at 200rpm. Results were compared to similar FSL-Se labelled surfaces infected with bacteria and after 10 minutes contact.

Results and interpretation

Results indicate that there was no benefit in incubating bacteria on surfaces for 120 minutes had no additional effect (Figure 42). Therefore, 10 minutes incubation of bacteria on surfaces was used as for standardised contact time before placing the swatches in growth medium.

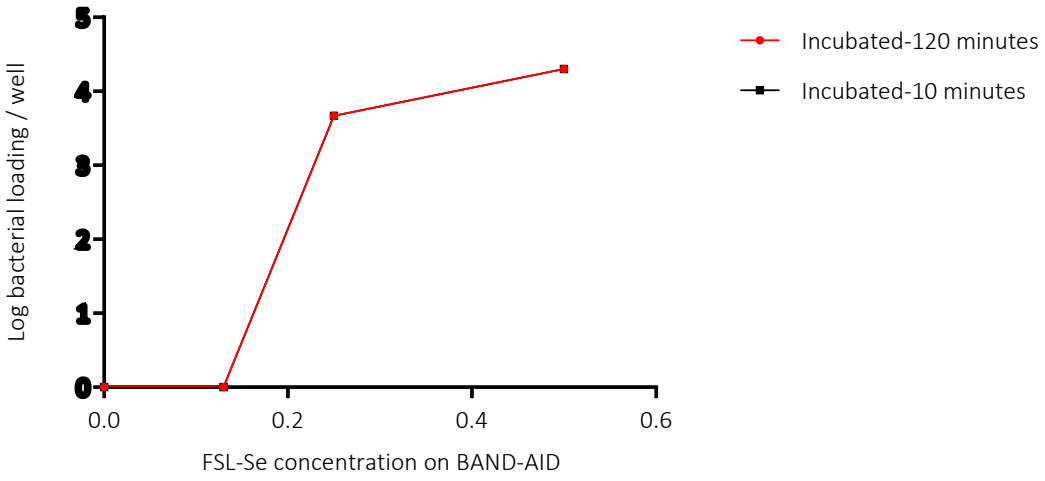

Figure 42. Antimicrobial activity of FSL-Se labelled BAND-AID®. 10-120min contact time with bacteria.

c) Antimicrobial efficacy of FSL-Se on BAND-AID® swatches against both gram-positive and gram-negative bacterium

Methodology overview

Each of four microorganisms were tested against FSL-Se at three concentrations. The four microorganisms were *S. aureus*, *S. epidermidis*, *E. coli* and *P. aeruginosa*. The bacterial concentrations were prepared as in section 4.1.1. and similar bacterial loadings concentrations were used for all bacteria. Results from the microplates were converted into colours and these are recorded in table format with pink indicating bacterial growth and blue indicating no growth (see also Figure 33)

Results and interpretation

A comparison of the antibacterial activity of FSL-Se labelled swatches was done against all four microorganisms tested. Results indicate that FSL-Se is effective against only gram-positive bacteria and has no effect against gram-negative bacteria (Table 12) even at high concentrations of FSL-Se. FSL-Se at 0.5 mM concentration had an antimicrobial effect at 4.6 log of bacterial loading while at 0.25 mM concentration it was only effective against *S. epidermidis* and at 0.13 mM FSL-Se did not have any antimicrobial activity.

Table 12. FSL-Se on BAND-AID® antimicrobial activity against *S. epidermidis.* The pink growth of bacteria blue colour indicating bactericidal activity.

		Log bacterial loading/ well		
	FSL-Se mM concentration	5.3	4.6	3.6
S. aureus	0.5			
	0.25			
	0.13			
S. epidermidis	0.5			
	0.25			
	0.13			
P. aeruginosa	0.5			
	0.25			
	0.13			
E. coli	0.5			
	0.25			
	0.13			

4.1.2 Antimicrobial effect of monolayer

Methodology overview

FSL-Se labelled surfaces were washed six times in DI water to establish a monolayer (and wash away the ablative layer) Swatches were dried and generic protocol was used to determine the antimicrobial activity of the monolayer in comparison to unwashed FSL-Se labelled surface (which also have the ablative layer)

Results and interpretation

Table 13 summarises the substainal loss of antimicrobial activity on washed surfaces and no inhibitory action of bacteria by the monolayer at least against 3.6 log of bacteria. This absence of antibacterial effect is probably low amount of FSL-Se remaining on the surface and not being enough to have an antimicrobial effect compared with the total amount present on the unwashed swatches.

Table 13. Loss of antimicrobial activity against gram-positive bacteria by FSL-Se labelled surfaces when reduced to a monolayer.

		Unwashed (ablative layer+ monolayer)			Washed (monolayer)		
		Log bacterial loading/ swatches					
	FSL -Se (mM)	5.3	4.6	3.6	5.3	4.6	3.6
S. aureus	0.5						
S. epidermidis	0.5						

4.1.3 Antimicrobial activity of FSL-SPM

Similarly to FSL-Se, FSL-SPM construct was tested for its antimicrobial efficacy on surfaces including BAND-AID®, SS and plastic in the form of a microtiter plate.

a) FSL-SPM on BAND-AID®

Methodology overview

The antimicrobial activity of FSL-SPM coating BAND-AID® was evaluated using resazurin dye as an indicator of bacterial growth. 50 µL of FSL-SPM (1.6 mM) was placed on 0.25 cm^2 square BAND-AID® swatches and dried at 80˚C for approximately 45 minutes. 10 µL of a desired concentration of bacteria in suspension was applied to the surface and inoculated swatches were incubated for 10 minutes at room temperature. Swatches were then placed in a 96 well microtiter plate along with resazurin dye containing growth medium (MH broth) and incubated at 37˚C for 24 hr to observe for a colour change. Samples were also subjected to SEM analysis to observe biofilm formation.

Results and interpretation

Pink colour in the presence of resazurin was seen in all the wells with BAND-AID® surfaces labelled with 1.6 mM FSL-SPM. Pink colour was seen with both higher (6.9 log bacterial loading) and lower (4.7 log) bacterial loading. This indicates that no growth inhibition was observed with 1.6 mM FSL-SPM. These results obtained were confirmed by SEM image analysis revealing bacterial growth on both positive control and FSL-SPM labelled surfaces (Figure 43). Results with *S. aureus* were symbolized as a interpretation of the effect observed with the four bacteria used. FSL-SPM on BAND-AID® surfaces has no inhibitory effect against all four microorganisms tested. Inhibitory action of the FSL-SPM occurred only when in solution phase and not when on surfaces.

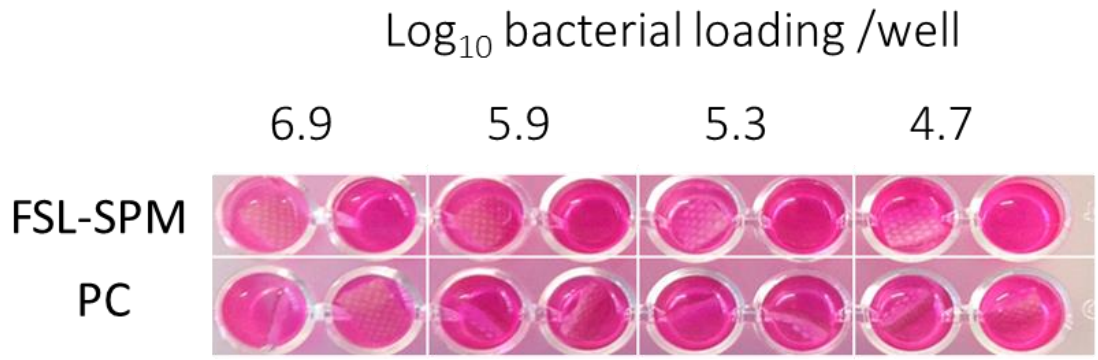

(i)

PC FSL-SPM labelled surface (1.6mM)

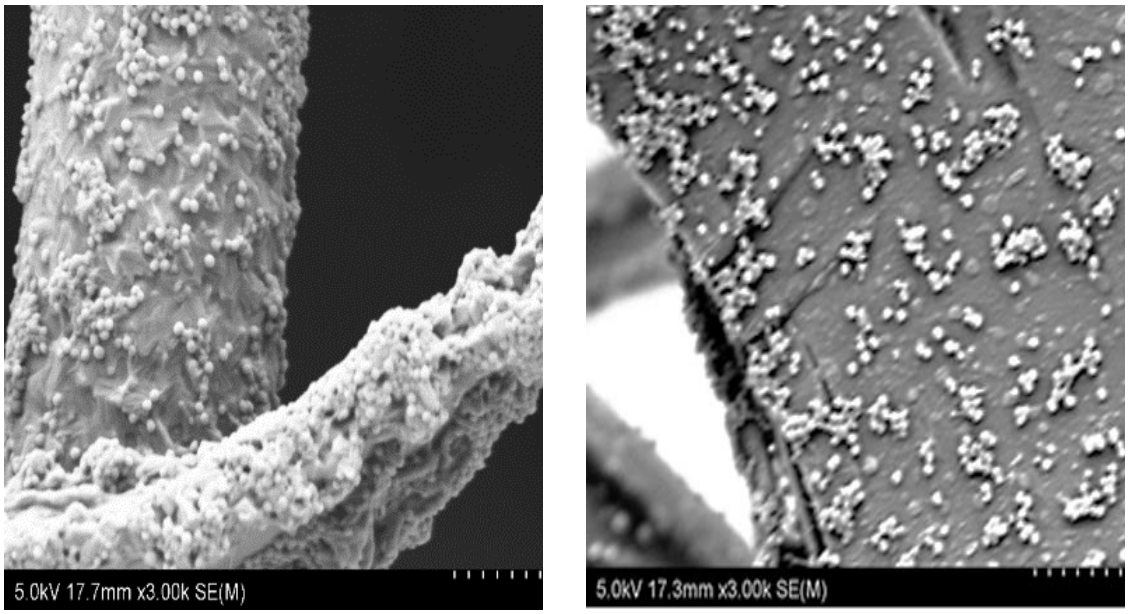

(ii)

Figure 43. Representation of the inability of FSL-SPM to bring in antimicrobial activity against gram-positive *S. aureus*. (i) Represent the growth on both the labelled and control surfaces (ii) SEM of BAND-AID® swatches is indicating bacterial growth on PC, and even at 1.6mM FSL-SPM labelled surfaces.

b) FSL-SPM on a microtiter plate

Methodology

A microtiter plate method was used to determine FSL-SPM's biofilm inhibition and crystal violet was used as an indicator to visualise the attached bacterial biofilm.

A stock concentration of 2 mM of FSL-SPM construct in water was prepared and pipetted into the first row of a 96 well plate. To all other wells, 50 µL of sterile water was added and serial dilutions were made using a multichannel pipette.

To each well was added 10 µL of resazurin (0.02%) and 30 µL of MH broth to ensure that the final volume of all the wells was 90 µL. Finally, 10 µL of bacterial suspension was added to each well. Bacteria were added in decreasing concentrations from the first column to the last.

Plates were incubated at 37 ˚C with shaking at 200 rpm. After 24 hr planktonic bacteria were removed by aspiration. The biofilm adhered to the microplate was dried and washed three times in sterile DI water and then dried. To all the microtiter wells 200 µL of 0.4% crystal violet was added, incubated for 10 minutes, washed six times and air dried. The crystal violet bound to the biofilm on the microtiter were removed with 95% ethanol and the amount of biofilm was estimated by OD 590 nm using a microplate reader.

Results and interpretation

Figure 44 shows that FSL-SPM at some concentrations enhanced *S.aureus* biofilm formation. At 0.25 mM of FSL-SPM showed no difference in bacterial growth than the PC. Maximal biofilm formation was seen over the range of 0.05-0.10 mM FSL-SPM and interstingly the lower the initial loading of bacteria the more biofilm was able to develope, 3 log was much better than 5 log. This was not further investigated. This graph shows the inabilty of FSL-SPM to inhibit biofilm developement and instead increased the ability of biofilm development particulrly at lower concentrations. This is supported by reports shows that SPM at lower concentrations can enhance bacterial growth[252].

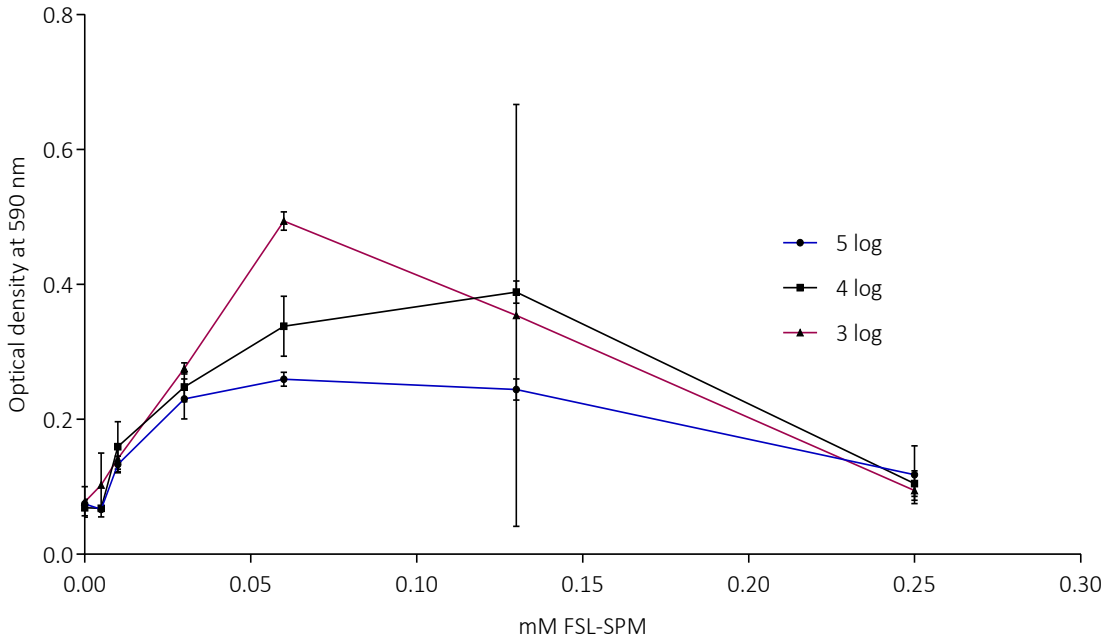

Figure 44. Antimicrobial activity of FSL-SPM on microtiter plates against *S. aureus* when stained with crystal violet.

A turkey comparision using Anova multiple comparision from Table 14 has shown that there is a significant difference between lower concentration of FSL-SPM and higher concentrations.

Table 14. Turkey comparision of 5 log bacterial loading and FSL-SPM concentration on the surface

Bacterial loading	Concentration of FSL-SPM on surface	Significant difference	Summary	P value
5 log	0.01 vs. 0.06	Yes	*	0.0211
	0.01 vs. 0.13	Yes	*	0.0218

c) FSL-SPM on Stainless steel

Methodology

Onto stainless steel (SS or 316SS) – industrial shim 0.051 mm (0.002”) surfaces 50 µL of 0.13mM FSL-SPM was dried. To the dried surface, 10 µL of 5 log of bacterial suspension was placed as a spot and allowed to stay on the surfaces for either 1 minute or 60 mins. These surfaces were then washed in sterile water and then placed in 1 mL of MH broth containing resazurin indicator. All the plates were incubated at 37˚C with shaking at 200 rpm. After 24 hr the SS surfaces were removed from the culture media and stained with 0.4% crystal violet. The degree of crystal violet

staining was determined by eluting it with 95% ethanol and measuring of OD at a 590 nM. Growth and sterility controls were included.

Results and interpretation

The values from Figure 45 shows the ability of FSL-SPM on the SS surface to enhance bacterial attachment compared to control with no FSL-SPM (PC). This enhanced microbial attachment was seen even when bacteria was in contact with the surface for only one minute. Even when a Anova multiple comparision using a Prism graphpad no significant variation between 1 minute and 60 minutes contact time was noted. These results indicate that FSL-SPM's antimicrobial ability is limited at best and instead enhances bacterial attachment and growth. As a consequence FSL-SPM was no longer considered a viable antimicrobial product, but it may have use in enhancing biofilm establishment.

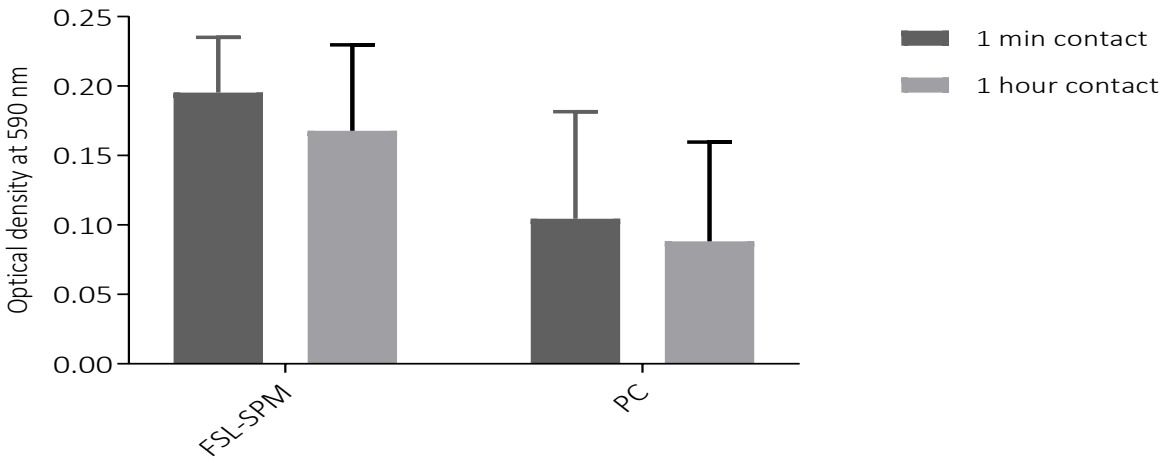

Figure 45. *S. aureus* attachment on FSL-SPM labelled 316SS when compared to control. Initial bacterial loading was 5 log per sample.

Methodology overview of extended bacterial adhesion studies

Based on the results obtained above, 0.13 mM FSL-SPM on SS surfaces were treated with the four clinical isolates. The bacterial loading was also increased by 1 log to place more bacteria on the surface. A comparison between one-minute and one-hr contact time was performed and images were taken after staining with crystal violet assay.

Results and interpretation

Figure 46 and Figure 47 show enhanced bacterial attachment of FSL-SPM labelled surfaces occurs after contact for 1 minute or 60 minutes for *S. aureus, S. epidermidis* and *E. coli.* However for *P. aeruginosa* required 60 minutes contact time for enhanced bacterial attachment to the surface in comparison to controls. In all examples FSL-SPM enhanced development of biofilms on 316ss.

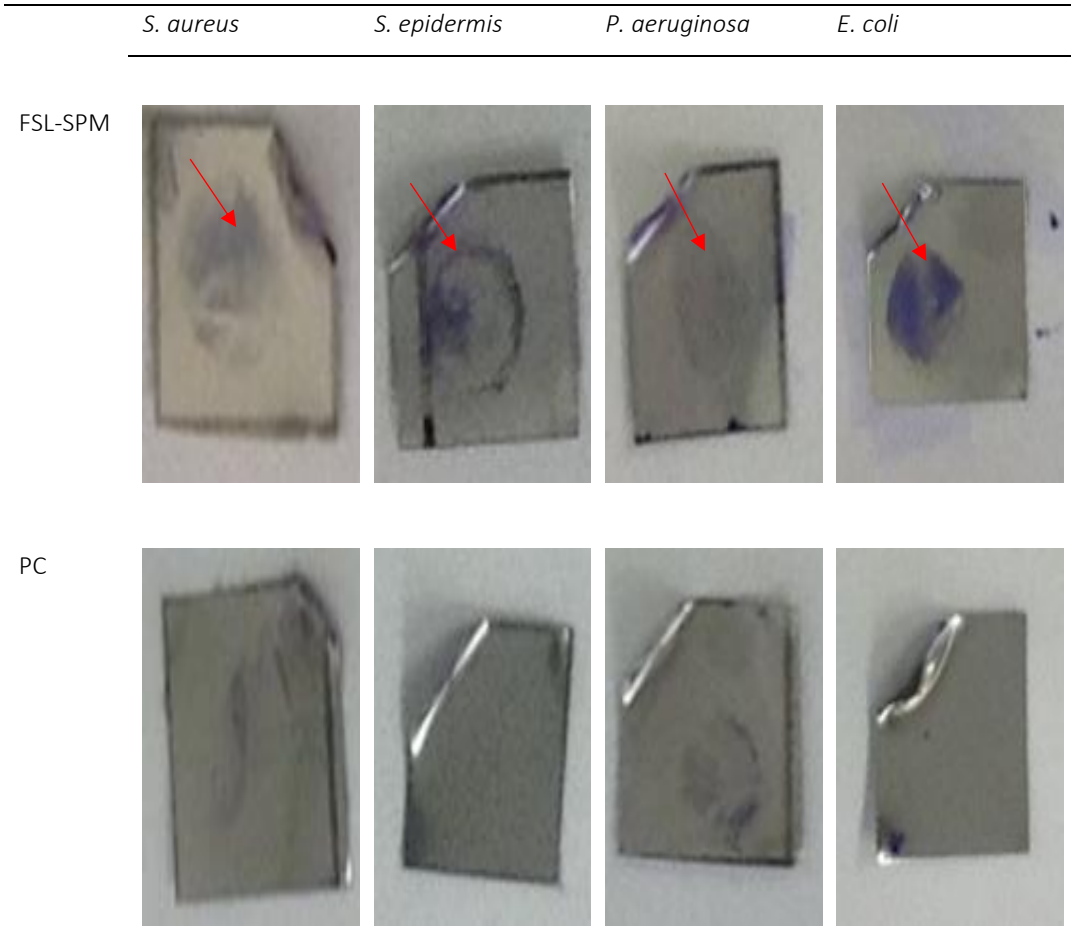

Figure 46. Bacterial attachment and growth after one-minute contact time on FSL-SPM labelled SS surfaces. The initial loading of bacterial loading was 6 log.

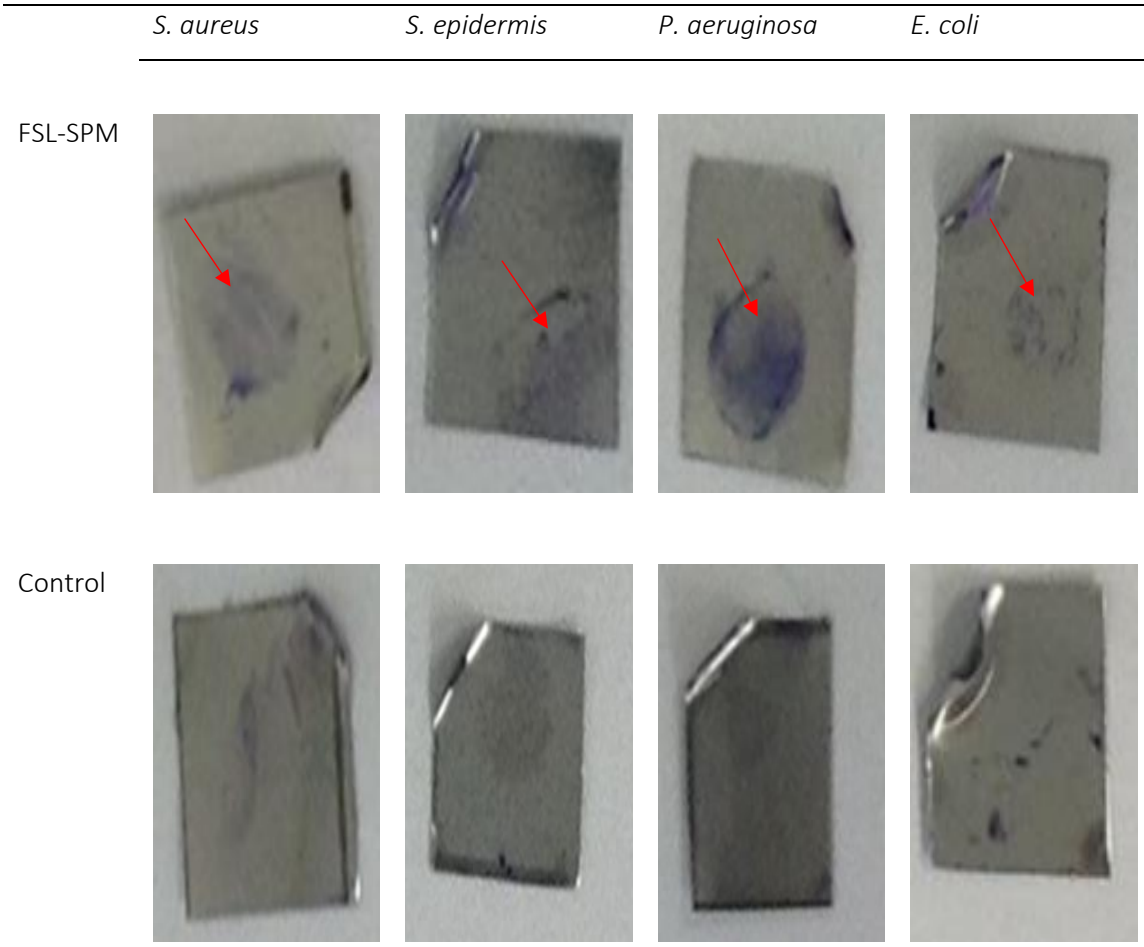

Figure 47. Bacterial attachment and growth after 60 mins contact time with FSL-SPM spotted SS surfaces with an initial bacterial loading of 6 logs.

4.1.4 Antibiofilm efficacy of FSL-RIP labelled surfaces

Although earlier described that FSL-RIP in solution has no antimicrobial activity, FSL-RIP labelled surfaces were tested to determine if they had any ability to prevent bacterial attachment onto surfaces.

a) Resazurin assay on SS surfaces

Methodology overview

Place 50 µL of 0.5 mM FSL-RIP into SS stamped wells and dry at 80˚C. Add 10 µL of *S. aureus* suspension and incubate for 10 minutes at RT. Placed innoculated surfaces into 24 well tissue culture plate and flood with one mL of MH broth containing resazurin at 0.02%. Each test was prepared in triplicate and incubated at 37 ˚C. Colour change was observed at 24 hr. Each assay had growth (PC) and a sterility controls (NC).

Results and interpretation

Pink indicates the presence of viable bacteria and as expected FSL-RIP did not inhibit bacterial growth (Figure 48). To establish if FSL-RIP affected biofilm develop, SS surfaces were analysed with the crystal violet biofilm assay, while bacteria on the BAND-AID ® were removed from the surfaces and subjected to determination of viability of bacteria. Both the 24 hours cultured SS and BAND-AID® surfaces were subjected to SEM imaging.

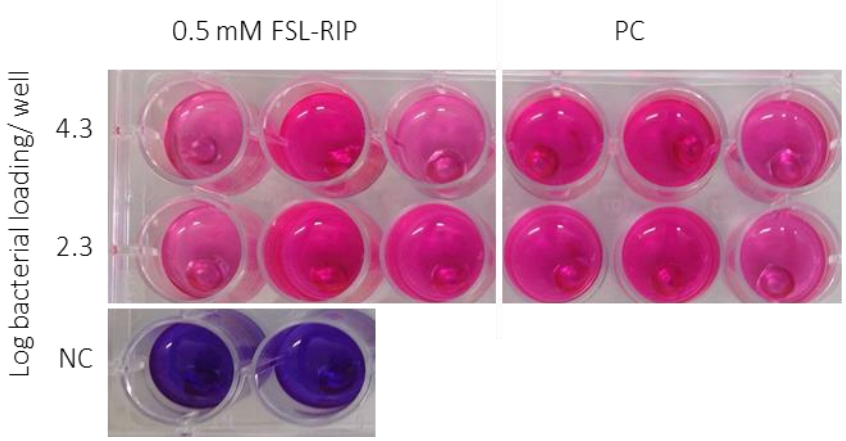

Figure 48.This image show the expected inability of FSL-RIP on SS surfaces to inhibit *S. aureus* bacterial growth. SS discs from these were subjected to SEM/CV analysis to determine of biofilm establishment was affected.

b) Crystal violet biofilm assay on SS surfaces

Methodology overview

After 24 hr culture the SS surfaces (as shown Figure 48) were washed once with sterile water, and then dried. Surfaces were then treated with 100 µL of 0.4% crystal violet and incubated at RT for 10 minutes. After incubation, these surfaces were washed 6 times with water and visualised for presence of bacteria as indicated by purple staining (Figure 49).

Results and interpretation

There appeared to be biofilm reduction on FSL-RIP treated surfaces as indicated by less crystal violet staining in comparison to a surface with no FSL-RIP (Figure 49).

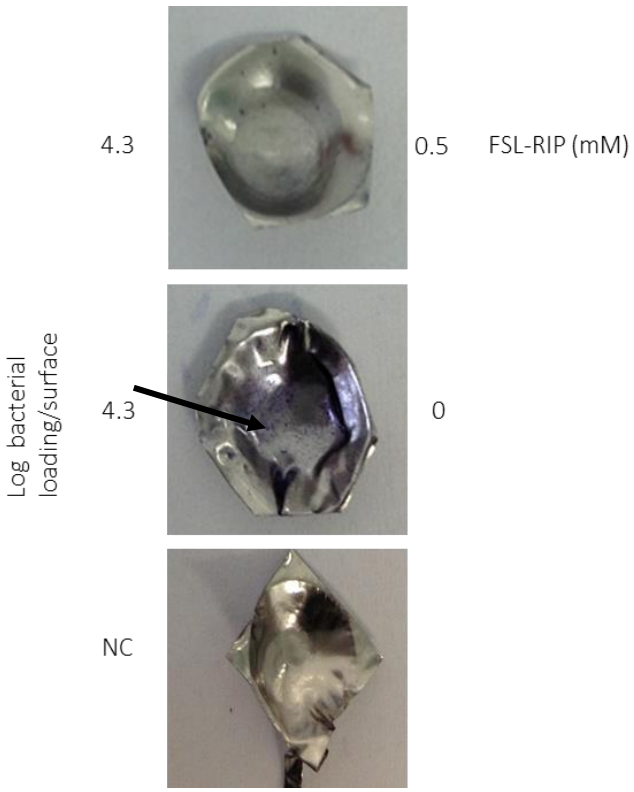

Figure 49. Crystal violet staining of biofilm on FSL-RIP labelled surface. Purple staining was seen on the surface with no RIP and was weak on the 0.5 mM FSL-RIP surfaces. NC was the sterility control. These results were obtained after 24 hr culture.

c) Viability count of bacteria removed from BAND-AID® surfaces

Methodology overview

BAND-AID® (0.25 cm^2) swatches were treated with 50 µL of 0.5 mM FSL-RIP and dried at 80˚C. 10 µL of *S. aureus* suspension was applied to the surface and incubated for 10 minutes at RT. Two different concentration of bacterial loadings (2.3 and 4.3 log) were used. Two lots were prepared, and one lot was washed 3 times with water after labelling with FSL-RIP, While the other was kept unwashed. All the surfaces were bacterially inoculated incubated for 10 minutes and then placed in 24 well tissue culture plate with one mL of MH broth containing resazurin at 0.02%. Each test was prepared in triplicate and incubated at 37 ˚C. Each plate had a growth control (PC) and a sterility control (NC). After 24 hr swatches were removed, washed once in sterile water and placed in 10 mL PBS for removal of viable bacteria. After vortexing for 30 seconds the eluates were serially diluted in 0.1% peptone and 100 µL of each dilution was plated onto Columbia sheep blood agar. Plates incubated for 24 hr at 37 ˚C and colonies were counted.

Results and interpretation

Figure 50 shows the viable bacteria removed from the labelled BAND-AID® surface (as colony forming units). The results obtained showed only a small reduction of bacteria growth on FSL-RIP labelled surfaces. There was no observable difference between washed surface and unwashed surfaces. This observation of bacterial growth by FSL-RIP labelled surfaces was probably due to both plantktonic bacteria and biofilm bound bacteria hence SEM analysis of these samples was carried out to measure effect on biofilm establihment.

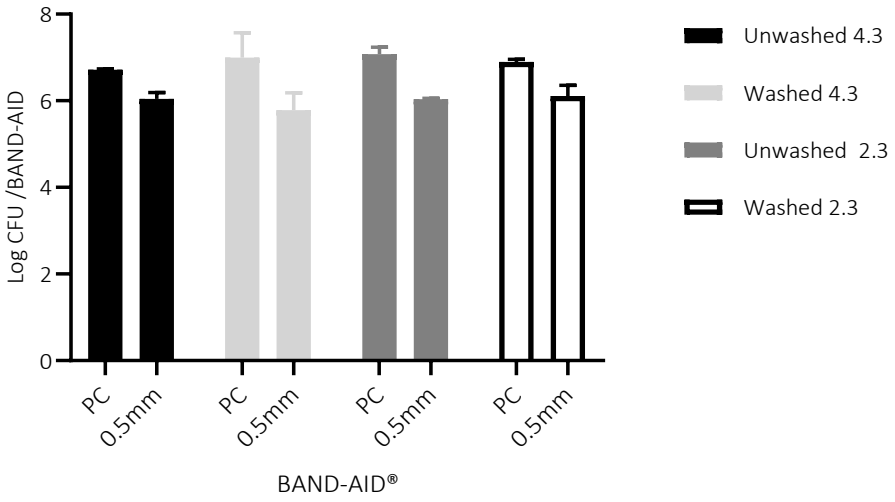

Figure 50. *S. aureus* CFU's removed from FSL-RIP labelled surfaces. This graph composes the presence of viable bacteria in the positive control (PC) compared with 0.5 mM FSL-RIP treated surfaces.

d) SEM analysis

Methodology overview

SEM imaging was used to determine the establishment of biofilms at the surface on both SS and BAND-AID® surfaces. Samples after 24-hr culture were rinsed in water, fixed with 2.5 % glutaraldehyde, washed and dried before platinum sputter coating for SEM analysis.

Results and interpretation

Images in Figure 51 reveal that FSL-RIP significantly reduced the establishment of *S. aureus* biofilm on FSL-RIP treated surface.

.	SS	BAND-AID®
PC	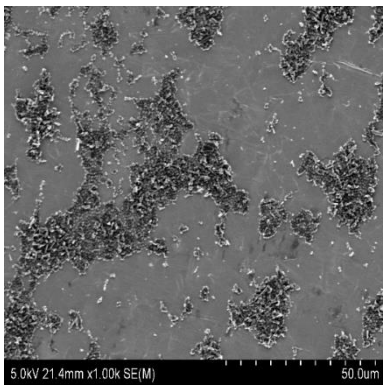	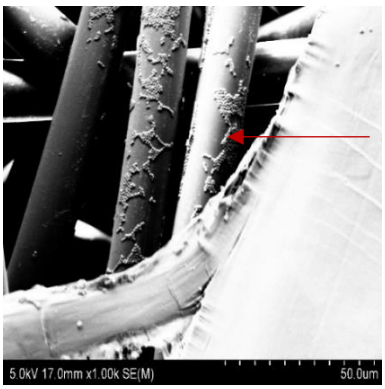
Unwashed	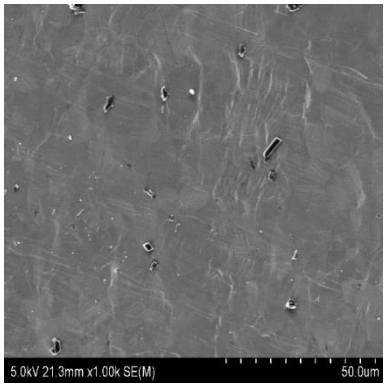	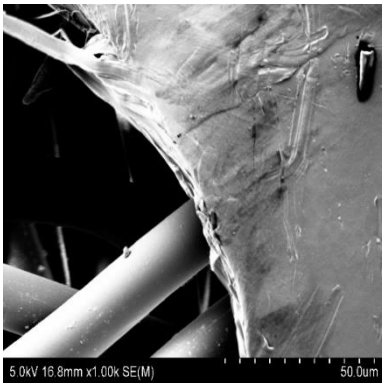
Washed	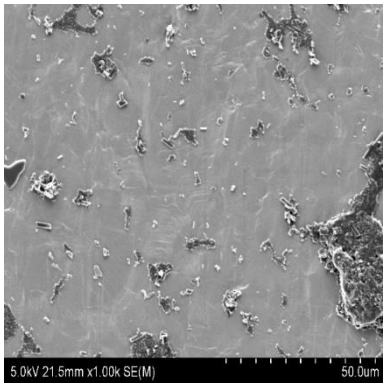	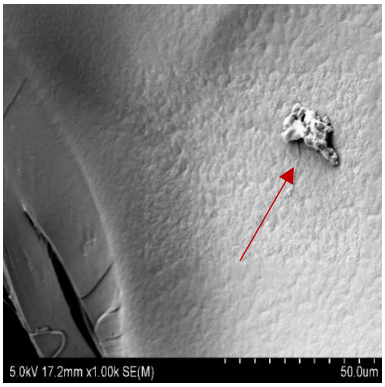

Figure 51. Biofilm formation of *S. aureus* after 1 day on the surfaces of SS, and BAND-AID® with and without washing the surface after labelling with FSL-RIP. Surfaces were inoculated with 2.3 log of S.aureaus. Image relates to surface obtained from the microplates in Figure 48.

4.2 Summary

To summarize three FSL constructs FSL-Se, FSL-SPM and FSL-RIP on surfaces were tested for antibiofilm activity. FSL-Se is the only construct to show antibiofilm activity when present on the surface, while FSL-SPM was shown to increase biofilm formation. FSL-RIP was shown to be able to potentially prevent bacteria from attaching to the surface but did not have any antimicrobial activity.

Chapter 5 Antimicrobial efficacy using FSL charge to capture bioactive compounds

In section 2.5 the ability of FSL molecules to associate with other compounds using charge was demonstrated with crystal violet and silver nanoparticles which was used as a method for detection of FSLs on the surface. The negative charged of the FSL spacer was shown to associate with the positive charge of crystal violet [Cv] (section 2.5.1) while positive charge of FSL-SPM associated with negative charged silver nanoparticles ([-]Agnp) (section 2.5.2). Both crystal violet and silver have antimicrobial activity in their own right. This ability to associate a charged antimicrobial molecules with FSL constructs has the potential to attach antimicrobial compounds to surfaces. The antimicrobial efficiency of the FSL modified surfaces using their associated charge for capture CV and silver on-surfaces was evaluated against four microorganisms (*S. aureus*, *S. epidermidis*, *E. coli* and *P. aeruginosa*).

5.1 Positive charge surface association with [-]Agnp

FSL-SPM is able to modify surfaces and label them with a positive charge, based on the cationic spermine present in the construct. These positive charged FSL-SPM surfaces have been previously established to associate negative charged [-]Agnp (section 2.5.2).

5.1.1 Antimicrobial efficacy of FSL-SPM associated with negative charged silver nanoparticles

In this section, the antimicrobial efficacy of FSL-SPM associated with negativly charged silver nanoparticles, FSL-SPM+ [-]Agnp, was evaluated against *S. aureus*, *S. epidermidis, E. coli* and *P. aeruginosa*.

Methodology

Preparation of FSL-SPM surfaces associated with [-]Agnp

On a 0.25 cm^2 square BAND-AID® swatches, 50 µL of 0.13 mM FSL-SPM in water was placed and dried at 80˚C. These FSL-SPM labelled surfaces were then washed three times in water. Following washing the swatches were placed in 1 mL of 7 % [-]Agnp [prepared as per section 2.5.1] and incubated at RT with shaking for one hr. FSL-SPM labelled BAND-AID® swatches with associated [-] Agnp, FSL-SPM+[-]Agnp, were removed from the solution and washed 3× with water. After drying at 80˚C these swatches were then placed in 96 well plates and infected with bacteria.

Preparation of bacterial inoculum

One loop of frozen bacterial stock culture was plated onto Columbia sheep blood agar using a flame sterilized loop. Plates were incubated at 37˚C for 18-22 hr. 3 colonies of bacterial culture were then inoculated into 10 mL of MH broth and propagated to log phase in a shaking incubator for 4 hr at 37˚C and 200 rpm. The OD of the bacterial culture was taken and adjusted to 0.3 OD for *S. aureus* and *S. epidermidis* and 0.2 OD for *P. aeruginosa* and *E. coli*.

Bacterial assay

The FSL-SPM+[-]Agnp labelled swatches in the microtiter plate were infected with 10 µL of the different bacterial suspensions and incubated at room temperature for 10 minutes. To all the surfaces 50 µL of sterile DI water was added, followed by 150 µL of MH broth containing 0.02% resazurin dye. Plates were then incubated at 37˚C for 24 hr.

Viability assay of bacteria removed from the surface

Each swatch was removed (10/batch) with sterile forceps and placed into a tube containing 10 mL PBS and vortexed for 30 seconds. 50 µL of suspension was removed and diluted 10-fold in 450 µL of 0.1% peptone water (10^{-1}-10^{-3}). 100 µL of undiluted sample and dilutions (10^{-1}-10^{-3}) were spread onto Columbia sheep blood agar with an L spreader. The plates were incubated at 37˚C for 24 hrs and colonies were counted.

Results and interpretation

a) Antimicrobial efficacy against bacteria by resazurin assay

Results in Figure 52 show that FSL-SPM+[-]Agnp surfaces could kill at least 5 log of *P. aeruginosa* and 3 log of *E. coli* (blue colour) initial loading. Individual components FSL-SPM and [+]Agnp on the surface did not show any antimicrobial killing effect against either *P. aeruginosa* or *E. coli* and they were similar to the PC control without any FSL-SPM or FSL-SPM associated [-]Agnp.

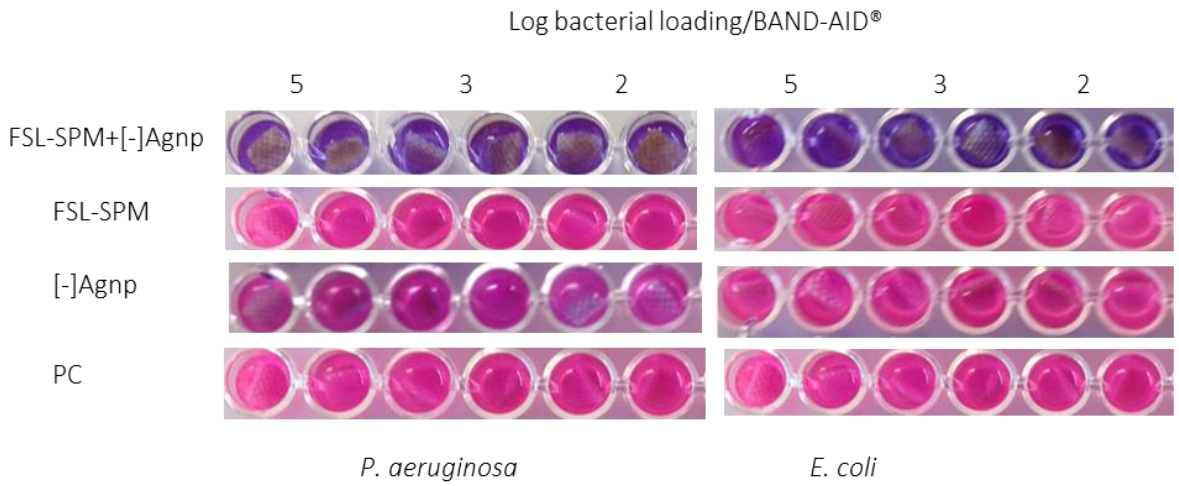

Figure 52. Antimicrobial activity of FSL-SPM+[-]Agnp coated surface against *P. aeruginosa* and *E. coli* showing bacterial growth inhibition at 5 log *P. aeruginosa* 3 log *E. coli* initial loading.

b) Antimicrobial efficacy of FSL-SPM+[-]Agnp labelled surfaces

The antimicrobial efficacy of FSL-SPM+[-]Agnp surfaces was tested against all four microorganisms. The results show the ability of FSL-SPM+[-]Agnp surfaces to inhibit nearly 4.5 log of *S. aureus, S. epidermidis* and *E.coli* initial bacterial loading and more than 6 log of *P. aeruginosa* (Figure 53).

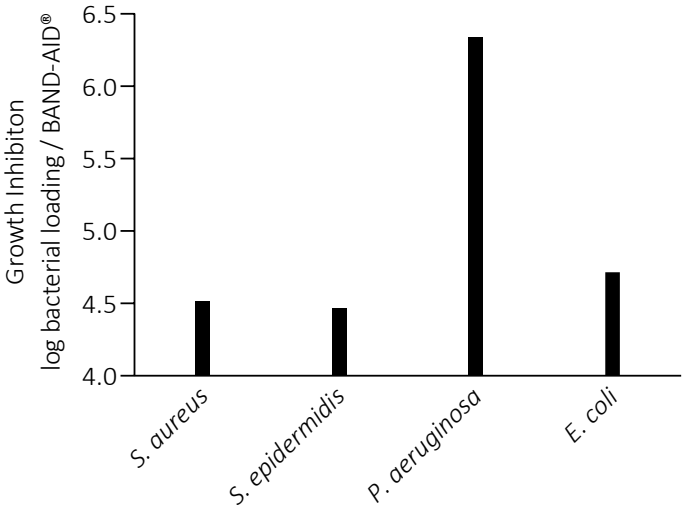

.

Figure 53. Antimicrobial efficacy of FSL-SPM+[-]Agnp on BAND-AID® surfaces. FSL-SPM+[-]Agnp labelled surfaces could inhibit about 4.5 log bacterial loading of *S. aureus, S. epidermis and E. coli* and 6.3 log of *P. aeruginosa.*

FSL-SPM+[-]Agnp surfaces had the most increased antimicrobial activity against *P. aeruginosa* while similar antimicrobial activity was seen with the gram-positive bacteria and *E.coli* . In summary, the presence of FSL-SPM on the surface with associated [-]Agnp could kill and inhibit the growth of both gram-positive and gram-negative bacteria with the highest activity seen against *P. aeruginosa* which previously could not be killed by FSL-Se and FSL-SPM labelled surfaces. (See section 4.1.1.c and 5.1.1.a).

5.2 Capture of positive charged compounds with negative charged FSLs

All CMG-based FSL constructs have a negativly charge spacer and the ability to associate with positive charged material (Section 2.5.1). In this section, the ability of negative charged FSL surfaces to associate with positive charged compounds such as positive charged silver nanoparticles [+]Agnp and Cv, were evaluated and tested for their antimicrobial efficiency. [+]Agnp were tested due to the antimicrobial efficacy previously established for [-]Agnp in section 5.1.1.

5.2.1 Negative charged FSL association with positive charged silver nanoparticles [+]Agnp

In this experiment FSL-Z was used as a model construct to label BAND-AID® surface with a negative charge.

Methodology overview

50 µL of FSL-Z in water was applied to the BAND-AID® surface at 0.13 mM concentration and dried at 80 ˚C. The labelled surfaces was placed in 7% [+]Agnp solution (preparation described in section 2.5.2.b) with shaking for one hr. A control surface with no FSL was included. Swatches were removed, and the absorbance of the remaining solution was read at 412 nm. Based on the values the efficiency of FSL-Z associated [+]AgNP was measured.

Results and interpretation

Result of efficiency % of [+]Agnp association to 0.13 mM labelled FSL-Z surfaces were negative and the same as the unlabelled control surface indicating no association.

This result is contradict to the positive and negative charge association taking place with 0.13 mM FSL-SPM (section 2.5.2.b.ii.) Negative charge FSLs were not used further to associate [+]Agnp.

5.2.2 Negative charge surfaces associate positive charge crystal violet

Crystal violet (Cv) is another positive charged antimicrobial compound, which has previously been demonstrated to associate with negative charged FSLs (FSL-Se) on surfaces (see Section 2.5.1). In this section the antimicrobial efficacy of Cv associated with FSLs was evaluated. Three different CMG based constructs (Figure 11,13 and 14) FSL-Se, FSL-Z and FSL-Bn were used to label the surface with a negative charge and then associate positive charged Cv.

a) Determination of the absorbance of Cv in solution

Calibration curve was created using Cv at different concentrations (0-1000 µM) prepared with 95% ethanol. 100 µL of each concentration was then placed into a 96 well plate and absorbance measured at 590nm. Sample blank was 95% ethanol. The absorbance and concentration of each standard and were plotted and a calibration curve was constructed (Figure 54) to be used to calculate the amount of Cv attached to a surface (after removable with ethanol and measurement of OD).

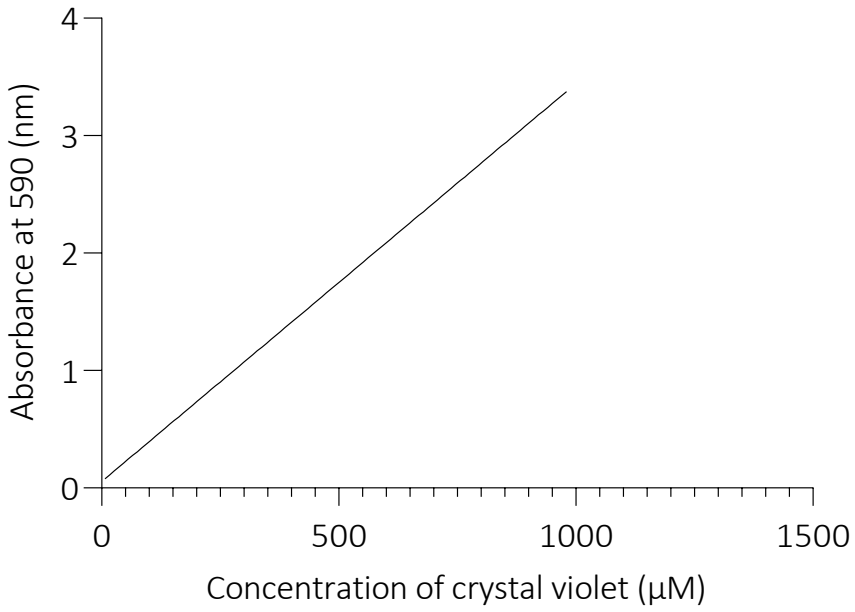

Figure 54. Calibration curve of crystal violet. Plotted by the measure of the absorbance at different concentration of crystal violet (µM). 1.0 OD units=256 µM crystal violet

b) Estimation of the amount of Cv bound to FSL labelled BAND-AID® surfaces

The amount of Cv associated with negativly charge FSL labelled surfaces (FSL-Bn, FSL-Z and FSL-Se) was evaluated to determine the amount of FSL that will associate with Cv. The amount of Cv associated with each FSL concentration was estimated based on the standard calibration curve in Figure 54 and the formula 1 OD unit=256 µM Cv.

Methodology

50 µL of a range of different concentrations of FSL was pipetted onto the BAND-AID® surface and dried at 80˚C. A control without FSL was included as the blank. To the FSL labelled surfaces 100 µL of 0.04% Cv diluted in 95% ethanol was added. After 10 minutes incubation at room temperature surfaces were washed 6 times with water and dried at 80˚C. 200 µL of 95% ethanol was then added to elute the Cv bound to the FSL labelled surface. 100 µL of the solution was transferred to a new microtiter plate and absorbance was read at 590 nm. Based on the calibration curve (Figure 54) the amount of Cv bound to the positively charged FSL labelled surfaces was calculated.

Results and interpretation

The relationship between the concentration of FSL construct on the surface, and the surface-bound Cv was calculated (Table 15).

Table 15. Estimation amount of crystal violet bound to FSL constructs.

FSL construct	mM concentration of FSL on BAND-AID® surface	µM of Cv bound to the surfaces
FSL-Se	1	59
	0.5	226
	0.25	365
	0.13	**264**
	0.06	197
FSL-B	1	134
	0.5	199
	0.25	565
	0.13	**359**
	0.06	199
FSL-Z	1	36
	0.5	367
	0.25	467
	0.13	**408**
	0.06	202

At higher concentrations of FSL the association with Cv decreased. This effect is possibly due to the loss of multilayer of FSL at higher concentrations during washing. Based on the values obtained in Table 15, 0.13 mM concentration was chosen as a working concentration for following experiments because it was the lowest concentration to give maximal associate with Cv.

c) Antimicrobial efficacy of FSL with associated Cv on BAND-AID® surfaces

In this experiment only FSL-Se was used on BAND-AID® surfaces for proof of concept and to reduce the group numbers and make handling easy.

Preparation of antimicrobial surface

50 µL of FSL-Se (0.13 mM) was pipetted onto the BAND-AID® surface and dried at 80˚C. A sterility control without FSL and bacteria, and growth control without FSL but with bacteria were included. To the FSL-Se labelled BAND-AID® surfaces 100 µL of 0.04% Cv diluted in 95% ethanol or water

was added. After incubation at room temperature for 10 minutes, surfaces were washed 6 times with sterile DI water and dried at 80˚C. Surfaces modified with FSL-Se and secondarily associated Cv are referred to as FSL-Se+Cv.

Bacterial assay

Each FSL-Se+Cv swatch was placed in 96 well plate, infected with 10 µL of the different bacterial suspensions and incubated at room temperature for 10 minutes. 50 µL of sterile DI water was then added to all surfaces followed by 150 µL of MH broth. The microtitre plates with the infected swatches in MH broth were then covered and incubated at 37˚C for 24 hr.

Viability assay of bacteria removed from the surface

Each swatch was removed (10/batch approx.) from 24 hr culture with sterile forceps, placed into a tube containing 10 mL PBS and vortexed for 30 seconds. 50 µL was then removed from the PBS and diluted 10-fold in 450 µL of 0.1% peptone water (10^{-1}-10^{-3}). 100 µL of undiluted sample and dilutions (10^{-1}-10^{-3}) were spread onto Columbia sheep blood agar with an L spreader. The plates were then incubated at 37˚C for 24 hr and colonies were counted.

Results and interpretation

Figure 55 shows the antimicrobial activity of FSL-Se+Cv surfaces as determined by viability of bacteria removed from the surface after 24 hr culture. FSL-Se+Cv surfaces had antimicrobial activity against 5 log of gram-positive *S. aureus* and gram-negative *E. coli.* FSL-Se+Cv had antimicrobial effect against 6 log of *S. epidermidis* but no effect against *E. coli* and *S. aureus* at that bacterial loading. FSL-Se+Cv surface had no antimicrobial activity against *P. aeruginosa* at both concentrations of bacterial loading.

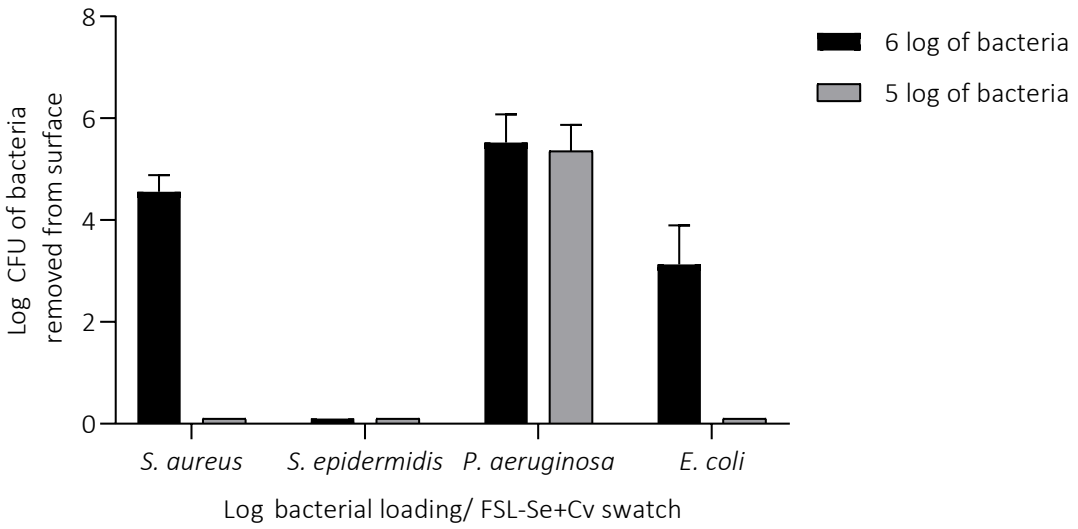

Figure 55. The bactericidal efficacy of FSL-Se+Cv coated BAND-AID® surfaces against four bacteria tested. No growth inhibition was seen against *P. aeruginosa*

Of note, FSL-Se as previously shown (in section 4.1) without the associated Cv had no antimicrobial activity against the tested microorganisms at 0.13 mM. However, of higher concentrations FSL-Se had antimicrobial activity against gram-positive bacteria although not against gram-negative bacteria (section 4.1.1.c). However when FSL-Se associated crystal violet now has antimicrobial activity against gram- negative *E. coli* and gram-positive bacteria.

d) Antimicrobial efficacy of surfaces prewashed before Cv association

In section 2.5.1.b it was shown that pre-washing FSL-Se coated surfaces prior to adding Cv resulted in reduced Cv association. Reduced crystal violet association is expected to result in reduced antimicrobial activity. To determine this washed FSL modified surfaces that contain reduced associated crystal violet and their antimicrobial efficacy were calculated.

Methodology overview

Surfaces were prepared as per methodology above (5.2.2.c). Antimicrobial efficacy of FSL-Se (0.13 mM) labelled surface with associated Cv were compared with FSL-Se surfaces washed 3 in water before used to capture Cv. Except that these surfaces were cultured in MH broth containing resazurin.These surfaces were treated with bacteria and incubated at 37˚C for 24 hr along with resazurin and MH broth.

Results and interpretation

The blue resazurin colour in Figure 56 shows that FSL-Se+Cv prepared without a prewash FSL-Se labelled surfaces, had high antimicrobial activity against 5 log of *S. aureus* bacterial loading while no antimicrobial activity was seen on the surfaces that were prewashed before the Cv association (pink colour). There was also a loss of antimicrobial activity when the surface were infected with less than 3 log of *S. aureus* loading. Similar results were seen with *E. coli* and *S. epidermidis* (data not shown).

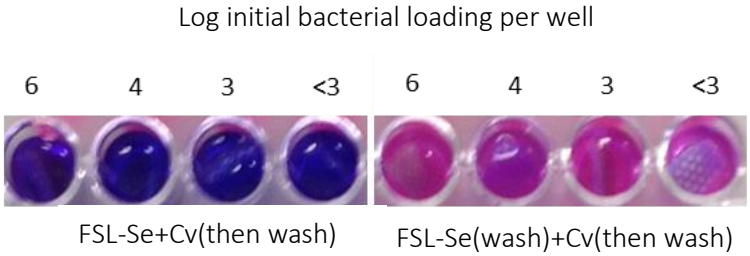

Figure 56. Effect of washing on antimicrobial efficacy of FSL–Se labelled surfaces before Cv association. Surfaces were infected with *S. aureus.* Prewashed FSL-Se (wash)+Cv(then washed) surfaces have lost their antimicrobial activity as indicated by the pink colour after 24 hr culture in the presence of resazurin indicator.

The loss of activity must therefore be due to washing the surfaces, potentially removing layers of FSLs from the surface, and resulting in a reduced amount of Cv association that in turn has affected antimicrobial efficacy. Therefore, following assays were performed without prewashing of the FSL-Se labelled surface before Cv association. It is important to note that washing still occurs but only post reactivity with Cv and it is probable that the Cv also stabilises the FSL layers at the surface,resulting is less loss during later washing phases.

5.2.3 Negative charged FSLs association with positive Cv and then negative charge [-]Agnp

FSL-Se+Cv-labelled BAND-AID® and FSL-SPM+[-]Agnp labelled BAND-AID® exhibited antimicrobial properties in the previous sections (5.2.1 and 5.2.2). Cv associated surfaces exhibited the highest antimicrobial activity against gram-positive bacteria while [-]Agnp associated surfaces exhibited highest activity against gram-negative bacteria. Therefore, a combination of both Cv and [-]Agnp could potentially inhibit both gram-positive and gram-negative bacteria. Based on the charged association, it is possible that a negative charge FSL labelled surface when associated with positive charged Cv could then associate with negative charged [-]Agnp. The following assays were carried

out to establish whether a surface labelled with a negatively charge FSL surface associated with Cv and could associate [-]Agnp, and have antimicrobial activity.

a) Establishing FSL-Se+Cv, FSL-Z+Cv and FSL-Bn+Cv labelled surface association with [-]Agnp

Methodology

Onto BAND-AID® swatches, 50 µL of FSL-Z (0.13 mM) was pipetted and dried at 80˚C. To the FSL-Z labelled surfaces, 100 µL of 0.04% Cv in water was added and incubated at RT for 10 minutes. FSL-Z+Cv labelled BAND-AID® surfaces were then washed 6× with sterile DI water and dried at 80˚C. FSL-Z+Cv associated swatches were then placed in 7% [-]Agnp solution (as per 5.2.1 methodology). Colour change on the surface were then visualized. The capture of Agnp was visualised as previously seen (section 5.2.1).

Results and interpretation

It was observed that FSL-Z+Cv labelled surfaces were not capable to associate [-]Agnp. Instead, Cv was removed from the surface as shown in Figure 57.

FSL-Z+Cv labelled BAND-AID®

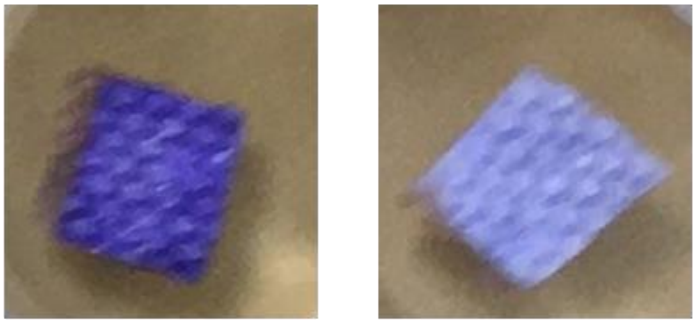

Before [-]Agnp association

After [-]Agnp association

Figure 57. Images of FSL-Z+CV BAND-AID® surfaces before and after [-]Agnp association.

This results observed were unlike the colour change with association of [-]Agnp by FSL-SPM labelled surfaces (section 5.2.1). Therefore the protocol for [-]Agnp association was modified and

[-]Agnp were deposited directly onto surfaces modified with FSL, rather than placing the swatches in a solution of [-]AgNP, as was done with the FSL-SPM+[-]Agnp association (section 5.2.1).

b) Antimicrobial efficacy of FSL-Se+Cv+[-]Agnp, FSL-Z+Cv+[-]Agnp and FSL-Bn+Cv+[-]Agnp surface

The antimicrobial efficacy of FSL-Se+Cv+[-]Agnp, FSL-Z+CV+[-]Agnp, FSL-Bn+Cv+[-]Agnp surfaces were tested for antimicrobial activity.

Methodology

Onto BAND-AID® swatches, 50 µL of FSL- Se/ FSL-Bn / FSL-Z (0.13 mM) was pipetted and dried at 80˚C. To the labelled surfaces 100 µL of 0.04% Cv in water was added and incubated at RT for 10 minutes. The swatches FSL+Cv were then washed 6 times with water and dried at 80˚C (FSL+Cv). 50 µL of [-]Agnp was then deposited on the dry FSL+Cv surface, and incubated for 10 minutes at RT. Swatches were washed 3 times with sterile milli Q water and dried at 80˚C. The FSL-Se+Cv+[-]Agnp, FSL-Bn+Cv+[-]Agnp, FSL-Z+CV+[-]Agnp swatches were placed in 96 well plates, innoculated with 10 µL of bacteria and incubated for 10 minutes at RT. 150 µL of MH broth and 50 µL of sterile water was added to all the surfaces and incubated at 24˚C for 24 hr. BAND-AID® labelled only with Cv or with Cv+[-]Agnp were also used as controls along with a sterility control without FSL and bacteria, and a growth control without FSL but with bacteria. After incubation the swatches were placed in 10 mL PBS and subjected to viability count assay of bacteria removed from the surface as described previously.

Results and interpretation

Figure 58 shows that all three negatively charged FSL constructs FSL-Se, FSL-Bne FSL-Z (FSL-Se+Cv+[-]Agnp, FSL-Bn+Cv+[-]Agnp and FSL-Z +Cv+[-]Agnp) have antimicrobial activity against all four bacteria tested. FSL-Bn+Cv+[-]Agnp had higher antimicrobial activity against *S. aureus* and *S. epidermidis,* while FSL-Z+Cv+[-]Agnp has higher antimicrobial activity against *P. aeruginosa.* FSL-Bn+Cv+[-]Agnp and FSL-Z+Cv+[-]Agnp have similar antimicrobial effect against *E. coli.* The sterility control had no growth indicating the complete process was carried out in sterile conditions. Controls (PC, Cv+[-]Agnp and [-]Agnp) had bacterial growth indicating the absence of antimicrobial effect on the unmodified surface

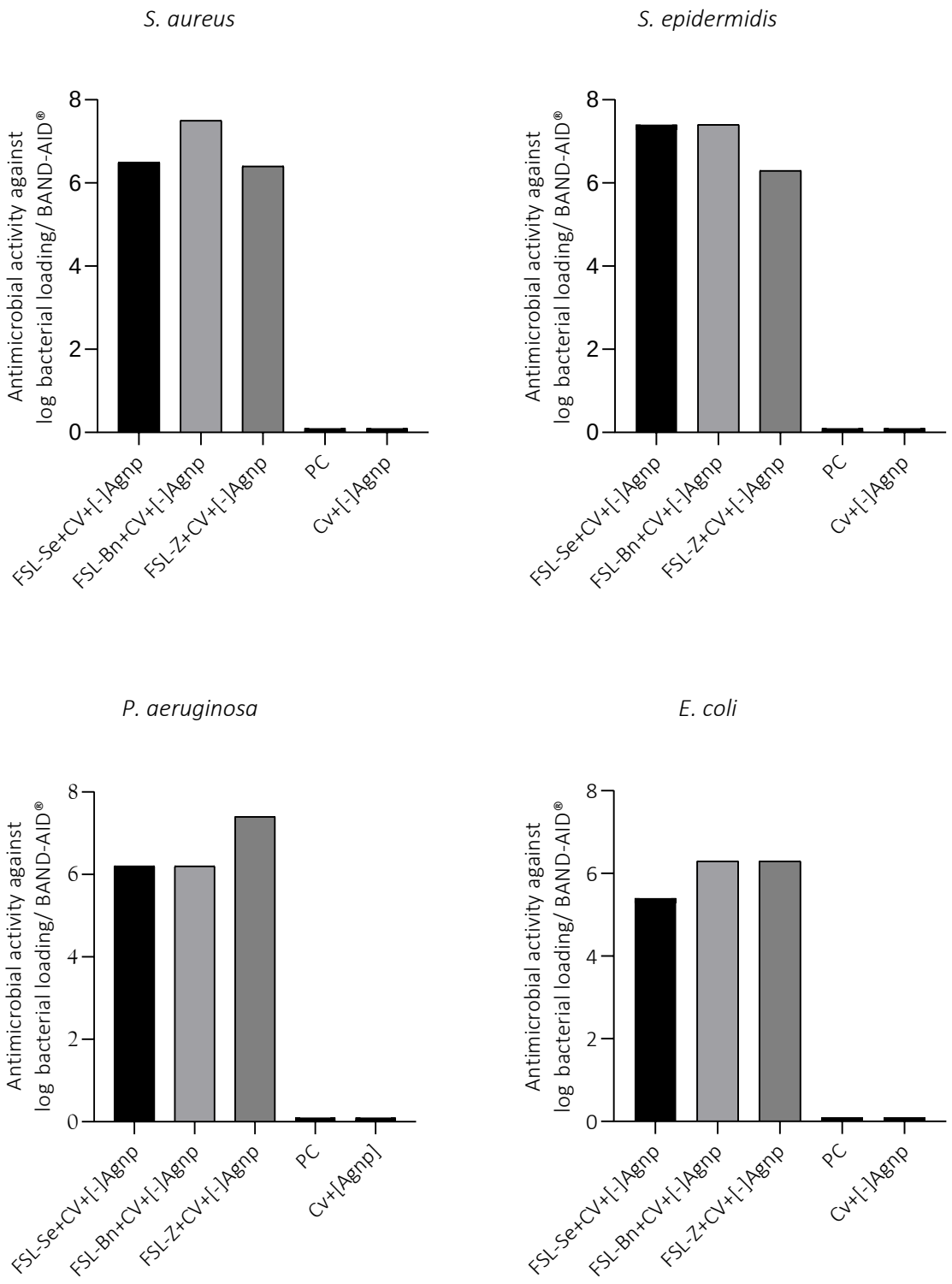

Figure 58. FSL+Cv+[-]Agnp activity against both gram- positive and gram-negative bacteria. The graphs show the log inhibition of each FSL+Cv+[-]Agnp against the four bacteria tested. FSL-Bn+Cv+[-]Agnp has higher antimicrobial activity against *S. aureus* and *S. epidermidis* while FSL-Z+Cv+[-]Agnp has higher antimicrobial activity against *P. aeruginosa.* However, FSL-Bn+Cv+[-]Agnp and FSL-Z+Cv+[-]Agnp have similar antimicrobial effect against *E. coli.*

The above results were statistically analysed using tukey's multiple comparisons for significance differences. The results in Table 16 reveal no significant difference in antimicrobial activity between the FSLs used.

Table 16. Tukey analysis comparison test between different FSLs to find the significant difference.

Tukey's multiple comparisons test	Mean Diff.	Significant?	Summary
FSL-Se+CV+[-]Agnp vs. FSL-Bn+CV+[-]Agnp	-0.49	No	ns
FSL-Se+CV+[-]Agnp vs. FSL-Z+CV+[-]Agnp	-0.24	No	ns
FSL-Bn+CV+[-]Agnp vs. FSL-Z+CV+[-]Agnp	0.25	No	ns

In summary, FSL surfaces were able to capture Cv+[-]Agnp onto BAND-AID® surfaces when the [-]Agnp were dried on the FSL coated surface. FSL associated Cv+[-]Agnp was then shown to have significant antimicrobial activity against both gram-positive and gram-negative bacteria. The requirement for the FSL to be present was proven by a lack of antimicrobial on surfaces without FSL but in the presence of Cv+[-]Agnp (Figure 58). The lack of antimicrobial activity on non-FSL Cv+[-]Agnp surfaces was probably a consequence of the loss of the compound during washing and prior to bacterial innoculation. Hence, the presence of FSL on the surface has resulted in immobilization Cv and [-]Agnp, which result in an antimicrobial surface with activity against both gram-positive and gram-negative bacteria.

5.2.4 Antimicrobial efficacy of FSL+Cv+$AgNO_3$

It was demonstrated that FSL constructs associated with Cv+[-]Agnp have antimicrobial activity. In this section, [-]Agnp the possibility of replacing was considered with $AgNO_3$ due to potential concerns of toxicity of nanoparticles to the human body. Additionally, $AgNO_3$ would act as a control to check if the antimicrobial activity observed to date was simply caused by silver or if it required by the presence of nanoparticles. BAND-AID® swatches coated with FSL-Se, FSL-Z and FSL-Bn, were associated with Cv and then $AgNO_3$ solutions (FSL+Cv+$AgNO_3$) and tested for antimicrobial activity. It should be noted that the FSL binding of negatively charged silver nanoparticles [-]Agnp to FSL+Cv requires a completely different mechanism of action to the potential association with uncharged $AgNO_3$ in solution. The potential that FSL+Cv could capture $AgNO_3$ was considered possible because it has been previously reported the $AgNO_3$ can associate with dyes[253].

Methodology

To BAND-AID® surfaces, 50 µL of FSL- Se/ FSL-Bn / FSL-Z (0.13 mM) was pipetted and dried at 80˚C. To these labelled surfaces, 100 µL of 0.04% Cv in water was added and incubated at RT for 10 minutes and then washed 6 times with water. Surfaces were dried at 80˚C and 50 µL of 1N $AgNO_3$ diluted in water was then deposited on the FSL coated surface and incubated for 10 minutes at RT. Swatches were washed 3 times with sterile water and dried at 80˚C. $AgNO_3$ associated surfaces (FSL-Se+Cv+$AgNO_3$, FSL-Bn+Cv+$AgNO_3$, FSL-Z+Cv+$AgNO_3$) were placed in 96 well plates, infected with 10 µL of bacteria and incubated for 10 minutes at RT. 150 µL of MH broth and 50 µL of sterile water was then added to all the surfaces and incubated at 37˚C for 24 hr. BAND-AID® labelled with Cv or $AgNO_3$ or FSL with associated Cv+[-]Agnp were used as controls along with a sterility (Nc) and growth (Pc) control. Swatches were placed in 10 mL PBS and subjected to the viability count assay of bacteria removed from the surface.

Results and interpretation

Bacteria removed from the BAND-AID® showed that surfaces labelled with FSL-Cv+$AgNO_3$ were highly active against both gram-positive and gram-negative bacteria. The bacterial sensitivity to FSL associated Cv followed by $AgNO_3$ was greater than FSL+Cv+[-]Agnp. Greater antimicrobial activity was noted with FSL-Bn+Cv+$AgNO_3$ and FSL-Z+Cv+$AgNO_3$ than to FSL-Se+CV+$AgNO_3$ (TTable 17). Broth plating agreed with the viability count of bacteria removed from the surface, i.e. when CFU of bacteria removed from the surface showed no bacterial growth, broth plating also showed no bacterial growth.

Table 17. Antimicrobial activity of FSL-Cv+$AgNO_3$ vs FSL-Cv+[-]Agnp coated BAND-AID® swatches.

		Log CFU removed/BAND-AID®						
	Initial bacterial loading	FSL-Se+Cv		FSL-Bn+Cv		FSL-Z+Cv		PC
		[-]Agnp	$AgNO_3$	[-]Agnp	$AgNO_3$	[-]Agnp	$AgNO_3$	
S. aureus	6.7	2.6	2.3	-	-	-	-	6.9
S. epidermidis	6.3	-	-	-	-	-	-	6.7
P. aeruginosa	6.0	3.0	4.8	3.9	-	5.5	-	7.2
E. coli	6.5	2.0	2.9	-	-	4.0	-	6.5

5.2.5 Antimicrobial efficacy of FSL-Z and FSL-Bn premixed with [Cv+$AgNO_3$] before applying on to the surfaces

a) BAND-AID®

To potentially minimise the steps involved, the ability to mix Cv and $AgNO_3$ solutions prior to contacting FSL was evaluated and the antimicrobial efficacy of the FSL contacted with a mix of Cv+$AgNO_3$ was tested.

Methodology

Preparation of FSL-[Bn/Z+[Cv+$AgNO_3$]] surface

Stock solutions of 8 mM Cv and 16 mM $AgNO_3$ were prepared in water and refrigerated until further use and $AgNO_3$ solution was protected from light with aluminium foil. 10 mL of 0.8 mM Cv (solution 1) in water and were prepared from 10 mL of 1.6 mM $AgNO_3$ in water (solution 2) by 10-fold dilution with water. A working [Cv+$AgNO_3$] solution was then prepared by adding equal volumes (5 mL + 5 mL) of solution 1 and 2. Negative FSLs at 0.13 mM were then prepared by adding the working Cv+$AgNO_3$ solution to the FSL powder and mixing to make FSL-[Z+[Cv+$AgNO_3$]] and FSL-[Bn+[Cv+$AgNO_3$]]. 50 µL of freshly reconstituted FSL-[Z+[Cv+$AgNO_3$]], and FSL-[Bn+[Cv+$AgNO_3$]] or controls were then added on to BAND-AID® swatch (0.25 cm^2) and dried. Surfaces were then washed 3× with water and dried at 80 ˚C. (Figure 59)

Antimicrobial assay of FSL-[Bn/Z+[Cv+$AgNO_3$]] labelled surface

Dried swatches were transferred to a sterile 96-well microplate, inoculated with 10 µL bacteria and incubated for 10 min at RT. To the infected swatches, 50 µL of water and 150 µL of MH broth was added and incubated for 24 hr at 37 ˚C with shaking at 200 rpm. Cultured swatches were picked (10/batch approx.) with sterile forceps and placed into Falcon tubes containing 10 mL PBS and vortexed for 30 seconds. 50 µL was removed from PBS and serially diluted in 0.1% peptone water (10^{-1}-10^{-3}) and 100 µL of undiluted sample and serial dilutions (10^{-1}-10^{-3}) were then plated onto Columbia sheep blood agar. Plates were incubated at 37˚C for 24 hr and then CFU were counted. The broth in which the BAND-AID® were placed for 24 hr culture was also plated onto Columbia sheep blood agar after removal of the swatches. Surfaces with Cv, $AgNO_3$, [Cv+$AgNO_3$], FSL+Cv, FSL+$AgNO_3$ were used as controls along with PC and NC. A second batch was prepared for SEM analysis. After 24 hr cultured surfaces were washed 1× with water, and placed in 2.5 % glutaraldehyde for 2 hr at RT. Surfaces were then washed 3 times in water and dried at RT overnight. Fixed samples were then platinum sputter coated for 100 seconds and imaged by SEM.

Results and interpretation

(i) Visual detection of FSL associated [Cv+$AgNO_3$] solution on BAND-AID® surfaces

Figure 59 shows BAND-AID® surface labelled with FSL-[Bn+[Cv+$AgNO_3$]] or FSL-[Z+[Cv+$AgNO_3$]] solution washed then dried at 80˚C, before innoculation with bacteria.

FSL-[Bn+[Cv+$AgNO_3$]]

FSL-[Z+[Cv+$AgNO_3$]]

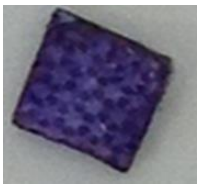

Figure 59. FSL-[Bn+[Cv+$AgNO_3$]] and FSL-[Z+[Cv+$AgNO_3$]] labelled BAND-AID® surface ready for inoculation.

(ii) Viability of bacteria removed from cultured surfaces

Viability of bacteria removed from surfaces after 24 hr cuture shows more growth than compared to FSL labelled surfaces that were prepared by adding Cv and $AgNO_3$ sequentially (Table 18). Both FSL-[Bn+[Cv+$AgNO_3$]] and FSL-[Z+[Cv+$AgNO_3$]] BAND-AID® surfaces show similar results when infected with 5.8 log *S. aureus*. FSL-Bn/Z+CV and FSL-[Bn/Z+[Cv+$AgNO_3$] shows no bacterial activity. While controls Cv, $AgNO_3$, Cv+$AgNO_3$ and [Cv+$AgNO_3$] have shown bacterial activity. However, its activity is less than the activity of PC.

Table 18 shows that of Cv and Cv+AgNO3 are added to the surface then sterility is not achived. (3.0 and 2.7 log growth). In contrast if Cv and Cv+AgNO3 are either added to FSL-Bn or added as a mixture to the surface then sterility is achieved (0 cfu's after 2+ hrs). However if Cv is added to FSL's in the absence of AgNO3 sterlity is not obtained.

Table 18. Antimicrobial activity of FSL association with Cv and $AgNO_3$ on surface when infected with 5.8 log of *S. aureus* loading.

Active component	Presence of component on the BAND-AID®								
Cv	+	+	+			+	+	+	
$AgNO_3$		+	+					+	
Mix [FSL+[Cv+$AgNO_3$]]				+					
FSL-B			+		+	+		+	
FSL-Z							+		
No FSL									+
Log CFU of bacteria removed from the surface after 24 hr culture	3.0	2.7	0	0	7.4	3.4	2.2	0	6.8

+ indicate presence of the active component on the surface.

It is a possibility that when FSL-[Bn/Z+[CV+$AgNO_3$]] added together form a complex which is able to bind more strongly to the surface than sequential addition which potentially results in loss of the molecules by washing. Labelling of the surface with FSL-[Bn/Z+[CV+$AgNO_3$] in a one step process and it showed greater antimicrobial activity than sequential addition of the components. Further experiments were performed with surfaces labelled with FSL-[Bn/Z+[CV+$AgNO_3$]].

(iii) Viability and SEM analysis of FSL-[Bn+[Cv+$AgNO_3$]] against *S. aureus, E. coli* and *P. aeruginosa*

The antimicrobial effect of FSL-[Bn+[Cv+$AgNO_3$]] on BAND-AID® surfaces are shown in Figure 60 by SEM images and viability count of *S. aureus* and *P. aeruginosa*. Both analyses show no bacterial growth on FSL-[Bn+[Cv+$AgNO_3$]] labelled BAND-AID® surfaces, when infected with *S. aureus* and *P. aeruginosa*. The PC had more than 7 log of bacterial growth after 24 hr in culture. Similar results were seen with *S. epidermidis* and *E. coli* (data not shown).

Bacteria	Log bacterial loading	FSL-[Bn+[Cv+$AgNO_3$]]	PC	Log CFU of bacteria removed from the BAND-AID® after 24 hr culture
S. aureus	6.5	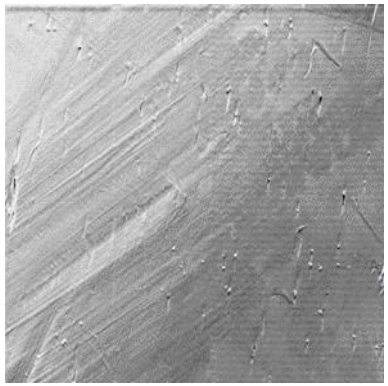	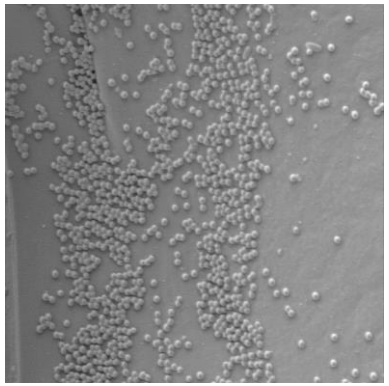	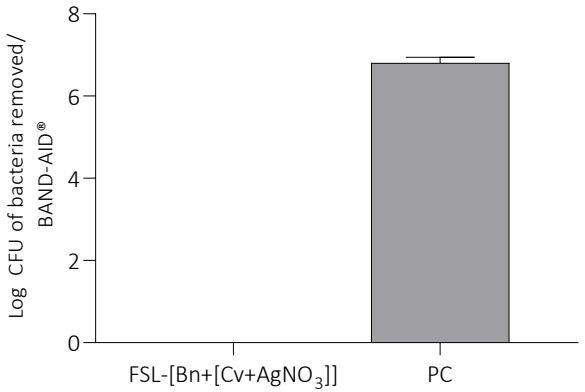
P. aeruginosa	6.9	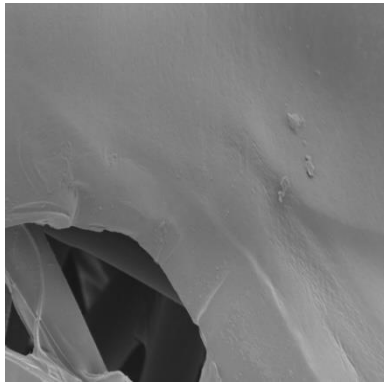	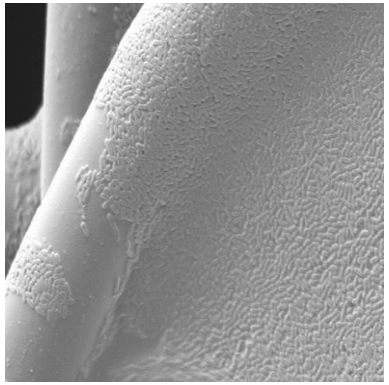	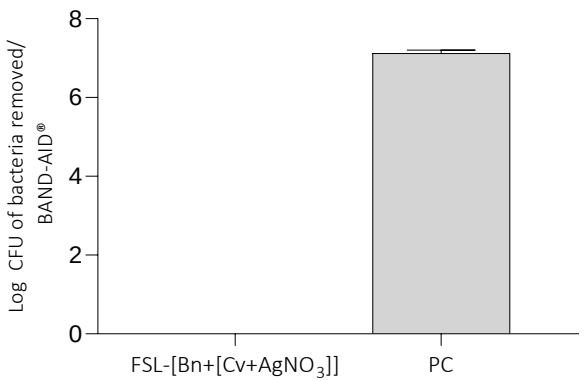

Figure 60. SEM images of FSL-[Bn+[Cv+$AgNO_3$]] BAND-AID® surfaces infected with 6.5 log *S. aureus* and 6.9 log *P. aeruginosa.* No bacterial growth was noted on the FSL-Bn+[Cv+$AgNO_3$] labelled surfaces in comparison to PC. The viability graphs show no bacterial growth on FSL-[Bn+[Cv+$AgNO_3$]] labelled surface. Magnification ×2000

In summary FSL-[Bn+[Cv+$AgNO_3$] on surfaces has antimicrobial activity against both gram-positive and gram-negative bacteria.

(iv) Antimicrobial efficacy of FSL-[Bn+[Cv+$AgNO_3$]] in comparison to silver bandages

Silver bandages are commercially available and widely used in clinical setting, so it was considered important to compare such bandages with FSL-[Bn+[Cv+$AgNO_3$]] labelled BAND-AID® surfaces.

Methodology overview

Antimicrobial efficacy was evaluated with FSL-[Bn+[Cv+$AgNO_3$]] labelled BAND-AID® and unmodified Ag bandage (Durafiber Ag, Smith & Nephew) following the methodology described in section (5.2.5.a). Viable bacteria removed from 24 hr culture were measured as previously described in section (5.2.5.a.ii.).

Results and interpretation

Figure 61 showed FSL-[Bn+[Cv+$AgNO_3$]] labelled BAND-AID® surfaces had antimicrobial efficacy against 7.9 log *S. aureus* loading while Ag bandage was ineffective. However FSL-Bn+[Cv+$AgNO_3$] was ineffective against 6.5 log of *P. aeruginosa* loading while Ag bandage was effective. Both FSL-[Bn+[Cv+$AgNO_3$]] and Ag bandages showed similar antimicrobial effects against *E. coli* and *S. epidermidis.* This similarity and the differences between FSL-Bn+[Cv+$AgNO_3$] and Ag bandage against the bacteria are shown in Table 19. The data shows that the activity of FSL-Bn+[Cv+$AgNO_3$] and Ag bandgaes on *E. coli* and *S. epiderimidis* are not significantly different, while with *S. aureus* and *P. aeruginosa* they differ.

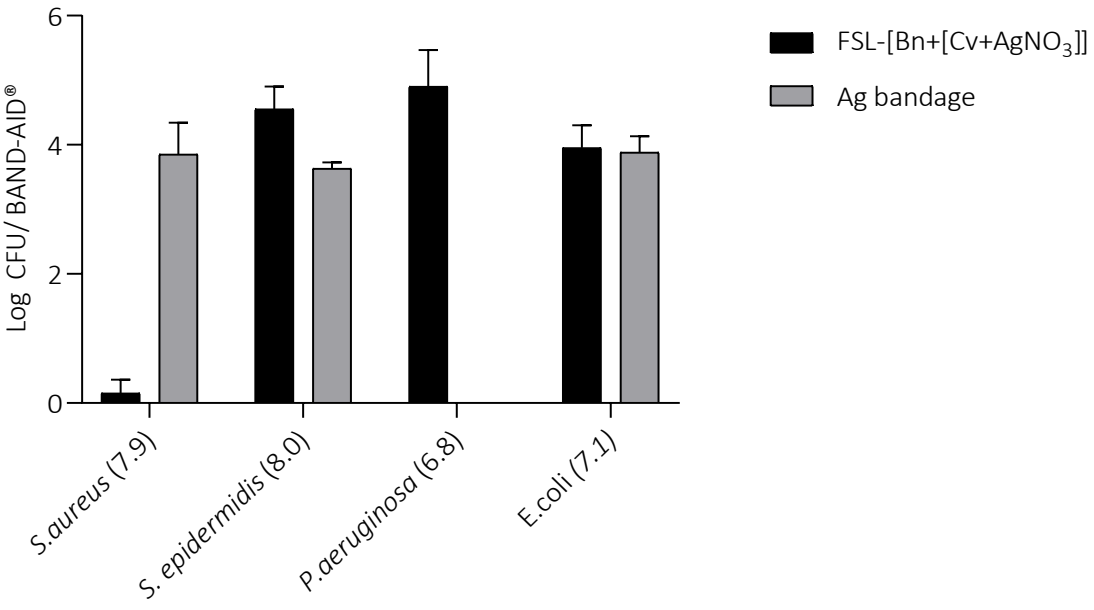

Figure 61. Antimicrobial efficacy of FSL-[Bn+[Cv+$AgNO_3$]] labelled BAND-AID® and Durafiber Ag bandages. The closer to zero the more antimicrobial activity of the sirface, as the assay measures CFU's after incubation.

The antimicrobial efficacy data obtained when comparing of FSL-[Bn+[Cv+$AgNO_3$]] labelled BAND-AID® and Durafiber Ag bandages were subjected to analysis of variance (ANOVA) to find the significant difference in antimicrobial activity of the surfaces against four microorganism (*S. aureus, S. epidermidis, P. aeruginosa* and *E. coli)*. The results (Table 19) from this test as well as those from ANOVA yielded a very low P value, thus indicating that the model was highly significant and reliable. A significant difference was shown in the antimicrobial activity between *S. aureus* and *P. aeruginosa*. The greater number of * reveal highly significant difference. Hence the data shown a significant diferrence.

Table 19. Sidak's multiple comparison test to show the difference in activity between FSL-Bn+[Cv+$AgNO_3$] labelled surfaces and Ag bandages.

	Mean Difference	Significant?	Summary
FSL-[Bn+[Cv+$AgNO_3$]] - Ag bandage			
S.aureus (7.9)	-3.700	Yes	****
S. epidermidis (8.0)	0.9200	No	ns
P.aeruginosa (6.8)	4.900	Yes	****
E.coli *(7.1)*	0.07000	No	ns

b) SS surfaces

Following the demonstration of antimicrobial activity of FSL+[Cv+$AgNO_3$] constructs on BAND-AID® surfaces, these constructs were tested on SS surfaces as an additional medical surface and their antimicrobial efficacy evaluated. FSL-[Bn+[Cv+$AgNO_3$]] and FSL-[Z+[Cv+$AgNO_3$]] were applied to SS surfaces were evaculated against *S. aureus*, *S. epidermidis*, *E. coli* and *P. aeruginosa*.

Methodology

Surface modification

1 cm^2 square SS surfaces were stamped in order to create a well that could hold 50 µL in which the FSLs could be coated. These stamped wells were made to differentiate between a treated side and untreated side (back) and to constrain reactants in a specific area.Stamped SS wells were placed in 24-well culture plates and 50 µL FSL-Bn+[Cv+$AgNO_3$] /FSL-Z+[Cv+$AgNO_3$] no FSL (or as control) was added to the well. Note only the well is coated. Surfaces were then dried at 80 ˚C, washed 3 times with 1 mL of water and dried at 80˚C (Figure 63).

Bacterial assay

Labelled wells surface were innoculated with 10 µL of (10×) bacteria, incubated for 10 minutes at RT. To the entire infected surfaces 1 mL MH broth+ resazurin (prepared as 23 mL of MH broth + 2 mL of 0.02% resazurin) was added and incubated for 24 hr at 37 ˚C shaking. The change in colour produced by the resazurin dye was photographed. Surfaces were then removed from culture and washed 1× by dipping in water and air dried at RT.

Staining with Cv

Cv was used to stain for bacteria biofilms. To the air-dried SS surfaces 100 µL of 0.4% CV in water was added and incubated at RT. After 10 minutes the surfaces were 6× with water and dried. The purple colour on surface was observed and indicated bacterial biofilms.

SEM analysis

Cultured samples were washed once with water and fixed in 2.5% glutaraldehyde, dried at RT and fixed in 2.5% glutaraldehyde for 2 hr. After 3 washes with water the surface was platinum sputter coated for 40 seconds and then imaged using SEM.

Result and interpretation

(i) Visual detection of FSL-[Bn+[Cv+$AgNO_3$]] on SS surface

When the SS surface was labelled with FSL-[Bn+[Cv+$AgNO_3$]] a purple colour was visible on the surface after washing. (Figure 62).

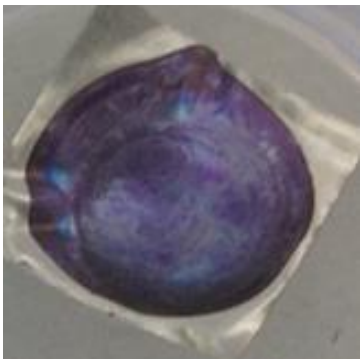

Figure 62. FSL-[Bn+[Cv+$AgNO_3$]] labelled SS surface. Dried at 80˚C.

(ii) Crystal violet biofilm assay

It was noted that after 24 h culture all surfaces including the FSL+[Cv+$AgNO_3$] labelled surfaces, no coloring at the surface was observed because the original bound Cv was lost which meant that the Cv biofilm staining assay was possible. When the SS surfaces were stained with Cv purple coloration was seen on the PC while on the FSL-[Bn+[Cv+$AgNO_3$]] and FSL-[Z+[Cv+$AgNO_3$]] labelled surfaces showed no purple coloration(Figure 63).

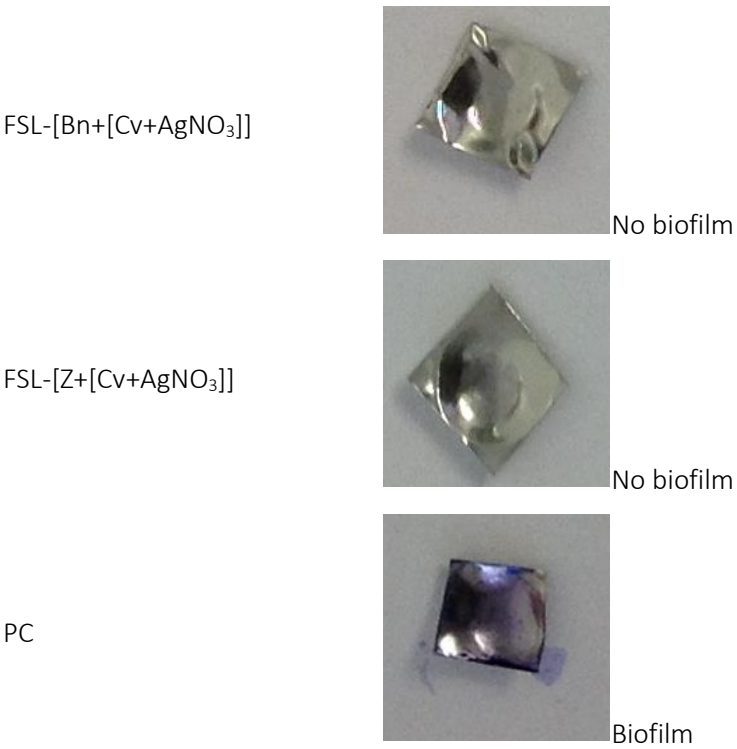

Figure 63. Cv biofilm assay on FSL-[Bn+[Cv+$AgNO_3$]] and FSL-[Z+[Cv+$AgNO_3$]] labelled SS surface when infected with 6.2 log *P. aeruginosa.* Purple colour biofilms seen on PC whereas FSL-[Bn+[Cv+$AgNO_3$]] and FSL-[Z+[Cv+$AgNO_3$]] labelled surfaces were negative for biofilm growth. Similar result was seen for all microorganisms tested.

(iii) SEM analysis

SEM analysis of FSL-[Z+[Cv+$AgNO_3$]] M SS surfaces 24 hr after culture showed no bacterial growth for all the three microorganisms (Figure 64). FSL-[Bn+[Cv+$AgNO_3$]] prevented biofilm formation of *S. aureus* and *E. coli* growth when infected with 6.7 and 6.5 log bacterial loading, respectively. FSL-[Bn+[Cv+$AgNO_3$]] was unable to prevent bacterial biofilm formation of 6.2 log of *P. aeruginosa* bacterial loading, although, reduction in bacterial growth in compared to the PC was observed.

	Log bacterial loading / SS surface	FSL-[Bn+[Cv+$AgNO_3$]]	FSL-[Z+[Cv+$AgNO_3$]]	PC
S. aureus	6.7	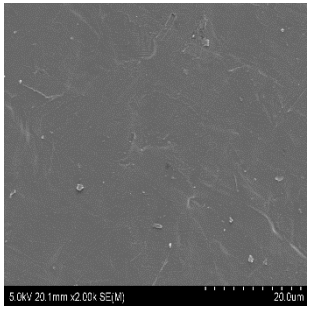	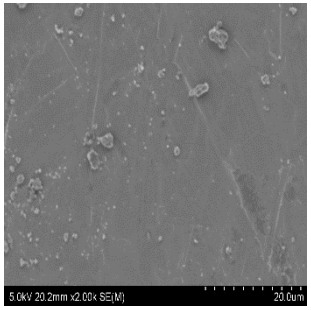	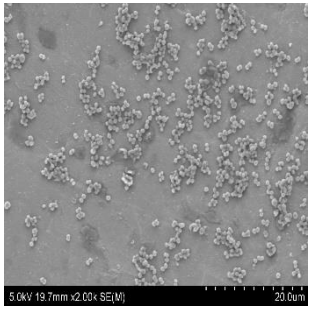
P. aeruginosa	6.2	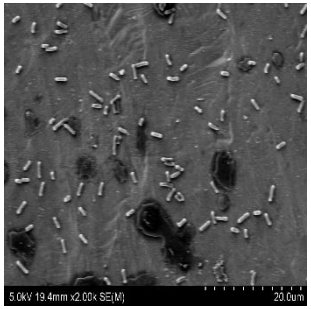	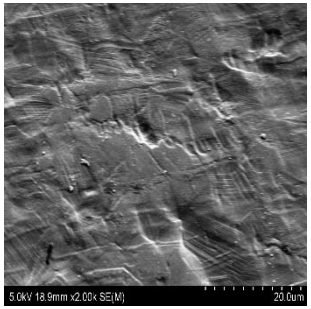	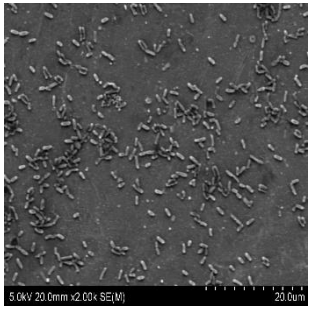
E. coli	6.5	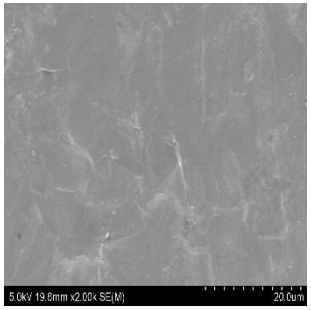	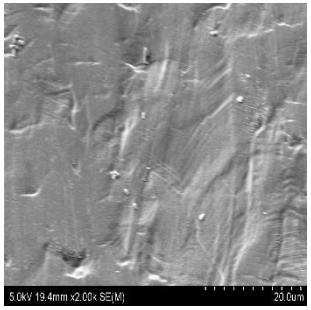	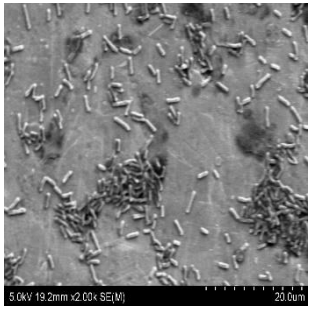

Figure 64. SEM imaging of FSL[Bn/Z+[Cv+$AgNO_3$]] labelled and unlabelled SS surfaces after 24 hr culture.

c) Stability of FSL-[Bn+[Cv+$AgNO_3$]]

(i) Antimicrobial efficacy of FSL-[Bn+[Cv+$AgNO_3$]] labelled BAND-AID® surfaces washed with serum/ plasma

Previous sections were conducted in the absence of serum while this section involves investigation of the antimicrobial effect of FSL-[Bn+[Cv+$AgNO_3$]] labelled surfaces, in the presence of plasma. It should be noted that the surface was washed with serum, but in a dried setting it would be expected that the bacterias would remain localised. Furthermore if sterility is achieved within a short time frame then prolonged explosive to serum is probably of no consequence.

Methodology overview

FSL-[Bn+[Cv+$AgNO_3$]] labelled BAND-AID® were prepared as described in section 5.2. and placed in 100 µL of serum or plasma after Incubate for 1 hr at 37˚C. They were washed 3 times in water and then inoculated with bacteria. Washung was required to remove any potential antimicrobial activity of the serum. All the surfaces were cultured for 24 hr in the presence of MH broth. After 24 hr culture, viable bacteria were removed from the surfaces to estimate the antimicrobial efficiency of the FSL-[Bn+[Cv+$AgNO_3$]] coating in the presence of serum or plasma.

Results and interpretation

Pretreatment of FSL-[Bn+[Cv+$AgNO_3$]] labelled BAND-AID® with serum or plasma reduced its antimicrobial efficacy (Figure 65) in comparison to untreated MH broth controls. Intinguisly serum has a greater reduction in antimicrobial efficacy in comparison to plasma, especially against gram-negative bacteria *P. aeruginosa* and *E. coli*. The reason for this is possibly because plasma contains EDTA which could contribute to an effect in killing bacteria.

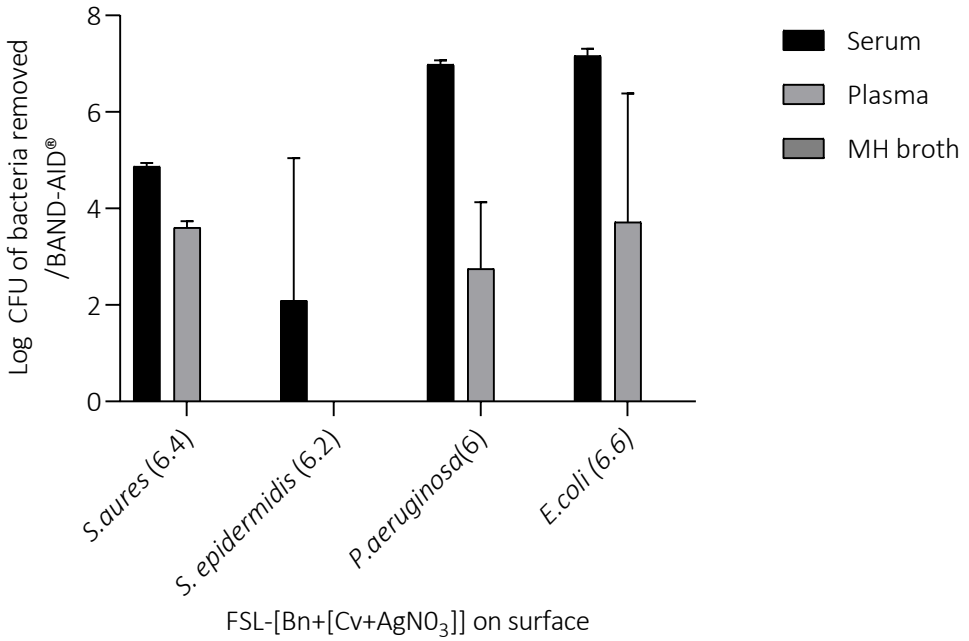

Figure 65. Antimicrobial efficacy of FSL-[Bn+[CV+$AgNO_3$]] in the presence of serum or plasma. Log bacterial loading per swatch is shown in brackets next to each organism.

Statistical analysis using ANOVA and Tukey's test revealed (Table 20) statistically significant differences in antimicrobial activity for serum vs plasma and serum/plasma vs MH broth.

Table 20. Tukeys multiple comparision test for antimicrobial activity in the presence of serum, plasma and MH broth.

Tukey's multiple comparisons test	Significant
Serum vs. plasma	Yes**
Serum vs. MH broth	Yes****
Plasma vs. MH broth	Yes**

(ii) Antimicrobial efficacy of FSL-[Bn+[Cv+$AgNO_3$]] on BAND-AID® in the presence of serum

The antimicrobial efficiency of FSL-[Bn+[Cv+$AgNO_3$]] in the presence of serum and plasma without washing was evaluated.

Methodology overview

FSL-[Bn+[Cv+$AgNO_3$]] solution was prepared as per methodology described in section 5.2.5 and 50 µL applied to BAND-AID® swatch as (0.25 cm^2), dried at 80˚C and then washed 3 times with DI water. Labelled swatches were transferred to sterile 96-well microplate and 50 µL (S 50), 20 µL (S 20) and 5 µL (S 5), of serum was added onto the swatch. The concentration of serum used was always 100% with only variation in only the volume used. One lot was placed in MH broth and incubated at 37˚C for 1 hr. The surfaces were then innoculated with 10 µL of bacteria and then incubated for 10 minutes at RT. 0 µL, 30 µL and 45 µL of water was added to each swatch to correct for volumes and 150 µL of MH broth was then added. Surfaces were incubated for 22 hrs at 37˚C for 200 rpm. Each swatch (10/batch approx) was then picked with sterile forceps and placed into a Falcon tube containing 10 mL PBS and vortexed for 30 seconds 50 µL was removed and serially diluted in 0.1% peptone water and then plated onto Columbia sheep blood agar with L spreader. Incubate following at 37 ˚C for 24 hr CFU were counted.

Results and interpretation

A reduction of antimicrobial efficacy of FSL-[Bn+[Cv+$AgNO_3$]] labelled BAND-AID® in the presence of serum when infected with 6.3 log *S. epidermidis* was seen. (Figure 66). Serum as low as 5 µL increased bacterial activity by 3 logs compared to no serum. A similar effect was seen with *S. aureus*, *P. aeruginosa* and *E. coli* (data not shown). Results clearly show that the presence of serum allowed for establishment of biofilms on the surface. Plesumably by removing or disrupting the FSL-[Bn+[Cv+$AgNO_3$]] layer of the surface.

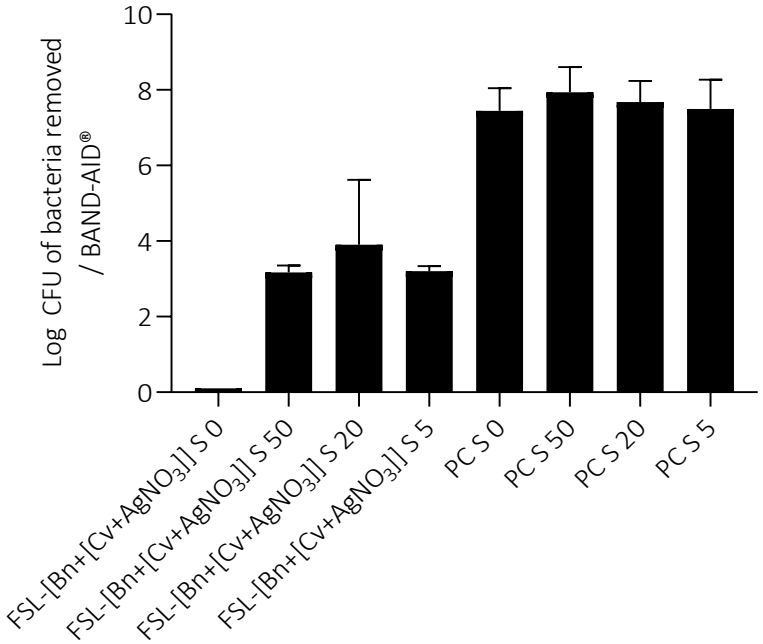

Figure 66. Effect of serum on the antimicrobial efficacy of FSL-[Bn+[Cv+$AgNO_3$]].

(iii) Antimicrobial efficacy of FSL-[Bn+[Cv+$AgNO_3$]] on SS in the presence of serum

The antimicrobial efficacy of FSL-[Bn+[Cv+$AgNO_3$]] on SS was previously established in section 5.2.5.b in-vitro. This section involves the effect of serum on antimicrobial efficiency of FSL-[Bn+[Cv+$AgNO_3$]] on SS.

Methodology overview

Stamped SS surfaces were placed in 24 well plates and were labelled with 50 µL FSL-[Bn+[Cv+$AgNO_3$]] or control, dried at 80˚C and washed 3 times with water. To the se labelled surfaces 50 µL (S 50), 20 µL (S 20) and 5 µL (S 5) of serum was added onto each surface and incubated at 37˚C for 1 hr. Surfaces were then innoculated with 10 µL bacteria, and incubated for 10 minutes at RT. To the appropriate surfaces 0 µL, 30 µL and 45 µL of water to correct of volumes followed by and 950 µL of MH broth. Plates were incubated for 22 hr at 37˚C with 200 rpm. Each surface was removed with sterile forceps and washed with water. Surfaces were dried at RTand stained with 0.4% Cv.

Results and interpretation

The presence of 50 µL of serum reduced the antimicrobial efficacy of FSL-[Bn+[Cv+$AgNO_3$]] OR seen by the presence of purple cv staining of the surfaces after 24 hr culture (Figure 67) (6.2 log *P. aeruginosa* loading). However 20 µL and 5 µL of serum showed less purple staining indicating some bactericidal activity. FSL-[Bn+[Cv+$AgNO_3$]] was negative for bacterial growth in the absence of serum while the PC showed bacterial growth with purple staining in both the presence and absence of serum.

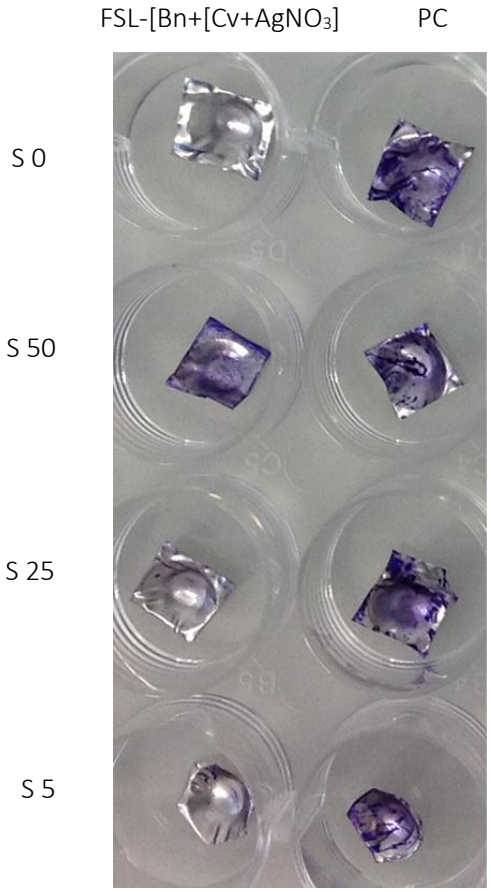

Figure 67. Antibiofilm efficacy of FSL-[Bn+[Cv+$AgNO_3$]] labelled SS surface in the presence of serum. Antimicrobial activity in the presence of serum 0, 50, 20 and 5 µL indicated as S 0, S 50, S 20 and S 5 respectively. 6.2 log *P. aeruginosa* loading.

(iv) Optimising concentrations of crystal violet and silver nitrate

The optimal concentration of Cv and Agno3 was determo by reducing the concentration of Cv and $AgNO_3$ used for the preparation of [Cv+$AgNO_3$] solution.

Methodology overview

Cv was prepared at 0.2, 0.4 and 0.8 mM concentrations while the Agno3 concentration was kept constant and then tested for efficiency as per the generic methodology (Section 5.1.7 methodology). Similarly, another lot was prepared with Agno3 at 0.4, 0.8 and 1.6 mM concentrations while the Cv concentration was kept constant. Antimicrobial efficacy was tested using the generic protocol with viable bacteria being removed from the surface of the BAND-AID® after 24 hr culture.

Results and interpretation

Reduction of Cv from 0.8 mm to 0.4 and 0.2 mM reduced the antimicrobial efficiency of all the four microorganisms tested (Table 21). Cv at 0.4 mM was only able to inhibit and kill *S. epidermidis* growth, but not at 0.2 mM concentration of bacterial at the loading. The best results were seen at 0.8mM of Cv

Table 21. Antimicrobial efficacy of FSL-[Bn+[Cv+$AgNO_3$]] at reducing concentration of Cv

		Log CFU removed/BAND-AID®		
	Log bacterial loading/ BAND-AID®	FSL-[Bn+[Cv+$AgNO_3$]] (Cv @0.2 mM)	FSL-[Bn+[Cv+$AgNO_3$]] (Cv @0.4 mM)	FSL-[Bn+[Cv+$AgNO_3$]] (Cv @0.8 mM)
S. aureus	6.9	3.1	1.7	-
S. epidermis	6.7	4.1	-	-
P. aeruginosa	6.3	3.9	3.2	-
E. coli	6.4	4.8	4.7	-

$AgNO_3$, when used at 0.8 mM concentration had antimicrobial activity against all microorganisms *S. epidermidis* and *E. col* and not against P. aeruginosa. Reduction to 0.4 mM showed a loss in antimicrobial activity against *S. aureus*, *S. epidermidis* and *P. aeruginosa* but was still able to kill *E. coli* (Table 22). The best concentration of $AgNO_3$ was 1.6 mM.

Table 22. Antimicrobial efficacy or FSL-[Bn+[Cv+$AgNO_3$]] labelled surface with reducing concentrations of $AgNO_3$

		Log CFU removed/BAND-AID®		
	Log bacterial loading/ BAND-AID®	FSL-[Bn+[Cv+$AgNO_3$]] ($AgNO_3$ @0.4 mM)	FSL-[Bn+[Cv+$AgNO_3$]] ($AgNO_3$ @0.8mM)	FSL-[Bn+[Cv+$AgNO_3$]] ($AgNO_3$ @1.6 mM)
S. aureus	6.4	4.6	-	-
S. epidermis	6.3	4.9	-	-
P. aeruginosa	6.5	4.8	4.1	-
E. coli	6.1	-	-	-

In Summary, 0.4 mM concentration of Cv and 0.8 mM of $AgNO_3$ solution have been shown to be the optimum concentration for antimicrobial activity against four types of bacteria.

(v) Freeze drying of FSL-[Bn+[Cv+$AgNO_3$]] solution

In the previous experiments a Cv solution is added to an $AgNO_3$ solution, which is then added to the FSL powder (three-steps). In considering a product for commercial use, a potential one-step process was evaluated. Freeze-drying the combined components in one vial for later reconstitution could be advantageous, as reconstitution would be easy and dry product is usually easier to store.

Methodology overview

0.13 mM FSL-[Bn+[Cv+$AgNO_3$]] was prepared a previously using FSL-Bn and [Cv+$AgNO_3$] solution containing Cv 0.4 mM and $AgNO_3$ 0.8 mM and freeze-dried. After reconstitute with 2 mL of water, and vortex 50 µL was added to the BAND-AID® surface (0.25 cm^2). FSL-[Bn+[Cv+$AgNO_3$]] freeze dried and freshly prepared FSL-[Bn+[Cv+$AgNO_3$]] solution was added to two different surfaces. Both surfaces were dried at 80 ˚C and washed 3 times with water and, dried again at 80 ˚C, then infected with bacteria and placed in broth for 24 hr. A viability count of the bacteria removed from cultured samples were done by plate on Columbia sheep blood agar.

Results and interpretation

Freeze dried FSL-[Bn+[Cv+$AgNO_3$]] did not reconstitute well with water and small precipitates formed that did not readily dissolve in water. In contrast FSL-[Bn+[Cv+$AgNO_3$]] when made fresh formed a clear solution.

When the reconstituted freeze dried FSL-[Bn+[Cv+$AgNO_3$]] solution was applied to the BAND-AID® the intensity of the color produced on the surface was reduced (Figure 68), compared to freshly prepared FSL-[Bn+[Cv+$AgNO_3$]], which produced a strong color on the surface of the BAND-AID®.

Figure 68. Reconstituted freeze dried FSL-[Bn+[Cv+$AgNO_3$]] and FSL-[Z+[Cv+$AgNO_3$]] solution applied to BAND-AID® surfaces.

When the antimicrobial efficacy was measured using the generic protocol the freeze dried FSL+[Cv+$AgNO_3$] surfaces had less antimicrobial efficacy (Table 23), compared to FSL complex where made up fresh. All four microorganisms were killed with freshly prepared FSL-[Bn+[Cv+$AgNO_3$]] and FSL-[Z+[Cv+$AgNO_3$]. Where the freeze dried FSL-[Bn+[Cv+$AgNO_3$]] and FSL-[Z+[Cv+$AgNO_3$]] had reduced antimicrobial activity against *S. aureus, E. coli* and *P. aeruginosa* . In the case of *S. epidermidis* freeze dried (FSL-[Bn+[CV+$AgNO_3$]]) had the same efficacy as that of freshly prepared FSL-[Bn+[Cv+$AgNO_3$]], while freeze dried FSL-[Z+[Cv+$AgNO_3$]] had reduced efficacy than freshly prepared. This reduction in antimicrobial efficacy of freeze dried solution was probably due to the precipitation of the Ag. Cv contains a chloride ion that could precipitate $AgNO_3$ as silver chloride. However further investigations are required to prove this.

Table 23. Antimicrobial efficacy of freeze dried FSL-[Cv+$AgNO_3$] on BAND-AID®

		Log CFU of bacteria removed from the BAND-AID®			
	Log bacterial loading/ swatch	FSL-[Bn+[Cv+$AgNO_3$]]		FSL-[Z+[Cv+$AgNO_3$]]	
		Fresh	Freeze dried	Fresh	Freeze dried
S. aureus	5.9	-	1.4	-	1.5
S. epidermidis	6.0	-	-	-	1.3
P. aeruginosa	6.0	-	5.6	-	5.8
E. coli	6.1	-	4.3	-	5.1

Chapter 6 Discussion

Medical surfaces such as stainless steel, contact lenses, surgical and commodity dressings are widely used and can potentially become bacterially contaminated and develop complex bacterial communities known as biofilms. These biofilms develop into an infection that can have profound consequences such as delay in wound healing, cause failure of implant surgery and prolong hospital stays. There is a need for prevention of the initial step of bacterial adhesion on medical surfaces in order to prevent establishment of infection and the complications that follow. Considering the importance of biofilms two approaches are used to prevent biofilm development (i) by preventing bacterial adherence and (ii) killing bacteria that come in contact with the surface. The well known ability of FSL constructs to adhere to surfaces was exploited with a view to attaching antimicrobial coatings to a surface. This thesis concentrated on developing antibiofilm coatings using Kode™ Technology Function-Spacer- lipid (FSL) constructs to

1. Develop FSL-antimicrobials (where the antimicrobial is covalently bound in form of an FSL construct)
2. Use FSLs to capture antimicrobials (where the antimicrobial component is secondarily captured by the FSL).

It is important to appreciate the context for this research; that is it was designed to develop the proof-of-concept principles that Kode Technology could be used as an antimicrobial coating on medical surfaces, and the Kode constructs used in this research are not necessarily those intended as a final product. It is envisioned that future researchers will use the principles developed here and probably exchange the bioactive Cv+$AgNO_3$ with an alternative compound of their own. However, it should also be appreciated that the final proof-of-concept product developed in this research, FSL-[Z+[Cv+$AgNO_3$]] is viable as a coating for medical surfaces.

6.1 Methodology used and its limitations

All methodology has limitations. In order to interpret the data, it is important to also consider the scope and limitations of the experimental procedures used in this research. There are three main aspects to this research to consider. The first is the micro-organisms, the second is the type of surfaces, and the third is the Kode constructs.

6.1.1 Micro-organisms and methods for their detection

a) Micro-organisms

A wide range of microorganisms cause biofilms on implant surfaces and *S. aureus*, *S. epidermidis*, *E. coli* and *P. aeruginosa* were chosen as representatives of bacteria well known and reported to be commonly isolated from infected surfaces. They were chosen as model bacterium to represent both gram-positive and gram-negative bacteria and due to their presence in the environment and ability to produce nosocomial infection[15,67,84,85].

Bacterial cultures were frozen until the time of use. Although there are many ways to store bacteria, storing at -80 °C with glycerol was the most recommended method of storage to keep bacterial cells viable to the freezing conditions and store at a greater cell density for better recovery[254] .

To obtain a pure isolated culture the frozen culture of bacteria was initially streaked on Columbia sheep blood agar. Based on the ability of microorganism to grow on this agar and differ in their haemolytic and morphological characteristics it serves as a primary quality check of the inoculum used.

The isolated colonies from the plates were propagated to a log phase by inoculating in MH broth for four hours. At this time duration all organisms reached a log exponential growth phase that were previously determined by growth curves experiments. At log phase increased number of faster growing cells are present and these are reported to have a maximum biofilm growth rate[255]. Therefore, for all biofilm assays exponentially growing bacteria were used to contaminate the surfaces.

Once the bacterial suspension has reached a log phase the desired concentration of bacteria was measured by adjusting optical density. This is a commonly used method for estimating the concentration of bacteria that represent living and dead bacterial cells in the suspension. In order to ensure the concentration of living cells in the inoculum, the number of viable cells present were validated with plate count agar method.

b) Method for detection

(i) Resazurin assay

In order to study the response of microorganisms to FSL coated BAND-AID® surfaces, conventional biofilm assays were performed to identify the presence of viable bacteria. Since the action of antimicrobial constructs results in killing or reduction of bacterial growth it poses a difficulty in identifying the presence of low bacterial counts. Therefore, in order to amplify the presence of low bacterial numbers, surfaces were placed in growth nutrients for 24 hr where multiplication of 1 or 2 viable bacteria to a detectable concentration (> 3 log) will occur. A colour based resazurin dye was used to visualise presence of bacteria on BAND-AID® and SS surface. As per a previous quantification report on using resazurin dye it was also shown that 3 log of bacteria was required to give in a slight colour change from blue[251]. Therefore, the presence of colour indicated multiplication of 1 or more bacteria present on the surface for a period of 24 hrs to >3 log, while no colour change indicated sterility. To reiterate, the first presence of colour change with resazurin dye was probably due to the presence of less than 10 viable bacteria on the treated surface. Although resazurin has been used as a simple technique to identify bacterial growth, additional quantification methods are also required to identify low biofilm concentration[256].

(ii) SEM (Scanning electron microscopy)

SEM analysis of biofilms on surfaces was used to validate the results obtained in resazurin assay. The presence of bacterial colonies on the surface have been previously reported to be identified with SEM[257]. However, SEM analysis of bacteria on BAND-AID® surfaces has several limitations. For example, the presence of one or two bacteria would not be identified using SEM. However, the presence of one or two bacteria were multiplied to a detectable number in a 24 hr culture they become easily visualised by SEM. Secondly SEM would be unable to identify low bacterial counts embedded between the layers of BAND-AID®. However, when resazurin had indicated bacterial growth by a colour change, bacterial colonies were also identified by SEM. Similarly, when resazurin had shown no colour change, SEM was also unable to detect any bacterial colonies on the surface, indicating sterility.

(iii) Viability of bacteria removed from the surface

Viability of bacteria removed from BAND-AID® was also done to validate the results obtained. For removal of bacteria from BAND-AID® surface vortexing was used. Though sonication and sonication vortexing together have been previously reported to efficiently remove bacteria, in this study vortexing alone was found to have resulted in removal of bacteria from BAND-AID®

surfaces[258,259]. It should however be appreciated, the vortexing will probably only remove some of the bacteria from the surface and is therefore only semi-quantitative. However, SEM analysis showed that when vortexed surfaces were visualised by SEM no bacteria were usually seen on the surface indicating good removal. Hence, vortexing was considered as a suitable method to remove sufficient bacteria from the surface to evaluate establishment of biofilms and sterility. The presence of viable bacteria was calculated using serial dilution of the removed bacteria and plating on Columbia sheep blood agar.

(iv) Crystal violet biofilm assay

The Cv biofilm assay was previously reported to be used to visualise the presence of biofilms[260]. Similarly, in this research the presence of biofilms on SS were visualised with Cv dye. Bacteria adhered to the surface as biofilms are visualised by purple staining. This assay was carried out along with resazurin and SEM imaging. Note, that in this study Cv was also used as an antimicrobial agent.

6.1.2 Surfaces and baseline FSLs

Commercially available BAND-AID® commodity dressings and 316 stainless steel surfaces were used as representative medical surfaces. Labelling of these surface will result in depositing of FSL as a adhered layer and an ablative layer. The adhered layer (FSL constructs that are attached to the surface) will not be easily removed by washing while the ablative layer (FSL constructs that are not directly attached to the surface but form a multilayer over the adhered layer) could be removed when placed in solution. This effect is seen when FSL-Bn labelled surfaces were washed 5× with PBS shown in Figure 21. FSL is seen to be distributed better with increased number of washing. This is due to the distribution of the multilayer or the ablative layer of the construct over the surface.

While labelling FSL onto stainless-steel surfaces due to the flat nature of the surfaces it showed an inability to retain liquid reagents, thereforewells were embossed into the SS surfaces to hold reactants. Apart from the embossed well the remaining regions of the surface were uncoated with FSL construct. However, when labelled surfaces were placed in solution, such as MH broth, removal of multilayers of FSL from the surface could potentially label other regions of the surface which initially were not labelled when the construct was first applied.

FSL-Bn was used as a model construct to exam the ability of FSL to label surfaces. This construct had already been proven to modify almost all surfaces[234], however the concentration used, and its stability on BAND-AID® needed to be studied. The presence of FSL-Bn on BAND-AID® with a well-established enzyme assay showed a stable interaction between FSL-Bn and the surface and this coating was unaffected by the presence of water and PBS. Ethanol, methanol and acetone resulted as expected in removal of the FSLs from the surface. This study confirmed the stable interaction of the FSL construct with surfaces as shown by Barr[234]. Thus, FSL modification techniques were confirmed as suitability to modify medical surface materials.

Baseline experiments of FSL construct interaction with microorganisms also showed the ability of FSL-Bn to label micoorganisms such as gram-positive and gram-negative as previously reported by Barr[234]. While eukaryotic cells such as yeast, *Candida* and *Rhodotorula sp*. were not labelled by FSL-Bn. Hence antimicrobial activity against eukaryotic cells were not considered for further experiments.

In summary FSL constructs were shown to label both medical and bacterial surfaces. FSL when applied to medical surfaces forms a removable ablative layer and an adhered layer. In a clinical setting the ablative layer is lost into solution when in contact with fluids. In such cases it should also be considered that there will be a secondary effect cause by solution phase on the micro-organism (by the FSL's lost from the surface).

6.2 Covalent FSL-antimicrobials

FSL constructs containing covalent antibiofilm functional heads were constructed based on the potential of selenium, spermine and the peptide RIP to inhibit biofilm formation by either preventing bacterial adherence and/or killing bacteria that contacts the surface[1,30,32,68,103,108,168-173.175,192,196,198]. The efficacy of FSL-antimicrobials (FSL-Se, FSL-SPM and FSL-RIP) on medical surfaces was investigated against both gram-positive and gram-negative representative bacteria.

6.2.1 FSL-Spermine (FSL-SPM)

Spermine has been previously reported to be effective in the reduction of planktonic bacteria and prevent biofilm formation[197,198]. Antimicrobial FSLs with covalent spermine were investigated for antimicrobial activity when applied to the surface.

a) Detection of FSL-SPM

Ninhydrin can be used to detect polyamines on paper, thin layer chromatography and electrophoretic procedures[261,262]. Ninhydrin was sprayed onto FSL-SPM labelled surfaces and colour developed by heating to 100˚C. Ninhydrin colour developed with > 0.1 mM of FSL-SPM on labelled surfaces. Additionally, a second detection method was employed using negatively charged silver nanoparticles ([-]Agnp) (section 2.5.2). As FSL-SPM carries a positive charged due to the presence of primary amine could captured [-]Agnp and detect a minimum of 0.03 mM FSL-SPM on BAND-AID® surfaces.

Note these detection methods employed were on prewashed FSL-SPM labelled surfaces (which do not have the additional ablative layers). This is different from the FSL-Se detection on unwashed surfaces (as FSL-Se could not be detected on prewashed labelled surfaces).

b) SPM Biofilm assay

When considering FSL-SPM in both biofilm assays both BAND-AID® surfaces and plastic microtiter plates were measured. Resazurin growth indications of FSL-SPM labelled BAND-AID® showed no growth inhibition of bacteria after 24 hr of culture (Figure 43), even when applied at very high concentrations of 1.6 mM of FSL-SPM.

Biofilm assays on microtiter plates unexpectedly showed enhancement bacterial growth (section 4.1.2.b) rather than inhibition of growth. In these biofilm assays, no growth inhibition was seen with high concentrations of FSL-SPM, while at low FSL-SPM concentrations enhanced bacterial attachment and biofilm formation was seen.

To further evaluate biofilm enhancement activity of FSL-SPM labelled surfaces, SS surfaces were also tested. For these assays high concentrations of FSL-SPM were not used and instead, 0.13mM FSL-SPM concentration was chosen due to its observed ability to increase bacterial growth. The results obtained were similar to that of the microtitre assay and bacterial growth enhancement of *S. aureus* was observed (Figure 44). This characteristic of enhancement of growth by FSL-SPM is probably caused by (i) increased adhesion of bacteria to surface or/and (ii) spermine playing an essential role in bacterial growth and having no significant bactericidal effect. Although this was an undesired outcome, the possibility that this could be a useful technique was explored.

c) Bacterial adhesion using FSL-SPM

Further bacterial adhesion studies were conducted to evaluate the ability of FSL-SPM to increase adhesion including its influence on bacterial contact (section 4.1.3.c). It was found that bacterial attachment on FSL-SPM labelled surfaces occurs with contact as short as one minute for *S. aureus, S. epidermidis* and *E. coli.* In contrast, *P. aeruginosa* required one hour of contact time for enhanced bacterial attachment to surface. Charge based adhesion was probably causing this effect [263]. As bacteria are negatively charged, they would be expected to be attracted to the positively charged FSL-SPM labelled surfaces which could result in the observed increased bacterial adhesion. However it has been reported by Gottenbos et.al. that positively charged surfaces inhibit growth of adhered bacteria, in contrast to the effect seen with FSL-SPM labelled surfaces[264]. It was also possible that released spermine of the FSL construct degradation could possibly enhance bacterial growth as it is an essential component for cell proliferation, growth and numerous other cellular functions[252]. In bacteria, spermine is not synthesized however exogenous spermine uptake is seen when grown in the presence of spermine[252]. There are reports suggesting both presence and absence of antimicrobial activity by spermines[193]. In our experiments FSL-SPM on surfaces had no antimicrobial activity and instead enhanced bacterial growth/ attachment. However, FSL-SPM in solution showed a dose dependent antimicrobial effect on gram-positive and gram-negative bacteria (Table 11). The possible mechanism for this observed activity is not known but activity of FSL-SPM in solution could be due to FSL-SPM existing as nanoparticles which enables the antimicrobial effect as previously reported.

The presence of FSL-SPM as nanoparticles was observed when 0.5 mM of FSL-SPM was analysed using a zeta sizer and the particle size was nearly 100 nm. Hence it is possible that FSL-SPM as nanopartilces could have affected the bacterial cell membrane resulting in bacterial killing, while as a layer on a surface it cannot exert this effect. The mechanism behind the observation was not resolved.

Spermine has been previously reported to have antimicrobial activity against different strains of *S. aureus* and *E.coli* and to produce strain dependent activity[193]. Similarly, when the antimicrobial activity of FSL-SPM in solution against both gram-positive and gram-negative bacteria was evaluated it was shown to exhibit activity against both types of bacteria but increased antimicrobial activity was seen against gram-positive bacteria and less activity against gram-negative bacteria unlike FSL-Se which had shown antimicrobial activity only against gram-positive bacteria. FSL-SPM and FSL-Se differ in their charge and it is unclear if the net charge of the construct affects its antimicrobial ability. But a study conducted on antimicrobial activity

of AMP explains that antimicrobial activity could be affected by charge[265]. That study stated that positively charged AMP could interact with the negatively charged gram-negative lipopolysaccharide and bring about an effect.

In summary, FSL-SPM in solution had antimicrobial activity but when FSL-SPM is applied to the surface the ability to exert an antimicrobial effect was lost and instead bacterial attachment was enhanced.

Despite this negative antimicrobial consequence, the enhancement of biofilm activity by FSL-SPM could have value in other fields. For example, using FSL-SPM, microbial colonies development could be encouraged to develop on surfaces where immobilised bacteria are used such as in some bioreactors[266]. A method for improving these processes could be of value and help to minimise the challenges in establishing biofilms in bioreactors. Further investigation into this enhancement method was outside the antimicrobial scope of this research and no further testing was done.

6.2.2 FSL-Selenium (FSL-Se)

Selenium in the form of nanoparticles or organoselenium has been previously reported to be incorporated onto surfaces such as cellulose discs, titanium surfaces, contact lens, glass, catheters and silicon surfaces and shown to inhibit gram-positive and gram-negative bacterial growth[166,168-170,172-176,179,181,183,236]. Previously, selenium coatings on surfaces were established by dropping desired selenium solution on a titanium surface and drying under laminar flow[179]. Similarly, FSL-Se coatings on surfaces were also evaluated by direct contacting of a desired concentration of FSL construct with the surface, and drying at 80˚C.

a) Detection

Selenium coatings on surfaces such as titanium alloy have been previously reported to be detected using SEM[179]. However, in this study, SEM was not a useful tool in detecting the presence of FSL-Se on BAND-AID surfaces with no differences observed between FSL-Se labelled and unlabelled surfaces. Higher SEM magnification was not suitable as it resulted in surface damage by the electron beam. Additionally, there was no suitable EIA or chemical stainingdetection system available for FSL-Se (low levels).

As a consequence, a charge-based detection method was employed to confirm the presence of FSL-Se on the surface. FSL-Se along with other FSLs such as FSL-Z and FSL-Bn carry a negative charge due to the presence of a CMG spacer. When these FSLs were applied to the surface, the surface is modified by the charge of the FSL that is, it becomes negatively charged. The presence of this negative charge was able to be detected with a positively charged dye Cv. The presence of 0.01 mM FSL-Se on the surface (including the monolayer and the capture of the ablative layer) was easily detected by Cv (Figure 26).

b) Ablative layer FSL-Se

Adding FSLs on to a surface results in attachment of FSLs as both a monolayer and an ablative layer, the latter being able to be removed (ablative) from the surface when in contact with solutions. This ablative layer is seen to be removed by the process of washing as identified by Cv (charge-based) detection techniques. Washed FSL-Se labelled surfaces do not react with Cv. In the case of FSL-Se labelled surfaces (FSL-Se was dried on to the surface and not washed), and the Cv was probably binding the ablative layer of FSLs to the surface. The washing process which sould have resulted in removal of the ablative layer of FSL-Se from the surface, did not appear to do this, suggesting that Cv when applied on to unwashed labelled surfaces binds the FSLs and prevents ablative layer from being lost during washing.

In a clinical/ product setting, the existence of an ablative layer, which is lost into solution could be advantaeous and securing it for slower release would be an important secondary advantage. The loss of these layers could potentially result in controlled release of antimicrobial components into the environment which would possibly result in improved prevention of biofilm initiation.

c) Reduction in hydrophilicity

FSL-Se modification of surfaces resulted in reduction in the hydrophilicity which was verified by contact angle analysis (section 2.5.1.b). This change in the surface property could potentially influence bacterial adhesion on to the surface[243], although in the presence of serum this effect would probably mitigated significantly.

d) Antimicrobial efficacy of FSL-Se modified surfaces

Antimicrobial efficacy of FSL-Se modified surfaces were initially determined with *S. aureus* as a model organism. FSL-Se when applied to the surface exhibited antimicrobial activity against these gram-positive bacteria. The antimicrobial ability of FSL-Se on BAND-AID® surfaces, estimated by

the resazurin indicator had clearly demonstrated the effectiveness of 0.5 mM concentration of FSL-Se to kill 4.3 log of bacteria (Figure 37). Along with resazurin assays, SEM analysis of inoculated FSL-Se surfaces grown for 24 hr also indicated prevention of bacterial adhesion and bacterial growth (Figure 38). This antimicrobial effect could be due to bactericidal activity by the selenium functional head in catalysing the production of superoxide radical that are cytotoxic to bacteria[168-170].

The ablative layer eluting from the labelled surface can form micelles and also bind to the bacterial cell witnbiotinpotentially bringing about a bactericidal effect. The ability of FSL to bind microbial surfaces have been previously shown with FSL-Bn. This labelling of bacteria by FSLs happens in both gram-positive and gram-negative bacteria (Figure 17). Though the precise mechanism of labelling and uptake of FSL constructs by the bacterial surface were not examined, it had been previously reported that benign FSL interaction with bacteria did not alter cell viability[234]. When labelling bacteria with the antimicrobial FSL-Se, the FSL construct will probably still produce superoxides when in contact with the bacterial surface. The superoxide radical gets converted into neutral hydroperoxyl radical in the presence of negatively charged bacterial cell membrane, passes through the cell membrane to form a free radical chain with unsaturated fatty acids of the bacterial cell resulting in bacterial cell death[171]. This antimicrobial activity of selenium has been previously reported for both cocci and bacilli[172]. However, in this study FSL-Se when on surfaces (vs when free in solution) had no antimicrobial activity against gram-negative bacteria. The reason for this is unclear.

e) Contact time

Various aspects were considered for antimicrobial activity. The change in contact time of bacteria with FSL-Se labelled surface shown not to alter the antimicrobial efficacy. i.e. a specific concentration of FSL-Se (0.5mg) affected a certain concentration of bacteria irrespective of the contact time (usually >1 min). When comparing the two gram-positive bacterium, a 0.5 mM concentration FSL-Se was required to kill *S. aureus*, while 0.25 mM was sufficient to kill *S. epidermidis* (Table 12). Of note 3 log of *S. epidermidis* loading could not be grown on untreated BAND-AID® surfaces indicating some existing intrinsic antimicrobial activity of the dressing. Hence the susceptibility of *S. epidermidis* to antimicrobial molecules when compared to *S. aureus* was possibly increased due to the innate antimicrobial effect of the BAND-AID® surface.

f) Monolayer

All these effects were observed on surfaces which had an ablative layer of FSL-Se but, when ablative layerwas reduced to a monolayer (produced by washing), there was a complete loss of antimicrobial activity against gram-positive bacteria (Table 13). Although not certain but based on observations from other FSLs it is assumed that a monolayer of FSL-Se remains present on washed surfaces (although it was below the level of detection of our available assays). This indicates that the amount of selenium present in a monolayer of FSL-Se (bound to the surface) is insufficient to bring about an antimicrobial effect or its mode of action is incompatible with being surface bound as an FSL.

g) FSL-Se in solution

In order to establish the effect of the FSL-Se ablative layer that goes into solution the effect of FSL-Se in solution was determined. The antimicrobial efficacy of FSLs in solution was estimated by resazurin growth indicator.

FSL-Se in solution, had an antimicrobial effect against gram-positive *S. epidermidis* and *S. aureus* while gram-negative bacteria *E. coli* and *P. aeruginosa* were not affected (Table 10). This inconsistency of selenium antimicrobial activity against bacterial strains could be due to the release of reactive ions and oxygen species to which gram-positive bacteria are more susceptible. A similar effect by selenium in the form of nanoparticles has been previously reported, where selenium nanoparticles were shown to exhibit antimicrobial activity against gram-positive *S. epidermidis* but were unable to inhibit *E. coli* [185]. Similarly, organoselenium compounds were found to have high activity against *S. aureus* but weak activity against gram-negative bacteria[179]. However, various studies have also reported that selenium and selenium compounds on surfaces could inhibit the activity of both gram-positive and gram-negative bacteria[166,173,179]. Similarly, Hariharan et al. reported that selenium composite has a higher zone of inhibition against gram-negative bacteria than gram-positive bacteria[187].

h) Selenous acid controls

In this research, FSL-Se in solution proved to have greater antimicrobial activity against *S. aureus* than selenous acid at the same molarity (Figure 35). The ability of the FSL construct to directly bind to the bacterial cell and produce a toxic effect could be the cause for the increased antimicrobial effect of the FSL construct, or the formation of micelles may impart a more powerful effect.

i) FSL-Se on surface and in solution

When FSL-Se on BAND-AID® surfaces were compared to FSL-Se in solution, less antibacterial activity was seen on modified surfaces (Figure 40). This reduction could be due to less availability of the functional head when layering of FSL-constructs occurs at the surface. Similarly, the antimicrobial activity of unlabelled BAND-AID® swatches placed in FSL-Se solution infected with bacteria were compared to FSL-Se labelled swatches. The first had shown a 0.4 log decrease in bacterial activity in comparison to FSL-Se labelled swatches. The minimal variation of activity could be probably be due to the availability of the antimicrobial components present as FSL on the surface.

In summary, FSL-Se could be applied on to medical surface (e.g. SS or dressing) and have antimicrobial activity against gram-positive bacteria.

6.2.3 FSL-antimicrobial peptide RIP (FSL-RIP)

The anti-adhesive property of coated dressing materials is an important factor for minimising bacterial biofilm formation. The ability of RIP (RNA III inhibiting protein) to prevent bacterial attachment by inhibiting the quorum sensing mechanism has been previously reported[267]. RIP has been reported to regulate the quorum sensing mechanism in gram-positive bacteria [102]. Based on this activity FSL-RIP construct was built and applied to surfaces to evaluate its ability to prevent bacterial biofilm establishment (section 4.1.3). The performance of FSL-RIP showed no inhibition of planktonic bacterial growth, no growth inhibition of biofilms, although on unwashed BAND-AID® surfaces (i.e. surfaces with an ablative layer) there was some antibiofilm activity in comparison to monolayer. The failure of washed surfaces to cause total inhibition was probably due to an insufficient FSL remaining bound to the surface to cause an effect, or the peptide being covalently bound to the FSL construct being unable to exert a full effect.

The results obtained with FSL-RIP this study showed some minor activity against *S. aureus* biofilm formation and planktonic bacteria.

In the case of FSL-RIP in solution, antimicrobial activity was tested only against *S. aureus* as it has been shown that the FSL has antibiofilm activity only against *S. aureus* (Figure 36). It is also known to exhibit only antibiofilm and not antimicrobial activity, i.e. RIP has been reported to prevent bacterial attachment to surfaces but not inhibit the growth of planktonic bacteria[103,108]. Similar effects were seen in this research, when tested in solution with resazurin growth indicator, no bacterial killing effect was observed even against 3.5 log of bacterial loading, indicating the

presence of planktonic bacteria and inability to affect bacterial growth. In summary, FSL-RIP has some antibiofilm activity when applied to a surface. These results were sufficiently encouraging that future work with other peptides is warranted. It is intriguing that the RIP peptide retained its functionality (or at least some of it) when covalently conjugated to the FSL. Although the exact mechanism of action for this was not investigated, it does open up the ability to use a large variety of other peptides. Further research in this area is warranted.

6.3 FSL secondary capture of antimicrobials

In an effort to provide a medical surface with an antibiofilm/ antimicrobial coating, the FSLs ability to capture antimicrobial compounds through a second approach utilising the inherent negative charge of the FSLs spacer to capture positively charged antimicrobial compounds was investigated. Negatively charged FSLs such as FSL-Z, FSL-Bn and FSL-Se were used to capture positively charged crystal violet (Cv). The resultant capture of Cv was then used to further capture silver nanoparticles ([-]Agnp). Silver nanoparticles (Agnp) in solution have been previously shown to exhibit antimicrobial activity [146,150,213] and has been reported that Agnp coating on medical devices like catheters, polyurethane foams, dressings have also shown high antimicrobial activity[153,154,268-270] . Additionally, Cv has been used on catheters and shown to have antimicrobial activity[210].

In addition to the use of FSLs with a negative charge, FSL-SPM with a positively charged functional heads was directly used to capture negatively charged antimicrobial compounds such as negatively charged ([-] Agnp.

6.3.1 Negatively charged FSL with captured Cv

Initially negatively charged FSLs with captured Cv were evaluated on surfaces. The antimicrobial activity of negatively charged FSL capture of Cv had high antimicrobial activity against 5 log of *S. aureus*, *S. epidermidis* and *E. coli* (Figure 55). The concentration of FSL-Se used for Cv capture was 0.13mM, as it had shown activity against gram-positive bacteria and gram-negative *E. coli*. *P. aeruginosa* was not susceptible to FSL+Cv (negative charge FSL captured Cv) surface, which is in agreement with literature where Cv is reported to be only moderately effective against *P. aeruginosa* [206]. The results observed clearly show that the antimicrobial activity of FSL+Cv surfaces is due to the presence of Cv on the surface.The presence of Se functional head of FSL had no significant part in bacterial killing similar effects were seen with FSL-Z and FSL-Bn and captured of Cv.

6.3.2 Positively charged FSL-SPM with captured [-]Agnp

FSL-SPM captured [-]Agnp surfaces showed antimicrobial activity against all four bacteria tested. It is of note that FSL-SPM alone does not exhibit antimicrobial activity when applied to the surface, while FSL-SPM+[-]Agnp (Figure 52) exhibited good antimicrobial activity against all four microorganisms including high activity against *P. aeruginosa*. These results were unlike the results observed when Agnp was coated onto plastic catheters by others, who found complete inhibition of *S. aureus* and *E. coli* and only 67% inhibition of *P. aeruginosa*[268]. In both situations with Cv or [-]Agnp capture, the FSLs were required to capture the antimicrobial agents onto the surface as demonstrated by an inability of Cv/[-]Agnp alone to adhere to surfaces without the FSL.

6.3.3 Antimicrobial efficacy of negatively charged FSL captured Cv captured [-]Agnp

FSK captured Cv showed highest activity against *S. aureus*, *S. epidermidis* and *E. coli* while [-]Agnp showed best activity against *P.aeruginosa*, therefore both these antimicrobial components were applied together to a single surface to potentially increase the antimicrobial activity against broad range of microorganisms. Negatively charged FSL labelled surfaces were used to capture positively charged Cv, which was then used to capture [-]Agnp (section 5.2.3) and as expected this coated surface had broad antibiofilm activity against both gram-positive *S. aureus* and *S. epidermidis* and gram-negative *P. aeruginosa* and *E.coli*. Without FSLs, there was no antimicrobial activity at the surface indicating the inability to capture of Cv and [-]Agnp to the surface. Therefore FSLs are essential in immobilising the antimicrobial component Cv (and secondarily [-]Agnp) at the surface (Figure 58).

The capture of Cv+[-]Agnp by FSLs is a charged based effect and a successful attachment of the two components to the surface was achieved by first adding Cv to a negatively charged FSL modified surfaces (with requisite drying). Then to this FSL+Cv coated surface was added [-]Agnp which resulted in the FSL+Cv+[-]Agnp coating. The requirement for drying before the addition of the [-]Agnp was important as direct contact with the [-]Agnp solution resulted in loss of surface bound Cv. In contrast positively charged FSL-SPM surfaces could be directly labelled by contact with [-]Agnp in solution.

The resultant FSL+Cv+[-]Agnp coated surfaces showed significant reduction in adhesion and proliferation of both gram-positive and gram-negative bacteria. This antimicrobial effect was seen with all the negative FSL constructs used (FSL-Se, FSL-Bn and FSL-Z) irrespective of the functional head, demonstrating the capture effect was as a consequence of the spacer. However,

a small difference of up to one log bacteria loading was seen between the different negatively charged FSLs used, suggesting there may be some additional effects/value from the functional head.

FSL-Cv+[-]Agnp surfaces showed antimicrobial activity against all four microorganisms tested and was effective in removal/killing of a minimum of 6 log initial bacterial loading. Moreover, this FSL+CV+[-]Agnp surface showed increased antimicrobial activity in comparison to a Cv or Agnp captured FSL surface (section 5.1.1.b and 5.2.2.c) probably due to combined effect caused by both the captured antimicrobial component Cv and [-]Agnp.

In addition, Cv+[-]Agnp on surfaces with no FSLs had no antimicrobial activity demonstrating the important role of the FSL in capturing Cv+[-]Agnp onto the surface.

6.3.4 Antimicrobial efficacy of negatively charged FSL captured Cv, captured $AgNO_3$

It was considered possible that the antimicrobial activity exhibited by [-]Agnp could also be caused by the presence of silver ions released from Agnp. To determine the reason for antimicrobial activity and significance of silver in [-]Agnp , $AgNO_3$ was considered in the place of [-]Agnp. The ability for silver ions to form complexes with dyes is seen in protein detection methods using electrophoresis and crystal violet [253,271].

When FSL+Cv surfaces were treated with silver in the form of [-]Agnp or $AgNO_3$ (TTable 17) Similar antimicrobial activity was observed. This confirms that silver in the form of [-]Agnp or $AgNO_3$ imparted antimicrobial activity against bacteria. Furthermore, FSL+Cv+$AgNO_3$ exhibited higher activity against gram-negative bacteria in comparison to FSL+Cv+[-]Agnp coated surfaces.
FSL-Bn/Z+Cv+$AgNO_3$ was effective against 6 log of *P. aeruginosa* loading, while FSL-B/Z+Cv+[-]Agnp failed to kill this high bacterial loading. The difference in the amount of silver captured by the two surfaces could probably be a reason for the effect. Additionally, differences in the functional head have shown a difference in antimicrobial effect produced. FSL-Se+Cv+$AgNO_3$ ability to kill bacteria was less when compared to FSL-Bn+Cv+$AgNO_3$ and FSL-Z+Cv+$AgNO_3$ (Table 17). The cause for this effect is unknown however, the orientation of the FSL construct on the surface may play an important role in its ability capture and may account for the variation in antimicrobial activity[272].

6.3.5 Negatively charged FSL captured [Cv and $AgNO_3$]

To minimise the steps involved in creation of FSL+Cv+$AgNO_3$ coated surfaces, Cv and $AgNO_3$ were premixed in solution to form a Cv+$AgNO_3$ complex. Cv was mixed with $AgNO_3$ and then resulting Cv+$AgNO_3$ complex was mixed with FSLs to form a FSL-[B/Z+[Cv+$AgNO_3$]]. This complex had antimicrobial activity against all the four microorganism tested. The results obtained by both SEM analysis and viability of bacteria removed from the surface showed the ability of the complex to prevent biofilm development (Figure 60).

When this complex was compared with commercial silver bandage, FSL-[Bn+[Cv+$AgNO_3$]] labelled BAND-AID® surfaces had antimicrobial efficacy against 7.9 log *S. aureus* loading while Ag bandage was ineffective. While, FSL-[Bn+[Cv+$AgNO_3$]] was ineffective against 6.5 log *P. aeruginosa* loading and Ag bandage was effective in killing this concentration of bacterial loading. Both FSL-[Bn+[Cv+$AgNO_3$]] and Ag bandages showed similar antimicrobial effects against *E. coli* and *S. epidermidis* (section 5.2.5.a.iv). The variation in antimicrobial activity against *S. aureus* and *P. aeruginosa* could possibly be attributed to the amount of Cv and silver present on the surface. The concentration of silver present in silver bandages is probably higher than the silver in FSL+[Cv+$AgNO_3$] and so is more effective in killing high gram-negative *P. aeruginosa* loading [150,154].

The antimicrobial activity of FSL-[Bn+[Cv+$AgNO_3$]] against high *S. aureus* loading could probably be due to the presence of Cv that is absent in the silver bandage. Hence Cv is effective in killing a high loading of gram-positive *S. aureus* while silver is effective in killing *P. aeruginosa*.

FSL-[Bn/Z+[Cv+$AgNO_3$]] had shown antimicrobial activity also on SS surfaces. The antimicrobial ability was detected with Cv biofilm staining techniques along with SEM analysis. Both the methods showed the ability of the complex to effectively prevent bacterial attachment of greater than 6 log bacterial loading of both *S. aureus* and *P. aeruginosa* by killing (Figure 63 and Figure 64.)

The bactericidal effect obtained by 0.8 mM Cv and 1.6 mM of $AgNO_3$ was striking. Reduced or no bactericidal effect was seen when the concentration of Cv and $AgNO_3$ were lowered. Reducing Cv concentration affected all bacteria tested except *S. epidermidis*. This indicates the amount of Cv present is crucial for binding of $AgNO_3$ to form a [Cv+$AgNO_3$] complex. Lowering the concentration of $AgNO_3$ reduced the bactericidal effect against *P. aeruginosa* at 0.8 mM concentration and at 0.4 mM concentration has reduced activity against *S. aureus*, *S. epidermidis* and *E. coli* was seen.

Hence the lower concentrations of $AgNO_3$ probably resulted in reduced silver availability which appears essential for the antimicrobial activity against *P. aeruginosa*.

While using implant surfaces in a clincal setting the antimicrobial activity and the bacterial binding capacity may increase or decrease when in contact with body fluids such as serum and plasma. Serum has been previously reported to affect antimicrobial activity of silver nanoparticles[273]. Similar loss of antimicrobial activity of the FSL-[Bn+[Cv+$AgNO_3$]} complex in the presence of serum and plasma was seen in this research. But the results with plasma showed greater ability to kill bacteria when compared to serum (section 5.2.5.c). This greater antimicrobial activity could be due to presence of EDTA in the plasma that has been previously reported to have antimicrobial activity[274]. In the case of serum, the volume of serum also plays a role in loss of antimicrobial activity. Higher volume of serum resuted in greater the reduction of antimicrobial activity. This was seen on both BAND-AID® and SS surface. The *in-vivo* consequences of the reduction of activity in the presence of serum are yet to be quantified.

In a commercial setting minimisation of steps in production is important. To evaluate this the preparation of a FSL-Bn+[Cv+$AgNO_3$]] as a freeze dried product was considered. However, freeze drying affected the ability of the complex to reconstitute in water and instead formed a precipitate. The precipitate was formed with both FSL-[Z+[Cv+$AgNO_3$]] and FSL-[Bn+[Cv+$AgNO_3$]] and the freeze dried complexes could not be reconstituted in water. The actual cause for the formation of precipitate is unknown and will be investigated in the future, as it would be desirable to have a simple product for immediate use.

6.4 Outcomes of this research

In conclusion, FSL constructs were found to effectively adhere and attach antimicrobials to the surfaces. Surface attachment of antimicrobials is either by a covalently attached antimicrobial or by secondarily captured antimicrobials. Covalently attached antimicrobials FSL-Se, FSL-SPM and FSL-RIP were analysed for their antimicrobial efficacy. Upon initial investigation FSL-Se and FSL-SPM when in solution could kill planktonic bacteria. FSL-Se had some effect a potency as an antimicrobial candiate against gram-positive bacteria when applied to a surface while FSL-RIP had a potency as an antibiofilm candidate against gram-positive *S. aureus.*

FSL secondary captured antimicrobials showed greater antimicrobial activity against all the four microganisms used. This study is the first to show the antibacterial activity of Cv and

silvernanoparticles captured as an antimicrobial and is an illustration of the potential mechanism of Kode technology as an anti-biofilm coating.

The constructs used in this research were developmental prototypes and significant potential exists to improve on them. All the same the antimicrobial effect exerted by the FSL-[Z+[Cv+$AgNO_3$]] exceeded that of silver dressings. The antimicrobial activity of FSL constructs used in the research are is as summarised in Table 24.

Table 24. Summary of antimicrobial ability of FSL construct

FSL construct and complexes	Antimicrobial activity						Comments on antimicrobial ability of FSL on surface
	In Solution	On surface	Gram-positive*		Gram-negative*		
			S. aureus	*S. epidermidis*	*E. coli*	*P. aeruginosa*	
FSL-Se	+	+	+	+	-	-	Antimicrobial activity against 4.6 log of bacterial loading
FSL-SPM	+	-	+	+	+	+	Enhancement of bacterial attachment
FSL-RIP	-	-	-	-	-	-	Prevention of bacterial attachment to surfaces but no growth inhibition
FSL-SPM+[-]Agnp	NT	+	+	+	+	+	Highest activity against *P. aeruginosa*
FSL-Bn/Z/Se+CV	NT	+	+	+	+	-	No antimicrobial activity against *P. aeruginosa*
FSL-Bn/Z/Se+Cv+[-]Agnp	NT	+	+	+	+	+	High antimicrobial activity against four organisms tested
FSL-Bn/Z+Cv+$AgNO_3$	NT	+	+	+	+	+	$AgNO_3$ replaced Agnp with high antimicrobial activity
FSL-[Bn/Z+[Cv+$AgNO_3$]]	NT	+	+	+		+ +	Premixed solution can be applied to any surface and can inhibit both gram-positive and gram-negative bacteria.

*+ indicates antimicrobial activity against the tested, - indicates no antimicrobial activity against the organisms tested, NT-Not tested.

6.5 Future prospects

The results from this study clearly demonstrate that FSLs associated with Cv and silver possess high antimicrobial activity against both gram-positive and gram-negative bacteria. Extension of this research is still required, particularly to establish stability and optimize coating processes and susceptibility of other microorganisms. It will also be desirable to understand the mechanisms of association/dissociation of the Cv and Ag with the FSL construct. It is the hope that this research will have laid down the proof-of concept for the development of Kode Technology for use in prevention of biofilm infection on implant surfaces and dressing materials.

Chapter 7 References

1. Nir S, Zanuy D, Zada T, et al. Tailoring the self-assembly of a tripeptide for the formation of antimicrobial surfaces. Nanoscale 2019;11:8752-9.
2. Ferrer-Espada R, Shahrour H, Pitts B, Stewart PS, Sánchez-Gómez S, Martínez-de-Tejada G. A permeability-increasing drug synergizes with bacterial efflux pump inhibitors and restores susceptibility to antibiotics in multi-drug resistant Pseudomonas aeruginosa strains. Scientific reports 2019;9:3452.
3. McDougal LK, Thornsberry C. The role of beta-lactamase in staphylococcal resistance to penicillinase-resistant penicillins and cephalosporins. Journal of Clinical Microbiology 1986;23:832-9.
4. Neu HC. The crisis in antibiotic resistance. Science 1992;257:1064-73.
5. Blanco P, Hernando-Amado S, Reales-Calderon JA, et al. Bacterial multidrug efflux pumps: much more than antibiotic resistance determinants. Microorganisms 2016;4:14.
6. Webber MA, Piddock LJV. The importance of efflux pumps in bacterial antibiotic resistance. Journal of Antimicrobial Chemotherapy 2003;51:9-11.
7. Hall-Stoodley L, Stoodley P. Evolving concepts in biofilm infections. Cellular Microbiology 2009;11:1034-43.
8. Richardson LA. Understanding and overcoming antibiotic resistance. PLoS biology 2017;15:e2003775.
9. Lambert PA. Bacterial resistance to antibiotics: Modified target sites. Advanced Drug Delivery Reviews 2005;57:1471-85.
10. Davies J. Inactivation of antibiotics and the dissemination of resistance genes. Science 1994;264:375-82.
11. Spratt B. Resistance to antibiotics mediated by target alterations. Science 1994;264:388-93.
12. Hughes G, Webber MA. Novel approaches to the treatment of bacterial biofilm infections. British journal of pharmacology 2017;174:2237-46.
13. Pascale GD, Wright GD. Antibiotic Resistance by Enzyme Inactivation: From Mechanisms to Solutions. ChemBioChem 2010;11:1325-34.
14. Wright GD. Aminoglycoside-modifying enzymes. Current Opinion in Microbiology 1999;2:499-503.
15. Davies J, Davies D. Origins and evolution of antibiotic resistance. Microbiology and molecular biology reviews : MMBR 2010;74:417-33.
16. Gupta A, Mumtaz S, Li C-H, Hussain I, Rotello VM. Combatting antibiotic-resistant bacteria using nanomaterials. Chemical Society Reviews 2019;48:415-27.
17. Sanchez LO, Gustot T. Multidrug-Resistant Bacterial Infection in Patients with Cirrhosis. A Review. Current Hepatology Reports 2019.
18. Mah T-FC, O'Toole GA. Mechanisms of biofilm resistance to antimicrobial agents. Trends in Microbiology 2001;9:34-9.
19. Spoering AL, Lewis K. Biofilms and planktonic cells of *Pseudomonas aeruginosa* have similar resistance to killing by antimicrobials. Journal of bacteriology 2001;183:6746-51.
20. Stewart PS. Mechanisms of antibiotic resistance in bacterial biofilms. International Journal of Medical Microbiology 2002;292:107-13.
21. Cloete TE. Resistance mechanisms of bacteria to antimicrobial compounds. International Biodeterioration & Biodegradation 2003;51:277-82.
22. Lewis K. Riddle of Biofilm Resistance. Antimicrobial Agents and Chemotherapy 2001;45:999-1007.
23. Bürger J, Akgün D, Strube P, Putzier M, Pumberger M. Sonication of removed implants improves microbiological diagnosis of postoperative spinal infections. European Spine Journal 2019:1-7.

24. Widmer AF. New Developments in Diagnosis and Treatment of Infection in Orthopedic Implants. Clinical Infectious Diseases 2001;33:S94-S106.
25. Buch PJ, Chai Y, Goluch ED. Treating Polymicrobial Infections in Chronic Diabetic Wounds. Clinical Microbiology Reviews 2019;32:e00091-18.
26. Akgün D, Bürger J, Pumberger M, Putzier M. C-reactive protein misdiagnoses delayed postoperative spinal implant infections in patients with low-virulent microorganisms. European Spine Journal 2019.
27. Neut D, van Horn JR, van Kooten TG, van der Mei HC, Busscher HJ. Detection of Biomaterial-Associated Infections in Orthopaedic Joint Implants. Clinical Orthopaedics and Related Research 2003;413:261-8.
28. Bürger J, Akgün D, Strube P, Putzier M, Pumberger M. Sonication of removed implants improves microbiological diagnosis of postoperative spinal infections. European Spine Journal 2019.
29. Mohan K, Cox JA, Dickey RM, et al. Treatment of Infected Facial Implants. Seminars in plastic surgery 2016;30:78-82.
30. Kunutsor SK, Beswick AD, Whitehouse MR, Wylde V, Blom AW. Debridement, antibiotics and implant retention for periprosthetic joint infections: A systematic review and meta-analysis of treatment outcomes. Journal of Infection 2018;77:479-88.
31. Qasim S, Swann A, Ashford R. The DAIR (debridement, antibiotics and implant retention) procedure for infected total knee replacement – a literature review2017.
32. Fink B, Anagnostakos K, Winkler H. Periprosthetic Joint Infection. 2019.
33. Argenson JN, Arndt M, Babis G, et al. Hip and knee section, treatment, debridement and retention of implant: Proceedings of international consensus on orthopedic infections. The Journal of Arthroplasty 2019;34:S399-S419.
34. Pfang BG, García-Cañete J, García-Lasheras J, et al. Orthopedic Implant-Associated Infection by Multidrug Resistant Enterobacteriaceae. Journal of Clinical Medicine 2019;8:220.
35. Darouiche RO. Treatment of infections associated with surgical implants. New England Journal of Medicine 2004;350:1422-9.
36. Davis SC, Ricotti C, Cazzaniga A, Welsh E, Eaglstein WH, Mertz PM. Microscopic and physiologic evidence for biofilm-associated wound colonization in vivo. Wound repair and regeneration : official publication of the Wound Healing Society [and] the European Tissue Repair Society 2008;16:23-9.
37. Bjarnsholt T, SpringerLink ebooks B, Life S. Biofilm infections. New York: Springer; 2011.
38. Sibbald RG, Woo K, Ayello EA. Increased bacterial burden and infection: the story of NERDS and STONES. Advances in skin & wound care 2006;19:447.
39. Armbruster CR, Parsek MR. New insight into the early stages of biofilm formation. Proceedings of the National Academy of Sciences 2018;115:4317-9.
40. Katsikogianni M, Missirlis Y. Concise review of mechanisms of bacterial adhesion to biomaterials and of techniques used in estimating bacteria-material interactions. Eur Cell Mater 2004;8:37-57.
41. Behlau I, Gilmore MS. Microbial biofilms in ophthalmology and infectious disease. Archives of Ophthalmology 2008;126:1572-81.
42. Chapman RG, Ostuni E, Liang MN, et al. Polymeric thin films that resist the adsorption of proteins and the adhesion of bacteria. Langmuir 2001;17:1225-33.
43. Dutta D, Cole N, Willcox M. Factors influencing bacterial adhesion to contact lenses. Molecular vision 2012;18:14-21.
44. Kawai K, Urano M, Ebisu S. Effect of surface roughness of porcelain on adhesion of bacteria and their synthesizing glucans. The Journal of Prosthetic Dentistry 2000;83:664-7.
45. Singh VA, Barbul A. Bacterial biofilms in wounds. Wound Repair and Regeneration 2008;16:1-.
46. Garrett TR, Bhakoo M, Zhang Z. Bacterial adhesion and biofilms on surfaces. Progress in Natural Science 2008;18:1049-56.

47. Board OS, Council NR. Opportunities for environmental applications of marine biotechnology: Proceedings of the october 5-6, 1999, workshop: National Academies Press; 2000.
48. Galié S, García-Gutiérrez C, Miguélez EM, Villar CJ, Lombó F. Biofilms in the Food Industry: Health Aspects and Control Methods. Frontiers in microbiology 2018;9:898-.
49. Wagner VE, Iglewski BH. P. aeruginosa Biofilms in CF Infection. Clinical Reviews in Allergy & Immunology 2008;35:124-34.
50. Mancl KA, Kirsner RS, Ajdic D. Wound biofilms: Lessons learned from oral biofilms. Wound Repair and Regeneration 2013;21:352-62.
51. Thomson CH. Biofilms: do they affect wound healing? International Wound Journal 2011;8:63-7.
52. Joo H-S, Otto M. Molecular basis of in vivo biofilm formation by bacterial pathogens. Chemistry & biology 2012;19:1503-13.
53. Zimmerli W. Prosthetic-joint-associated infections. Best Practice & Research Clinical Rheumatology 2006;20:1045-63.
54. Bjarnsholt T. The role of bacterial biofilms in chronic infections. APMIS 2013;121:1-58.
55. Scanlon E. Wound infection and colonisation. Nursing Standard 2005;19:57.
56. Edwards R, Harding KG. Bacteria and wound healing. Current Opinion in Infectious Diseases 2004;17:91-6.
57. Alrawi M, Crowley TP, Pape SA. Bacterial colonisation of the burn wound: A UK experience. Journal of Wound Care 2014;23:274-7.
58. Swindt JK. Wound infection. The American Journal of Surgery 1929;6:137-9.
59. Meers PD, Ayliffe GAJ, Emmerson AM, et al. Wound infections. Journal of Hospital Infection 1981;2:29-34.
60. Peleg AY, Hooper DC. Hospital-Acquired Infections Due to Gram-Negative Bacteria. New England Journal of Medicine 2010;362:1804-13.
61. Ishigami J, Trevisan M, Xu H, Coresh J, Matsushita K, Carrero J-J. Estimated GFR and hospital-acquired infections following major surgery. American Journal of Kidney Diseases 2019;73:11-20.
62. Querido MM, Aguiar L, Neves P, Pereira CC, Teixeira JP. Self-disinfecting surfaces and infection control. Colloids and Surfaces B: Biointerfaces 2019;178:8-21.
63. Hitchman LH, Smith GE, Chetter IC. Prosthetic infections and high-risk surgical populations. Surgery (Oxford) 2019;37:38-44.
64. Hetrick EM, Schoenfisch MH. Reducing implant-related infections: active release strategies. Chemical Society Reviews 2006;35:780-9.
65. Montanaro L, Speziale P, Campoccia D, et al. Scenery of Staphylococcus implant infections in orthopedics. Future microbiology 2011;6:1329-49.
66. Raafat D, Otto M, Reppschläger K, Iqbal J, Holtfreter S. Fighting S*taphylococcus aureu*s Biofilms with Monoclonal Antibodies. Trends in Microbiology 2019;27:303-22.
67. Flurin L, Greenwood-Quaintance KE, Patel R. Microbiology of polymicrobial prosthetic joint infection. Diagnostic Microbiology and Infectious Disease 2019.
68. Hischebeth GT, Randau TM, Ploeger MM, et al. Staphylococcus aureus versus Staphylococcus epidermidis in periprosthetic joint infection—Outcome analysis of methicillin-resistant versus methicillin-susceptible strains. Diagnostic Microbiology and Infectious Disease 2019;93:125-30.
69. Allerberger F, Kasten M, Cockerill F, Krismer M, Dierich M. Listeria monocytogenes infection in prosthetic joints. International orthopaedics 1992;16:237-9.
70. Štádler P, Bìlohlávek O, Špaček M, Michálek P. Diagnosis of vascular prosthesis infection with FDG-PET/CT. Journal of Vascular Surgery 2004;40:1246-7.
71. Joint Lm, Group BIS, Leclercq A, et al. *Listeria monocytogene*s–Associated Joint and Bone Infections: A Study of 43 Consecutive Cases. Clinical Infectious Diseases 2011;54:240-8.
72. Hanssen AD, Brandt CM, Osmon DR, et al. *Staphylococcus aureus* prosthetic joint infection treated with debridement and prosthesis retention. Clinical Infectious Diseases 1997;24:914-9.

73. Wekwejt M, Dziaduszewska M, Pałubicka A. The problem of infections associated with implants–an overview. EJMT 2018;4:21.
74. Hofling-Lima AL, Branco BC, Romano AC, et al. Corneal infections after implantation of intracorneal ring segments. Cornea 2004;23:547-9.
75. Control CfD, Prevention. Invasive Streptococcus pyogenes after allograft implantation--Colorado, 2003. MMWR Morbidity and mortality weekly report 2003;52:1174.
76. Fiaux E, Titecat M, Robineau O, et al. Outcome of patients with streptococcal prosthetic joint infections with special reference to rifampicin combinations. BMC infectious diseases 2016;16:568-.
77. Bulut T, Tahta M, Akgun U, Zengin EC, Ozcan C, Afsar I. Overview of Implant Infections in Orthopaedics Department: Retrospective Study. Journal of Clinical And Analytical Medicine 2016;7:240-3.
78. Wang L, Shang X, Hao Y, et al. Bi-functional titanium-polydopamine-zinc coatings for infection inhibition and enhanced osseointegration. RSC Advances 2019;9:2892-905.
79. Jung J, Schmid NV, Kelm J, Schmitt E, Anagnostakos K. Complications after spacer implantation in the treatment of hip joint infections. International Journal of Medical Sciences 2009;6:265-73.
80. Petersen S, Henke G, Freitag M, Faulhaber A, Ludwig K. Deep prosthesis infection in incisional hernia repair: predictive factors and clinical outcome. European Journal of Surgery 2001;167:453-7.
81. Ronde-Oustau C, Lustig S, Dupieux C, Ferry T, Lyon BJISg. Implant-associated ESBL-Klebsiella pneumonia producing small colony variant bone and joint infection in a healthy 40-year-old man. BMJ Case Reports 2017;2017:bcr2016217542.
82. Sacar S, Turgut H, Toprak S, et al. A retrospective study of central nervous system shunt infections diagnosed in a university hospital during a 4-year period. BMC Infectious Diseases 2006;6:43.
83. Morand PC, Billoet A, Rottman M, et al. Specific distribution within the Enterobacter cloacae complex of strains isolated from infected orthopedic implants. Journal of Clinical Microbiology 2009;47:2489-95.
84. Scotland KB, Lo J, Grgic T, Lange D. Ureteral stent-associated infection and sepsis: pathogenesis and prevention: a review. Biofouling 2019:1-11.
85. Papadopoulos A, Ribera A, Mavrogenis AF, et al. Multidrug-resistant and extensively drug-resistant Gram-negative prosthetic joint infections: Role of surgery and impact of colistin administration. International Journal of Antimicrobial Agents 2019;53:294-301.
86. Costerton JW, Stewart PS, Greenberg EP. Bacterial biofilms: A common cause of persistent infections. Science 1999;284:1318-22.
87. Verstraelen H, Swidsinski A. The biofilm in bacterial vaginosis: implications for epidemiology, diagnosis and treatment: 2018 update. Current opinion in infectious diseases 2019;32:38-42.
88. Xu L-C, Siedlecki CA. Submicron-textured biomaterial surface reduces staphylococcal bacterial adhesion and biofilm formation. Acta Biomaterialia 2012;8:72-81.
89. Yeo I-S, Kim H-Y, Lim KS, Han J-S. Implant Surface Factors and Bacterial Adhesion: A Review of the Literature. The International Journal of Artificial Organs 2012;35:762-72.
90. Busscher HJ, Rinastiti M, Siswomihardjo W, van der Mei HC. Biofilm formation on dental restorative and implant materials. Journal of Dental Research 2010;89:657-65.
91. Danese PN. Antibiofilm approaches: Prevention of catheter colonization. Chemistry & Biology 2002;9:873-80.
92. Raja RH, Raucci G, Hook M. Peptide analogs to a fibronectin receptor inhibit attachment of *Staphylococcus aureus* to fibronectin-containing substrates. Infection and Immunity 1990;58:2593-8.
93. Bračič M, Fras-Zemljič L, Pérez L, et al. Protein-repellent and antimicrobial nanoparticle coatings from hyaluronic acid and a lysine-derived biocompatible surfactant. Journal of Materials Chemistry B 2017;5:3888-97.

94. Gao Q, Yu M, Su Y, et al. Rationally designed dual functional block copolymers for bottlebrush-like coatings: In vitro and in vivo antimicrobial, antibiofilm, and antifouling properties. Acta Biomaterialia 2017;51:112-24.
95. Pan C, Zhou Z, Yu X. Coatings as the useful drug delivery system for the prevention of implant-related infections. Journal of orthopaedic surgery and research 2018;13:220-.
96. Silva-Dias A, Palmeira-de-Oliveira A, Miranda I, et al. Anti-biofilm activity of low-molecular weight chitosan hydrogel against *Candida species*. Medical Microbiology and Immunology 2014;203:25-33.
97. Li P, Poon YF, Li W, et al. A polycationic antimicrobial and biocompatible hydrogel with microbe membrane suctioning ability. Nature Materials 2010;10:149.
98. Harris LG, Tosatti S, Wieland M, Textor M, Richards RG. *Staphylococcus aureus* adhesion to titanium oxide surfaces coated with non-functionalized and peptide-functionalized poly(l-lysine)-grafted-poly(ethylene glycol) copolymers. Biomaterials 2004;25:4135-48.
99. Wong TW, Ramli NA. Carboxymethylcellulose film for bacterial wound infection control and healing. Carbohydrate polymers 2014;112:367-75.
100. Nowatzki PJ, Koepsel RR, Stoodley P, et al. Salicylic acid-releasing polyurethane acrylate polymers as anti-biofilm urological catheter coatings. Acta Biomaterialia 2012;8:1869-80.
101. Pompilio A, Scocchi M, Pomponio S, et al. Antibacterial and anti-biofilm effects of cathelicidin peptides against pathogens isolated from cystic fibrosis patients. Peptides 2011;32:1807-14.
102. Cirioni O, Giacometti A, Ghiselli R, et al. RNAIII-inhibiting peptide significantly reduces bacterial load and enhances the effect of antibiotics in the treatment of central venous catheter—associated staphylococcus aureus infections. The Journal of Infectious Diseases 2006;193:180-6.
103. Gov Y, Bitler A, Dell'Acqua G, Torres JV, Balaban N. RNAIII inhibiting peptide (RIP), a global inhibitor of Staphylococcus aureus pathogenesis: structure and function analysis. Peptides 2001;22:1609-20.
104. Novick RP. Activation and Inhibition of the Staphylococcal AGR System. Science 2000;287:391a-.
105. Giacometti A, Cirioni O, Gov Y, et al. RNA III inhibiting peptide inhibits in vivo biofilm formation by drug-resistant Staphylococcus aureus. Antimicrobial Agents and Chemotherapy 2003;47:1979-83.
106. Otto M. Quorum-sensing control in *Staphylococci* – a target for antimicrobial drug therapy? FEMS Microbiology Letters 2004;241:135-41.
107. Bryers JD, Ratner BD. Bioinspired implant materials befuddle bacteria. American Society for Microbiology 2004;70:232-.
108. Balaban N, Cirioni O, Giacometti A, et al. Treatment of Staphylococcus aureus Biofilm Infection by the Quorum-Sensing Inhibitor RIP. Antimicrobial Agents and Chemotherapy 2007;51:2226-9.
109. Anguita-Alonso P, Hanssen AD, Patel R. Prosthetic joint infection. Expert review of anti-infective therapy 2005;3:797-804.
110. Kaplan JB. Therapeutic potential of biofilm-dispersing enzymes. The International Journal of Artificial Organs 2009;32:545-54.
111. Jorge P, Alves D, Pereira MO. Catalysing the way towards antimicrobial effectiveness: a systematic analysis and a new online resource for antimicrobial enzyme combinations against Pseudomonas aeruginosa and Staphylococcus aureus. International journal of antimicrobial agents 2019.
112. Pavlukhina SV, Kaplan JB, Xu L, et al. Noneluting enzymatic antibiofilm coatings. Acs Applied Materials & Interfaces 2012;4:4708-16.
113. Whitchurch CB, Tolker-Nielsen T, Ragas PC, Mattick JS. Extracellular DNA Required for Bacterial Biofilm Formation. Science 2002;295:1487-.
114. Swartjes JJTM, Das T, Sharifi S, et al. A Functional DNase I Coating to Prevent Adhesion of Bacteria and the Formation of Biofilm. Advanced Functional Materials 2013;23:2843-9.

115. Kerrigan JE, Ragunath C, Kandra L, et al. Modeling and biochemical analysis of the activity of antibiofilm agent Dispersin B. Acta biologica Hungarica 2008;59:439-51.
116. Soccol VT, Pandey A, Resende RR. Current Developments in Biotechnology and Bioengineering: Human and Animal Health Applications: Elsevier; 2016.
117. DeMarco ML. Three-Dimensional Structure of Glycolipids in Biological Membranes. Biochemistry 2012;51:5725-32.
118. Dusane DH, Pawar VS, Nancharaiah YV, Venugopalan VP, Kumar AR, Zinjarde SS. Anti-biofilm potential of a glycolipid surfactant produced by a tropical marine strain of Serratia marcescens. Biofouling 2011;27:645-54.
119. Araujo LVd, Guimarães CR, Marquita RLdS, et al. Rhamnolipid and surfactin: Anti-adhesion/antibiofilm and antimicrobial effects. Food Control 2016;63:171-8.
120. Sekhon Randhawa KK, Rahman PKSM. Rhamnolipid biosurfactants-past, present, and future scenario of global market. Frontiers in Microbiology 2014;5:454-.
121. Nickzad A, Déziel E. The involvement of rhamnolipids in microbial cell adhesion and biofilm development – an approach for control? Letters in Applied Microbiology 2014;58:447-53.
122. Haba E, Pinazo A, Jauregui O, Espuny MJ, Infante MR, Manresa A. Physicochemical characterization and antimicrobial properties of rhamnolipids produced by Pseudomonas aeruginosa 47T2 NCBIM 40044. Biotechnology and Bioengineering 2003;81:316-22.
123. Al-Tahhan RA, Sandrin TR, Bodour AA, Maier RM. Rhamnolipid-induced removal of lipopolysaccharide from pseudomonas aeruginosa: Effect on cell surface properties and interaction with hydrophobic substrates. Applied and Environmental Microbiology 2000;66:3262-8.
124. Sotirova A, Spasova D, Vasileva-Tonkova E, Galabova D. Effects of rhamnolipid-biosurfactant on cell surface of Pseudomonas aeruginosa. Microbiological Research 2009;164:297-303.
125. Sotirova AV, Spasova DI, Galabova DN, Karpenko E, Shulga A. Rhamnolipid–Biosurfactant Permeabilizing Effects on Gram-Positive and Gram-Negative Bacterial Strains. Current Microbiology 2008;56:639-44.
126. de Araujo LV, Abreu F, Lins U, Anna LMdMS, Nitschke M, Freire DMG. Rhamnolipid and surfactin inhibit Listeria monocytogenes adhesion. Food Research International 2011;44:481-8.
127. Cortés-Sánchez AdJ, Hernández-Sánchez H, Jaramillo-Flores ME. Biological activity of glycolipids produced by microorganisms: New trends and possible therapeutic alternatives. Microbiological Research 2013;168:22-32.
128. Fux CA, Costerton JW, Stewart PS, Stoodley P. Survival strategies of infectious biofilms. Trends in Microbiology 2005;13:34-40.
129. Chen W, Liu Y, Courtney HS, et al. In vitro anti-bacterial and biological properties of magnetron co-sputtered silver-containing hydroxyapatite coating. Biomaterials 2006;27:5512-7.
130. Zhang R, Jones MM, Moussa H, et al. Polymer–antibiotic conjugates as antibacterial additives in dental resins. Biomaterials science 2019;7:287-95.
131. Hu S, Cai X, Qu X, et al. Preparation of biocompatible wound dressings with long-term antimicrobial activity through covalent bonding of antibiotic agents to natural polymers. International Journal of Biological Macromolecules 2019;123:1320-30.
132. Thatiparti TR, Shoffstall AJ, von Recum HA. Cyclodextrin-based device coatings for affinity-based release of antibiotics. Biomaterials 2010;31:2335-47.
133. Del Real R, Padilla S, Vallet-Regí M. Gentamicin release from hydroxyapatite/poly (ethyl methacrylate)/poly (methyl methacrylate) composites. Journal of biomedical materials research 2000;52:1-7.
134. Shen S-C, Letchmanan K, Chow PS, Tan RBH. Antibiotic elution and mechanical property of TiO2 nanotubes functionalized PMMA-based bone cements. Journal of the Mechanical Behavior of Biomedical Materials 2019;91:91-8.
135. Stigter M, Bezemer J, de Groot K, Layrolle P. Incorporation of different antibiotics into carbonated hydroxyapatite coatings on titanium implants, release and antibiotic efficacy. Journal of Controlled Release 2004;99:127-37.

136. Newman GR, Walker M, Hobot JA, Bowler PG. Visualisation of bacterial sequestration and bactericidal activity within hydrating Hydrofiber® wound dressings. Biomaterials 2006;27:1129-39.
137. Hobot J, Walker M, Newman G, Bowler P. Effect of Hydrofiber® wound dressings on bacterial ultrastructure. Journal of Electron Microscopy 2008;57:67-75.
138. Coelho CC, Araújo R, Quadros PA, Sousa SR, Monteiro FJ. Antibacterial bone substitute of hydroxyapatite and magnesium oxide to prevent dental and orthopaedic infections. Materials Science and Engineering: C 2019;97:529-38.
139. Babushkina IV, Mamontova IA, Gladkova EV. Metal nanoparticles reduce bacterial contamination of experimental purulent wounds. Bulletin of Experimental Biology and Medicine 2015;158:692-4.
140. Grass G, Rensing C, Solioz M. Metallic copper as an antimicrobial surface. Applied and Environmental Microbiology 2011;77:1541-7.
141. Schrand AM, Rahman MF, Hussain SM, Schlager JJ, Smith DA, Syed AF. Metal-based nanoparticles and their toxicity assessment. Wiley interdisciplinary reviews: Nanomedicine and Nanobiotechnology 2010;2:544-68.
142. MubarakAli D, Manzoor MAP, Sabarinathan A, et al. An investigation of antibiofilm and cytotoxic property of MgO nanoparticles. Biocatalysis and Agricultural Biotechnology 2019;18:101069.
143. Palza H. Antimicrobial polymers with metal nanoparticles. International journal of molecular sciences 2015;16:2099-116.
144. Ren G, Hu D, Cheng EWC, Vargas-Reus MA, Reip P, Allaker RP. Characterisation of copper oxide nanoparticles for antimicrobial applications. International Journal of Antimicrobial Agents 2009;33:587-90.
145. Dizaj SM, Lotfipour F, Barzegar-Jalali M, Zarrintan MH, Adibkia K. Antimicrobial activity of the metals and metal oxide nanoparticles. Materials Science and Engineering: C 2014;44:278-84.
146. Bergin S, Wraight P. Silver based wound dressings and topical agents for treating diabetic foot ulcers. Cochrane Database of Systematic Reviews 2006.
147. Munteanu A, Florescu IP, Nitescu C. A modern method of treatment: The role of silver dressings in promoting healing and preventing pathological scarring in patients with burn wounds. Journal of medicine and life 2016;9:306-15.
148. Carlson C, Hussain SM, Schrand AM, et al. Unique cellular interaction of silver nanoparticles: Size-dependent generation of reactive oxygen species. The Journal of Physical Chemistry B 2008;112:13608-19.
149. Rai M, Yadav A, Gade A. Silver nanoparticles as a new generation of antimicrobials. Biotechnology Advances 2009;27:76-83.
150. Kim JS, Kuk E, Yu KN, et al. Antimicrobial effects of silver nanoparticles. Nanomedicine: Nanotechnology, Biology and Medicine 2007;3:95-101.
151. Gasquères C, Schneider G, Nusko R, Maier G, Dingeldein E, Eliezer A. Innovative antibacterial coating by anodic spark deposition. Surface and Coatings Technology 2012;206:3410-4.
152. Pal S, Tak YK, Song JM. Does the antibacterial activity of silver nanoparticles depend on the shape of the nanoparticle? A study of the gram-negative bacterium Escherichia coli. Appl Environ Microbiol 2007;73:1712-20.
153. Paladini F, Pollini M, Deponti D, Di Giancamillo A, Peretti G, Sannino A. Effect of silver nanocoatings on catheters for haemodialysis in terms of cell viability, proliferation, morphology and antibacterial activity. Journal of Materials Science: Materials in Medicine 2013;24:1105-12.
154. Mogrovejo-Valdivia A, Rahmouni O, Tabary N, et al. In vitro evaluation of drug release and antibacterial activity of a silver-loaded wound dressing coated with a multilayer system. International Journal of Pharmaceutics 2019;556:301-10.
155. Ruparelia JP, Chatterjee AK, Duttagupta SP, Mukherji S. Strain specificity in antimicrobial activity of silver and copper nanoparticles. Acta Biomaterialia 2008;4:707-16.

156. Ismail WA, Ali ZA, Puteh R. Transparent nanocrystallite silver for antibacterial coating. J Nanomaterials 2013;2013:54-.
157. Trujillo NA, Oldinski RA, Ma H, Bryers JD, Williams JD, Popat KC. Antibacterial effects of silver-doped hydroxyapatite thin films sputter deposited on titanium. Materials Science and Engineering: C 2012;32:2135-44.
158. Bosetti M, Massè A, Tobin E, Cannas M. Silver coated materials for external fixation devices: in vitro biocompatibility and genotoxicity. Biomaterials 2002;23:887-92.
159. Kone BC, Kaleta M, Gullans SR. Silver ion (Ag+)-Induced increases in cell membrane K+ and Na+ permeability in the renal proximal tubule: Reversal by thiol reagents. The Journal of Membrane Biology 1988;102:11-9.
160. Takenaka S, Karg E, Roth C, et al. Pulmonary and systemic distribution of inhaled ultrafine silver particles in rats. Environmental Health Perspectives 2001;109 Suppl 4:547-51.
161. McAuliffe ME, Perry MJ. Are nanoparticles potential male reproductive toxicants? A literature review. Nanotoxicology 2007;1:204-10.
162. Prabhu S, Poulose EK. Silver nanoparticles: mechanism of antimicrobial action, synthesis, medical applications, and toxicity effects. International Nano Letters 2012;2:32.
163. Munteanu A, Florescu I, Nitescu C. A modern method of treatment: The role of silver dressings in promoting healing and preventing pathological scarring in patients with burn wounds. Journal of medicine and life 2016;9:306.
164. Silver S, Phung LT, Silver G. Silver as biocides in burn and wound dressings and bacterial resistance to silver compounds. Journal of Industrial Microbiology & Biotechnology 2006;33:627-34.
165. Landsdown ABG, Williams A. Bacterial resistance to silver in wound care and medical devices. Journal of Wound Care 2007;16:15-9.
166. Reid T, Cortez J, Hamood A, et al. Medical devices coated with Organo-Selenium inhibit bacterial and cellular attachment2010.
167. Tran PA, Taylor E, Sarin L, Hurt RH, Webster TJ. Novel Anti-Cancer, Anti-Bacterial Coatings for Biomaterial Applications: Selenium Nanoclusters. MRS Proceedings 2009;1209:1209-YY08-04.
168. Tran P, Hamood A, Mosley T, et al. Organo-Selenium-containing Dental Sealant Inhibits Bacterial Biofilm. Journal of Dental Research 2013;92:461-6.
169. Tran PL, Patel S, Hamood AN, et al. A Novel Organo-Selenium Bandage that Inhibits Biofilm Development in a Wound by Gram-Positive and Gram-Negative Wound Pathogens. Antibiotics 2014;3:435.
170. Vercellino T, Morse A, Tran P, et al. Attachment of organo-selenium to polyamide composite reverse osmosis membranes to inhibit biofilm formation of S. aureus and E. coli. Desalination 2013;309:291-5.
171. Vercellino T, Morse A, Tran P, et al. The use of covalently attached organo-selenium to inhibit S. aureus and E. coli biofilms on RO membranes and feed spacers. Desalination 2013;317:142-51.
172. Khiralla GM, El-Deeb BA. Antimicrobial and antibiofilm effects of selenium nanoparticles on some foodborne pathogens. LWT - Food Science and Technology 2015;63:1001-7.
173. Tran PL, Hammond AA, Mosley T, et al. Organoselenium Coating on Cellulose Inhibits the Formation of Biofilms by Pseudomonas aeruginosa and Staphylococcus aureus. Applied and Environmental Microbiology 2009;75:3586-92.
174. Nguyen THD, Vardhanabhuti B, Lin M, Mustapha A. Antibacterial properties of selenium nanoparticles and their toxicity to Caco-2 cells. Food Control 2017;77:17-24.
175. Reid T, Tran P, Cortez J, et al. Medical devices coated with organo-selenium inhibit bacterial and cellular attachment. Int Med Dev 2010;5:23-31.
176. Filipović N, Veselinović L, Ražić S, et al. Poly (ε-caprolactone) microspheres for prolonged release of selenium nanoparticles. Materials Science and Engineering: C 2019;96:776-89.
177. Ramos JF, Webster TJ. Cytotoxicity of selenium nanoparticles in rat dermal fibroblasts. International Journal of Nanomedicine 2012;7:3907.

178. Zonaro E, Lampis S, Turner RJ, Qazi SJS, Vallini G. Biogenic selenium and tellurium nanoparticles synthesized by environmental microbial isolates efficaciously inhibit bacterial planktonic cultures and biofilms. Frontiers in Microbiology 2015;6.
179. Holinka J, Pilz M, Kubista B, Presterl E, Windhager R. Effects of selenium coating of orthopaedic implant surfaces on bacterial adherence and osteoblastic cell growth. The Bone & Joint Journal 2013;95-B:678-82.
180. Kochkodan V, Hilal N. A comprehensive review on surface modified polymer membranes for biofouling mitigation. Desalination 2015;356:187-207.
181. Piętka-Ottlik M, Wójtowicz-Młochowska H, Kołodziejczyk K, Piasecki E, Młochowski J. New organoselenium compounds active against pathogenic bacteria, fungi and viruses. Chemical and Pharmaceutical Bulletin 2008;56:1423-7.
182. Holinka J, Pilz M, Kubista B, Presterl E, Windhager R. Effects of selenium coating of orthopaedic implant surfaces on bacterial adherence and osteoblastic cell growth. The bone & joint journal 2013;95:678-82.
183. Bartůněk V, Vokatá B, Kolářová K, Ulbrich P. Preparation of amorphous nano-selenium-PEG composite network with selective antimicrobial activity. Materials Letters 2019;238:51-3.
184. Sonkusre P, Singh Cameotra S. Biogenic selenium nanoparticles inhibit Staphylococcus aureus adherence on different surfaces. Colloids and Surfaces B: Biointerfaces 2015;136:1051-7.
185. Nastulyavichus A, Kudryashov S, Smirnov N, et al. Antibacterial coatings of Se and Si nanoparticles. Applied Surface Science 2019;469:220-5.
186. Hariharan H, Al-Harbi N, Karuppiah P, Rajaram S. Microbial synthesis of selenium nanocomposite using *Saccharomyces cerevisiae* and its antimicrobial activity against pathogens causing nosocomial infection. Chalcogenide Lett 2012;9:509-15.
187. Sharma S, Dua A, Malik A. Third generation materials for wound dressings. International Journal of Pharmaceutical Sciences and Research 2014;5:2113.
188. Burkatovskaya M, Tegos GP, Swietlik E, Demidova TN, P Castano A, Hamblin MR. Use of chitosan bandage to prevent fatal infections developing from highly contaminated wounds in mice. Biomaterials 2006;27:4157-64.
189. Muzzarelli RAA. Chitins and chitosans for the repair of wounded skin, nerve, cartilage and bone. Carbohydrate Polymers 2009;76:167-82.
190. Larqué E, Sabater-Molina M, Zamora S. Biological significance of dietary polyamines. Nutrition 2007;23:87-95.
191. El-Halfawy OM, Valvano MA. Non-genetic mechanisms communicating antibiotic resistance: rethinking strategies for antimicrobial drug design. Expert opinion on drug discovery 2012;7:923-33.
192. Rider J, Hacker A, Mackintosh C, Pegg A, Woster P, Casero R. Spermine and spermidine mediate protection against oxidative damage caused by hydrogen peroxide. Amino Acids 2007;33:231-40.
193. Kwon D-H, Lu C-D. Polyamine effects on antibiotic susceptibility in bacteria. Antimicrobial Agents and Chemotherapy 2007;51:2070-7.
194. Kikuchi K, Bernard EM, Sadownik A, Regen SL, Armstrong D. Antimicrobial activities of squalamine mimics. Antimicrobial agents and chemotherapy 1997;41:1433-8.
195. Razin S, Rozansky R. Mechanism of the antibacterial action of spermine. Archives of Biochemistry And Biophysics 1959;81:36-54.
196. Zhu S, Ashok M, Li J, et al. Spermine protects mice against lethal sepsis partly by attenuating surrogate inflammatory markers. Molecular Medicine 2009;15:275-82.
197. Goytia M, Dhulipala VL, Shafer WM. Spermine impairs biofilm formation by Neisseria gonorrhoeae. FEMS microbiology letters 2013;343:64-9.
198. Nesse LL, Berg K, Vestby LK. Effects of norspermidine and spermidine on biofilm formation by potentially pathogenic Escherichia coli and Salmonella enterica wild-type strains. Appl Environ Microbiol 2015;81:2226-32.
199. Mårdh P-A, Colleen S. Antimicrobial activity of human seminal fluid. Scandinavian Journal of Urology And Nephrology 1975;9:17-23.

200. Joshi GS, Spontak JS, Klapper DG, Richardson AR. Arginine catabolic mobile element encoded speG abrogates the unique hypersensitivity of Staphylococcus aureus to exogenous polyamines. Molecular microbiology 2011;82:9-20.
201. Ashton NN, Allyn G, Porter ST, et al. In vitro testing of a first-in-class tri-alkylnorspermidine-biaryl antibiotic in an anti-biofilm silicone coating. Acta Biomaterialia 2019.
202. Kim MS, Diamond SL. Controlled release of DNA/polyamine complex by photoirradiation of a solid phase presenting o-nitrobenzyl ether tethered spermine or polyethyleneimine. Bioorganic & Medicinal Chemistry Letters 2006;16:5572-5.
203. Ghorai SK, Maji S, Subramanian B, Maiti TK, Chattopadhyay S. Coining attributes of ultra-low concentration graphene oxide and spermine: An approach for high strength, anti-microbial and osteoconductive nanohybrid scaffold for bone tissue regeneration. Carbon 2019;141:370-89.
204. Wang EW, Agostini G, Olomu O, Runco D, Jung JY, Chole RA. Gentian Violet and Ferric Ammonium Citrate Disrupt Pseudomonas Aeruginosa Biofilms. The Laryngoscope 2008;118:2050-6.
205. Maley AM, Arbiser JL. Gentian violet: a 19th century drug re-emerges in the 21st century. Experimental dermatology 2013;22:775-80.
206. Bakker P, Van Doorne H, Gooskens V, Wieringa NF. Activity of gentian violet and brilliant green against some microorganisms associated with skin infections. International Journal of Dermatology 1992;31:210-3.
207. Saji M, Taguchi S, Uchiyama K, Osono E, Hayama N, Ohkuni H. Efficacy of gentian violet in the eradication of methicillin-resistant Staphylococcus aureus from skin lesions. Journal of Hospital Infection 1995;31:225-8.
208. Noimark S, Weiner J, Noor N, et al. Dual-Mechanism Antimicrobial Polymer–ZnO Nanoparticle and Crystal Violet-Encapsulated Silicone. Advanced Functional Materials 2015;25:1367-73.
209. Chaiban G, Hanna H, Dvorak T, Raad I. A rapid method of impregnating endotracheal tubes and urinary catheters with gendine: a novel antiseptic agent. Journal of Antimicrobial Chemotherapy 2005;55:51-6.
210. Hanna H, Bahna P, Reitzel R, et al. Comparative in vitro efficacies and antimicrobial durabilities of novel antimicrobial central venous catheters. Antimicrobial Agents and Chemotherapy 2006;50:3283-8.
211. Moreno S, Gadelha FR, Docampo R. Crystal violet as an uncoupler of oxidative phosphorylation in rat liver mitochondria. Journal of Biological Chemistry 1988;263:12493-9.
212. Sehmi SK, Noimark S, Pike SD, et al. Enhancing the Antibacterial Activity of Light-Activated Surfaces Containing Crystal Violet and ZnO Nanoparticles: Investigation of Nanoparticle Size, Capping Ligand, and Dopants. ACS Omega 2016;1:334-43.
213. Adams E. The antibacterial action of crystal violet*. Journal of Pharmacy and Pharmacology 1967;19:821-6.
214. Cheng G, Xue H, Li G, Jiang S. Integrated antimicrobial and nonfouling hydrogels to inhibit the growth of planktonic bacterial cells and keep the surface clean. Langmuir 2010;26:10425-8.
215. Sadrearhami Z, Shafiee FN, Ho KKK, et al. Antibiofilm Nitric Oxide-Releasing Polydopamine Coatings. ACS Applied Materials & Interfaces 2019;11:7320-9.
216. Darouiche RO, Mansouri MD, Gawande PV, Madhyastha S. Antimicrobial and antibiofilm efficacy of triclosan and DispersinB® combination. Journal of Antimicrobial Chemotherapy 2009;64:88-93.
217. Tetz GV, Artemenko NK, Tetz VV. Effect of DNase and Antibiotics on Biofilm Characteristics. Antimicrobial Agents and Chemotherapy 2009;53:1204-9.
218. Khalid HF, Tehseen B, Sarwar Y, et al. Biosurfactant coated silver and iron oxide nanoparticles with enhanced anti-biofilm and anti-adhesive properties. Journal of hazardous materials 2019;364:441-8.
219. Stemberger A, Gollwitzer H, Meyer H, Ibrahim K, Busch R, Mittelmeier W. Antibacterial poly(d,l-lactic acid) coating of medical implants using a biodegradable drug delivery technology. Journal of Antimicrobial Chemotherapy 2003;51:585-91.

220. Fang F, Xiao D, Zhang X, et al. Construction of intumescent flame retardant and antimicrobial coating on cotton fabric via layer-by-layer assembly technology. Surface and Coatings Technology 2015;276:726-34.
221. Kulkarni Aranya A, Pushalkar S, Zhao M, LeGeros RZ, Zhang Y, Saxena D. Antibacterial and bioactive coatings on titanium implant surfaces. Journal of biomedical materials research Part A 2017;105:2218-27.
222. Zhang P, Zhang Z, Li W. Antibacterial coating incorporating silver nanoparticles by microarc oxidation and ion implantation. Journal of Nanomaterials 2013;2013:8.
223. Lugovskoy A, Lugovskoy S. Production of hydroxyapatite layers on the plasma electrolytically oxidized surface of titanium alloys. Materials Science and Engineering: C 2014;43:527-32.
224. Durdu S, Usta M. The tribological properties of bioceramic coatings produced on Ti6Al4V alloy by plasma electrolytic oxidation. Ceramics International 2014;40:3627-35.
225. Sreekanth D, Rameshbabu N. Development and characterization of MgO/hydroxyapatite composite coating on AZ31 magnesium alloy by plasma electrolytic oxidation coupled with electrophoretic deposition. Materials Letters 2012;68:439-42.
226. Henry SM, Komarraju S, Heathcote D, Rodionov IL. Designing peptide-based FSL constructs to create Miltenberger kodecytes. ISBT Science Series 2011;6:306-12.
227. Henry SM, Bovin NV. Kode Technology–a universal cell surface glycan modification technology. Journal of the Royal Society of New Zealand 2018:1-14.
228. Korchagina EY, Henry SM. Synthetic glycolipid-like constructs as tools for glycobiology research, diagnostics, and as potential therapeutics. Biochemistry (Moscow) 2015;80:857-71.
229. Lan C-C, Blake D, Henry S, Love DR. Fluorescent function-spacer-lipid construct labelling allows for real-time in vivo imaging of cell migration and behaviour in zebrafish (danio rerio). Journal of Fluorescence 2012;22:1055-63.
230. Henry S, Williams E, Barr K, et al. Rapid one-step biotinylation of biological and non-biological surfaces. Scientific Reports 2018;8:2845.
231. Henry SM, Barr KL, Oliver CA. Modeling transfusion reactions with kodecytes and enabling ABO-incompatible transfusion with function-spacer-lipid constructs. ISBT Science Series 2012;7:106-11.
232. Williams E, Korchagina E, Frame T, Ryzhov I, Bovin N, Henry S. Glycomapping the fine specificity of monoclonal and polyclonal Lewis antibodies with type-specific Lewis kodecytes and function-spacer-lipid constructs printed on paper. Transfusion 2016;56:325-33.
233. Ilyushina NA, Chernyy ES, Korchagina EY, Gambaryan AS, Henry SM, Bovin NV. Labeling of influenza viruses with synthetic fluorescent and biotin-labeled lipids. Virologica Sinica 2014;29:199-210.
234. Barr K. Bio-modification of non-biological surfaces with function-spacer-lipid constructs by methods including bioprinting: Auckland University of Technology; 2013.
235. Barr K, Kannan B, Korchagina E, et al. Biofunctionalizing nanofibers with carbohydrate blood group antigens. Biopolymers 2016;105:787-94.
236. Tran P, Hamood A, Webster D, Jarvis C, Hanes R, Reid T. Selenium Contact Lens Hydrogel Polymer: Inhibition of Bacterial Biofilm Formation. Investigative Ophthalmology & Visual Science 2013;54:514-.
237. Tantra R, Schulze P, Quincey P. Effect of nanoparticle concentration on zeta-potential measurement results and reproducibility. Particuology 2010;8:279-85.
238. Botstein D, Chervitz SA, Cherry M. Yeast as a model organism. Science 1997;277:1259-60.
239. Williams E, Barr K, Korchagina E, Tuzikov A, Henry S, Bovin N. Ultra-Fast Glyco-Coating of Non-Biological Surfaces. International Journal of Molecular Sciences 2016;17:118.
240. Korchagina E, Tuzikov A, Formanovsky A, Popova I, Henry S, Bovin N. Toward creating cell membrane glyco-landscapes with glycan lipid constructs. Carbohydrate Research 2012;356:238-46.
241. Henry S, Perry H, Bovin N. Applications for kodecytes in immunohaematology2017.

242. Cheng KH, Leung SL, Hoekman HW, et al. Incidence of contact-lens-associated microbial keratitis and its related morbidity. The Lancet 1999;354:181-5.
243. Oliveira R, Azeredo J, Teixeira P, Fonseca A. The role of hydrophobicity in bacterial adhesion. 2001.
244. Busscher HJ, Weerkamp AH. Specific and non-specific interactions in bacterial adhesion to solid substrata. FEMS Microbiology Reviews 1987;3:165-73.
245. An YH, Friedman RJ. Concise review of mechanisms of bacterial adhesion to biomaterial surfaces. Journal of biomedical materials research 1998;43:338-48.
246. Asadinezhad A, Novák I, Lehocký M, et al. A physicochemical approach to render antibacterial surfaces on plasma-treated medical-grade pvc: Irgasan coating. Plasma Processes and Polymers 2010;7:504-14.
247. Friedman M. Applications of the ninhydrin reaction for analysis of amino acids, peptides, and proteins to agricultural and biomedical sciences. Journal of Agricultural and Food Chemistry 2004;52:385-406.
248. Kazemzadeh-Narbat M, Lai BFL, Ding C, Kizhakkedathu JN, Hancock REW, Wang R. Multilayered coating on titanium for controlled release of antimicrobial peptides for the prevention of implant-associated infections. Biomaterials 2013;34:5969-77.
249. Sarker SD, Nahar L, Kumarasamy Y. Microtitre plate-based antibacterial assay incorporating resazurin as an indicator of cell growth, and its application in the in vitro antibacterial screening of phytochemicals. Methods 2007;42:321-4.
250. Elshikh M, Ahmed S, Funston S, et al. Resazurin-based 96-well plate microdilution method for the determination of minimum inhibitory concentration of biosurfactants. Biotechnol Lett 2016;38:1015-9.
251. Van den Driessche F, Rigole P, Brackman G, Coenye T. Optimization of resazurin-based viability staining for quantification of microbial biofilms. Journal of Microbiological Methods 2014;98:31-4.
252. Shah P, Swiatlo E. A multifaceted role for polyamines in bacterial pathogens. Molecular Microbiology 2008;68:4-16.
253. Jin LT, Hwang SY, Yoo GS, Choi JK. Sensitive silver staining of protein in sodium dodecyl sulfate-polyacrylamide gels using an azo dye, calconcarboxylic acid, as a silver-ion sensitizer. Electrophoresis 2004;25:2494-500.
254. Guerin-Danan C. Storage of intestinal bacteria in samples frozen with glycerol. Microbial Ecology in Health and Disease 1999;11:180-2.
255. Kroukamp O, Dumitrache RG, Wolfaardt GM. Pronounced Effect of the Nature of the Inoculum on Biofilm Development in Flow Systems. Applied and Environmental Microbiology 2010;76:6025-31.
256. Sandberg ME, Schellmann D, Brunhofer G, et al. Pros and cons of using resazurin staining for quantification of viable Staphylococcus aureus biofilms in a screening assay. Journal of Microbiological Methods 2009;78:104-6.
257. Perloff JR, Palmer JN. Evidence of bacterial biofilms on frontal recess stents in patients with chronic rhinosinusitis. American Journal of Rhinology 2004;18:377-80.
258. Portillo ME, Salvadó M, Trampuz A, et al. Sonication versus vortexing of implants for diagnosis of prosthetic joint infection. Journal of Clinical Microbiology 2013;51:591-4.
259. Kobayashi H, Oethinger M, Tuohy MJ, Procop GW, Bauer TW. Improved detection of biofilm-formative bacteria by vortexing and sonication: A pilot study. Clinical Orthopaedics and Related Research 2009;467:1360-4.
260. Coffey BM, Anderson GG. Biofilm formation in the 96-well microtiter plate. Pseudomonas Methods and Protocols: Springer; 2014:631-41.
261. Fujita K, Nagatsu T, Shinpo K, Maruta K, Teradaira R, Nakamura M. Improved analysis for urinary polyamines by use of high-voltage electrophoresis on paper. Clinical Chemistry 1980;26:1577-82.

262. Herbst EJ, Keister DL, Weaver RH. The separation of aliphatic amines by paper chromatography or paper electrophoresis. Archives of biochemistry and biophysics 1958;75:178-85.
263. Lichter JA, Van Vliet KJ, Rubner MF. Design of antibacterial surfaces and interfaces: polyelectrolyte multilayers as a multifunctional platform. Macromolecules 2009;42:8573-86.
264. Gottenbos B, Grijpma DW, van der Mei HC, Feijen J, Busscher HJ. Antimicrobial effects of positively charged surfaces on adhering Gram-positive and Gram-negative bacteria. Journal of Antimicrobial Chemotherapy 2001;48:7-13.
265. Wang C-K, Shih L-Y, Chang KY. Large-Scale Analysis of Antimicrobial Activities in Relation to Amphipathicity and Charge Reveals Novel Characterization of Antimicrobial Peptides. Molecules 2017;22:2037.
266. Berlanga M, Guerrero R. Living together in biofilms: the microbial cell factory and its biotechnological implications. Microbial Cell Factories 2016;15:165.
267. Zhu Z, Wang Z, Li S, Yuan X. Antimicrobial strategies for urinary catheters. Journal of Biomedical Materials Research Part A 2019;107:445-67.
268. Roe D, Karandikar B, Bonn-Savage N, Gibbins B, Roullet J-B. Antimicrobial surface functionalization of plastic catheters by silver nanoparticles. Journal of Antimicrobial Chemotherapy 2008;61:869-76.
269. Jain P, Pradeep T. Potential of silver nanoparticle-coated polyurethane foam as an antibacterial water filter. Biotechnology and bioengineering 2005;90:59-63.
270. Verd Soriano J, Rueda Lpez J, Martnez Cuervo F, Soldevilla Agreda J. Effects of an activated charcoal silver dressing on chronic wounds with no clinical signs of infection. Journal of wound care 2004;13:419-23.
271. Satapathy MK, Das P. Optimization of crystal violet dye removal using novel soil-silver nanocomposite as nanoadsorbent using response surface methodology. Journal of Environmental Chemical Engineering 2014;2:708-14.
272. Zalygin A, Solovyeva D, Vaskan I, et al. Structure of Supramers Formed by the Amphiphile Biotin-CMG-DOPE. ChemistryOpen 2020;9:641.
273. Gnanadhas DP, Thomas MB, Thomas R, Raichur AM, Chakravortty D. Interaction of silver nanoparticles with serum proteins affects their antimicrobial activity in vivo. Antimicrobial agents and chemotherapy 2013;57:4945-55.
274. Finnegan S, Percival SL. EDTA: An Antimicrobial and Antibiofilm Agent for Use in Wound Care. Adv Wound Care (New Rochelle) 2015;4:415-21.